This is to certify that the
dissertation entitled

ELUCIDATING THE STRUCTURE AND KINETICS OF THE APOCYTOCHROME B mRNA/gRNA COMPLEX IN *TRYPANOSOMA BRUCEI* MITOCHONDRIA

presented by

Laura Elizabeth Yu

has been accepted towards fulfillment
of the requirements for the

Ph.D. degree in Cell and Molecular Biology

Major Professor's Signature

10/25/06

Date

MSU is an Affirmative Action/Equal Opportunity Institution

ELUCIDATING THE STRUCTURE AND KINETICS OF THE APOCYTOCHROME B mRNA/gRNA COMPLEX IN *TRYPANOSOMA BRUCEI* MITOCHONDRIA

By

Laura Elizabeth Yu

A DISSERTATION
Submitted to
Michigan State University
in partial fulfillment of the requirements
for the degree of

DOCTOR OF PHILOSOPHY

Cell and Molecular Biology Program

2006

ABSTRACT

ELUCIDATING THE STRUCTURE AND KINETICS OF THE APOCYTOCHROME B mRNA/gRNA COMPLEX IN *TRYPANOSOMA BRUCEI* MITOCHONDRIA

By

Laura Elizabeth Yu

Expression of mitochondrial genes in *Trypanosoma brucei* requires RNA editing of its mRNA transcripts. During editing, uridylates are precisely inserted and deleted as directed by the guide RNA (gRNA) template to create the protein open reading frame. This process involves the bimolecular interaction of the gRNA with its cognate pre-edited mRNA and the assembly of a protein complex. The importance of RNA structure in establishing a functional editing complex is poorly understood. Previous experiments indicate that different mRNA/gRNA pairs can form similar secondary structures suggesting that a common core architecture may be important for editosome recognition and function. Using solution structure probing, we have investigated the structure of the initiating gRNA, gCYb-558, in the mRNA/gRNA complex. The data indicate that the stem-loop formed by the guiding region of the gRNA alone is maintained in its interaction with the pre-edited message. In addition, the data suggest that a gRNA stem-loop structure is maintained through the first few editing events by the use of alternative base pairing with the U-tail. This suggests that the gRNA stem-loop is an important component of the initial editing complex.

In trypansomes, RNA editing of the mitochondrial mRNAs is developmentally regulated in a transcript specific manner. We hypothesize that regulation involves the structure of the mRNA and its ability to interact with its gRNA. Surface plasmon resonance was used to measure the kinetics of gRNA binding for three separate

mRNA/gRNA pairs; two mRNA substrates with predicted single stranded anchor binding sites (ABS) and one mRNA substrate with the ABS located within a thermodynamically stable stem-loop. The stability of the mRNA stem-loop appears to affect the gRNA anchor target binding and results in a slower association rate as well as a faster dissociation rate. In contrast, the mRNAs with an open ABS associate with their cognate gRNAs at a much faster rate. In addition, they have a surprisingly slow dissociation rate. This slow dissociation rate may be necessary to allow the editosome protein complexes to recognize and assemble onto the mRNA/gRNA pair.

Editing of the mRNA, results in a progressive lengthening of the anchor helix. Using apocytochrome b (CYb) mRNA and 2 partially edited CYb mRNAs, the kinetic effects of editing for the CYb mRNA/gRNA interaction were investigated. The CYb mRNA forms a stable stem-loop that the gRNA anchor has difficulty invading to base pair at the anchor binding site (ABS). Each editing event appears to result in a decreased dissociation rate that may be important for editing progression. In addition, the U-tail targets one side of the stem-loop for binding and this appears to increase the association rate constant two fold when the gRNA binds the unedited CYb mRNA providing a new and exciting function for the U-tail.

To my husband, Min, and my family and friends for their love and support

ACKNOWLEDGEMENTS

First I would like to thank my husband, Min Yu. Without his love and support I would never have made it through graduate school. He has been the best helpmate and sounding board on earth, and for his finite patience and never-ending love I thank him. I'd like to thank my family and friends from home for their love and support; especially Frank and Sylvia Bean, my parents, and Bob and Christina Bean, my brother and sister, and all my aunts, uncles and cousins. I'd also like to thank my friend, Angie Blazek, who knows me best. I'd also like to thank my friend, Michelle Degnan, who I partied and studied with as an undergrad, and who was crazy like me and went to graduate school.

I would like to thank my advisor, Donna Koslowsky. She is a wonderful example of a female scientist and an excellent role model. As a mentor, she spent many, many hours advising me on experiments, writing, and scientific protocol. For her diligence, I thank her. I would also like to thank my guidance committee members, Shelagh Ferguson-Miller, Jim Geiger, Charles Hoogstraten, and Ron Patterson for their help and dedication. I owe special thanks to Dr. Patterson and Dr. Hoogstraten. Dr. Patterson was always available to provide a listening ear and sound advice. Dr. Hoogstraten was invaluable with good discussion and advice for my Biacore and kinetics data.

The Koslowsky lab has been a wonderful environment for friendship as well as learning. I'd like to thank former lab member, Dr. Sandra Clement, for her unwavering support, excellent ideas (scientific and social), and wonderful friendship. I could never have made it through graduate school without Larissa Reifur, who has been my right hand woman in the lab. Larissa has been an awesome friend, excellent partner in crime

in the lab, and she is always willing to read and edit everything. Playing volleyball with Larissa helped me stay sane. I'd also like to thank Melissa Mingler for her spunky attitude and sparkling personality. The undergraduates coming through our lab have been invaluable; I'd especially like to thank Remy Brim, Andrea Hingst, Tanojo Mustika, and Aimee Sutherland.

The faithful members of the MSU RNA Journal Club have been very supportive. They have been especially helpful with ideas, listening, and evaluation of presentations. I'd especially like to thank the members of the Donna Koslowsky lab (Donna, Sandi, Larissa, and Mel), the Charles Hoogstraten lab (Charlie, James, and Kristy), the Ron Patterson Lab (Ron, Kevin, and Weizhong) and the John Wang lab (John, Rich, and Patty) for their patience, good ideas, and helpful advice.

I'd like to thank Dr Robert Hausinger, MSU Microbiology and Molecular Genetics, and Dr. Zachary Burton, MSU Biochemisty and Molecular Biology, for their help with rate constant equations for my kinetics data and good discussion and advice. I'd also like to thank Dr. Joseph Leykam and the members of the Macromolecular Structure Facility in the Biochemistry and Molecular Biology Department for the use of the Biacore machine.

I'd like to thank the Cell and Molecular Biology program for the support and training I've received as well as the faculty and staff of the Department of Microbiology and Molecular Genetics for all their help and assistance. I'd especially like to thank former graduate secretary Angie Zell and current graduate secretary Christine VanDeuren for fixing my messes within the MSU bureaucracy, and there have been a few.

TABLE OF CONTENTS

LIST OF TABLES

LIST OF FIGURES

LIST OF FIGURES (CON'T)

Images in this dissertation are presented in color.

LIST OF EQUATIONS

KEY TO ABBREVIATIONS

A	adenosine
ABS	anchor binding site
C	cytosine
CYb	apocytochrome b
CYbU	partial CYb mRNA Unedited
CYbPES1	partial CYb mRNA Partially Edited through Site 1
CYbPES3	partial CYb mRNA Partially Edited through Site 3
DEPC	diethyl pyrocarbonate
G	guanosine
gCYb-558	initiating CYb gRNA
gRNA	guide RNA
K_D	dissociation constant
k_{obs}	observed rate constant
k_{off}	dissociation rate constant
k_{on}	association rate constant
MBN	mung bean nuclease
NgCYb-558	new gCYb-558 gRNA with a U-tail
NgCYb-558sU	new gCYb-558 gRNA without a U-tail
nt	nucleotide
RU	resonance unit
SPR	surface plasmon resonance
T1	RNase T1
T2	RNase T2
U	uridine
U-tail	uridine tail
UV	ultra-violet light
V1	RNase V1

CHAPTER 1

INTRODUCTION

History of Human African Trypanosomiasis

Trypanosomes are motile, protozoan parasites with a life cycle that includes two hosts, insects and mammals. *Trypanosoma brucei gambiense* and *Trypanosoma brucei rhodesiense* are African species that infect man and wild game; they cause the disease human African trypanosomiasis (HAT), also known as sleeping sickness. HAT threatens over 60 million people in 36 sub-Saharan African countries. Only 3 to 4 million of those at risk have access to health care that provides screening and treatment (WHO, 2001). *Trypanosoma brucei brucei* (*T brucei*), the form studied in our lab, does not infect man but causes the wasting disease, nagana, in ruminants. The effects of nagana are equally devastating to the population as the disease places a major constraint on agricultural development in many of the poorer countries. Nagana infects 46 million cattle in Africa and causes the death of three million cattle a year (Unisci, 2001). The economic loss associated with African trypanosomiasis is estimated to be $4.5 billion each year (Mattock & Pink, 2003-2004).

T. brucei is transmitted through the saliva of a bite from a tsetse fly (*Glossina* ssp.) as it takes a blood meal from the new vertebrate host. The area of Africa where the tsetse fly breeds covers over 10 million square kilometers (WHO, 2001; Kuzoe & Schofield, 2004) creating a major challenge to both the prevention of parasite transmission as well as treatment of infected humans and animals. Other problems associated with treating humans with trypanosomiasis include inadequate resources, surveillance, disease knowledge, and diagnostic tools. The drugs available are expensive; most cause adverse side effects and cannot be administered without medical aid (Mattock & Pink, 2003-2004).

Historically, the spread of infection was primarily controlled by destroying the breeding grounds of the tsetse fly, spraying of pesticides, and reduction of wild game populations. Using these techniques, the number of cases of trypanosomiasis (over 50,000 reported cases of infection in 1940) was drastically reduced by the 1960's (less than 10,000 reported cases of infection) (Kuzoe & Schofield, 2004). Unfortunately, with the decrease in the numbers of afflicted, interest in HAT declined resulting in a reduction of control activities and a resurgence of human and animal trypanosomiasis (with close to 40,000 reported cases of infection by 2000). In addition, political instability, wars, and civil unrest have led to further blocks in control activities (Kuzoe & Schofield, 2004). The World Health Organization (WHO) estimates that 300,000 to 500,000 people are in danger of HAT infection every year, but the instability of the most affected areas means there are no accurate numbers to support these estimates (Mattock & Pink, 2003-2004).

A renewed interest in HAT prevention, through WHO and other non-profit groups has begun measures to try to reduce infection. Past methods of tsetse vector control described earlier are no longer recommended as they cause other secondary environmental concerns. Newer methods of control include traps and screens to capture and kill flies, live bait techniques (treating cattle with insecticides), and sterile insect technique (releasing mass numbers of sterile male tsetse flies) (Kuzoe & Schofield, 2004).

Trypanosomes

The life cycle of the trypanosome includes two hosts. Part of the life cycle is spent in an insect vector (procyclic stage) and part in a mammalian host (bloodstream stage) (Fig. 1). When an infected tsetse fly takes a blood meal, the trypanosomes are injected through

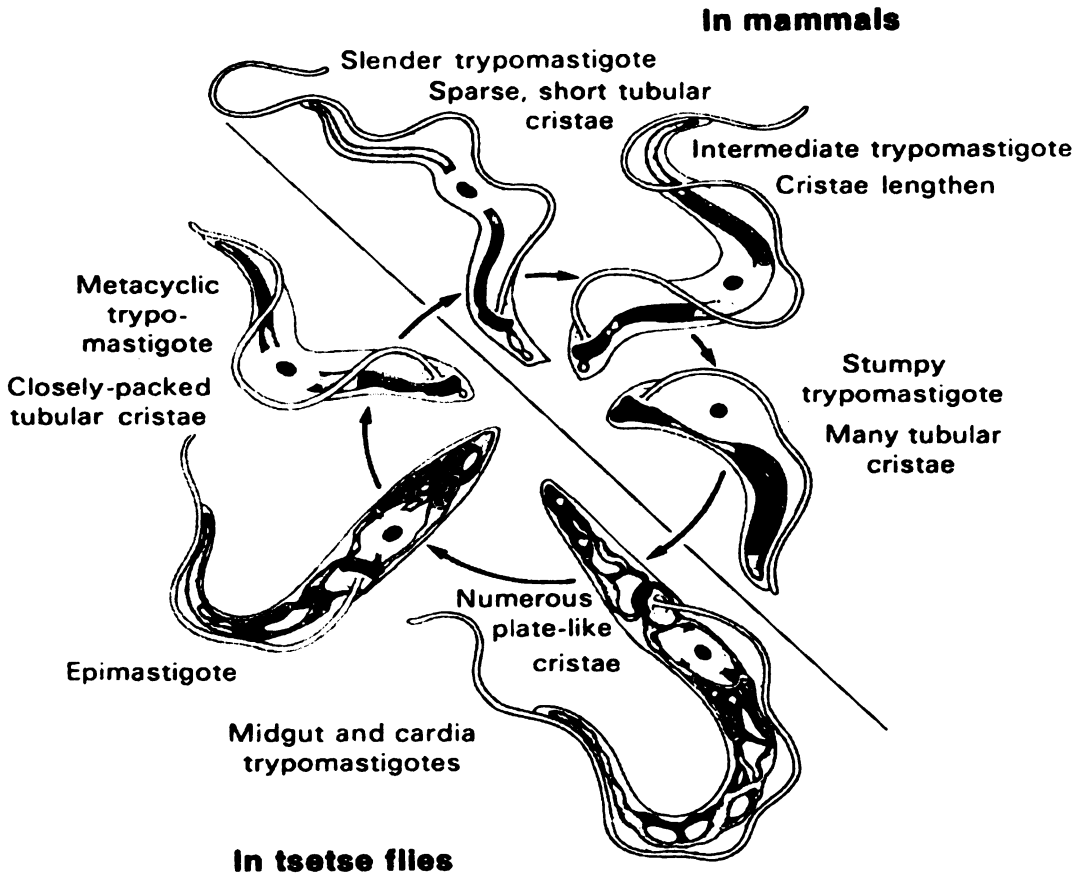

Figure 1. The life cycle of the trypanosome includes mammalian and insect hosts. In the tsetse fly, the mitochondrion is large and reticulated, and ATP is produced through electron transport and oxidative phosphorylation. In contrast, during the bloodstream stage of the life cycle, the trypanosome derives most of its energy from glycolysis. The mitochondrion is less active and has a compact morphology. From: Vickerman, K. 1971. In Fallis, A.M., ed. Ecology and Physiology of Parasites. University of Toronto Press, Toronto.

the salivary glands and enter the bloodstream. In the bloodstream, the parasites proliferate in waves as morphologically slender forms. They are able to thwart the human immune system by having a protein coat composed of a variant specific glycoprotein (VSG) with thousands of genetic variations that change with each wave of parasitemia (Vickerman, 1985). During each proliferative wave, as parasite numbers increase, differentiation to the short, stumpy form occurs. Cell division is arrested in this form, and the trypanosome is pre-adapted for transmission to the insect host. When an insect becomes infected through a trypanosome enriched blood meal, the stumpy forms travel to the mid-gut of the insect where they develop into the procyclic form. Procyclic forms lose the VSG coat and develop a coat of procyclins. Trypansomes in the mid-gut arrest in division and migrate to the salivary glands. They attach themselves to the walls of the salivary gland as epimastigote forms to proliferate. As epimastigote numbers rise, the trypanosomes differentiate into metacyclic forms that are non-proliferative and develop the VSG coat. The metacyclic forms are then ready to infect a new host (Matthews, 2005).

One unique feature in trypanosomes is the change in energy metabolism that is reflected in the extreme morphological difference in mitochondrion structure between the two hosts (Vickerman, 1965). Trypanosomes do not store carbohydrates, so they must obtain their energy supply directly from a host. In the insect vector, the trypanosome has a fully active and more developed mitochondrion that produces ATP through electron transport and oxidative phosphorylation. During this stage, the mitochondrion grows long and reticulated and develops a mitochondrial network where most of the cristae are plate-like (Brown et al., 1973). In the mammalian host, the trypanosome oxidizes

glucose from the bloodstream using an organelle unique to trypanosomes, the glycosome, while most mitochondrial functions are suppressed. Morphological changes in the structure of the mitochondrion reflect its suppressed function as it becomes a linear canal extending the length of the trypanosome and containing some tubular cristae (Brown et al., 1973). Glycosomes are peculiar peroxisomes that compartmentalize the first seven steps of glycolysis as well as the pentose phosphate pathway. The changes in morphology and content of this organelle lead to large differences in the metabolism of trypanosomes in the separate hosts. The trypanosome is able to effect a rapid change in its development, morphology, and energy metabolism in response to an instantaneous difference in temperature (insect 27°C, mammal 37°C), cellular environment, and immune response that is brought on by a change of host (Brown & Neva, 1983).

Metabolism of Trypanosomes

The metabolism of trypanosomes allows a large amount of flexibility in order to respond to sudden changes in nutrition as well as a change of host. In the mammalian bloodstream, compartmentalization of glycolysis in the glycosome appears to regulate the amount of ATP that is accessible to hexokinase and phosphofructokinase (Fig. 2). These glycolytic enzymes are unusual as they are unregulated in trypanosomes and could cause a toxic accumulation of glycolytic intermediates if allowed unlimited access to ATP (Hannaert et al., 2003). The glycosome allows no net change in ATP to occur through the first seven steps of glycolysis. Afterward, 3-phosphoglycerate is shuttled to the cytoplasm for the last three steps of glycolysis to produce two net ATP and pyruvate. Even though the mitochondrion is largely repressed during the mammalian stage, a putative glycerol 3-phosphate/DHAP shunt runs between the glycosome and the

mitochondrion. This shunt helps to maintain the NAD+/NADH balance with the help of a glycerol 3-phosphate dehydrogenase and the terminal alternative oxidase (Michels et al., 2000). During this stage of the life cycle, the mitochondrion lacks most Krebs cycle enzymes as well as a cytochrome containing respiratory chain. However, it does maintain an electron membrane potential through F_0F_1-ATPase (Nolan & Voorheis, 1992; Schnaufer et al., 2005).

When living in a procyclic host, the trypanosome has a more elaborate energy and carbohydrate metabolic network (Fig. 3) that includes the mitochondrial Krebs cycle and a respiratory chain (Fig. 4) (Hannaert et al., 2003; Coustou et al., 2005). The glycosome enzyme content changes and resembles succinic fermentation in anaerobic organisms versus lactic acid fermentation favored while in the mammalian bloodstream. This shift toward succinic fermentation allows the trypanosome to require 50% less pyruvate to maintain energy production (Hannaert et al., 2003). During this stage of the life cycle, the trypanosome is able to metabolize both glucose and amino acids (mainly proline) as its energy source (Lamour et al., 2005). However, it appears that neither energy source is fully converted to CO_2 despite the presence of a fully functional Krebs cycle and respiratory chain. Instead, glucose is converted to succinate, acetate, lactate, and alanine, while proline is converted to succinate (Coustou et al., 2005).

Kinetoplast

The mitochondrion of trypanosomes is called a kinetoplast because of the unique and complex structure formed by the kinetoplast DNA (kDNA). The mitochondrial DNA in these organisms is incredibly bizarre, consisting of thousands of minicircles (1.0 kb each) and 40-50 maxicircles (23 kb) that are topologically interlocked forming a compact disk

Energy Metabolism in the Bloodstream-Long, Slender form

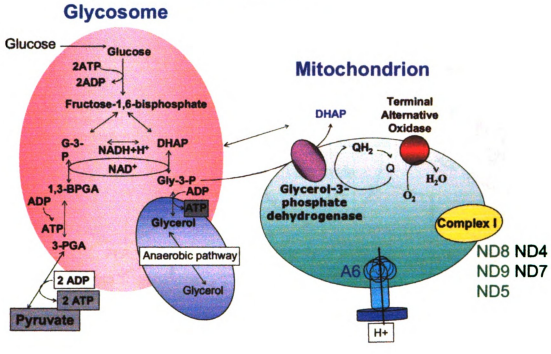

Figure 2. Diagram of energy metabolism in the mammalian host. The glycosome is a peculiar organelle that houses the first seven steps of glycolysis as well as much of the pentose phosphate pathway. During the bloodstream stage, trypanosomes use glucose as their main energy source. The glycosome is thought to act as an energy regulator to keep glycolytic intermediates from accumulating. The last three steps of glycolysis are cytoplasmic after 3-phosphoglycerate is shuttled to the cytoplasm to result in two net ATP. The mitochondrion is largely repressed; however, a putative glycerol 3-phosphate/DHAP shunt to the mitochondrion is thought to help maintain NAD+/NADH balance via glycerol 3-phosphate dehydrogenase and the terminal alternative oxidase. The transcription and editing of some of the mRNAs from Complex I of the respiratory chain are upregulated in the bloodstream stage. A F_0F_1-ATPase also maintains an electron membrane potential as well. A6 = ATPase subunit 6, BPGA = 1,3-bisphosphoglycerate, DHAP = dihydroxyacetone phosphate, G-3-P = glyceraldehydes 3-phosphate, ND = NADH dehydrogenase, 3PGA = 3-phosphoglycerate, QH2/Q = ubiquinone. Hannaert, V. *et al.* (2003) Evolution of energy metabolism and its compartmentation in Kinetoplastida. Kinetoplastid Biology and Disease. 2:11.

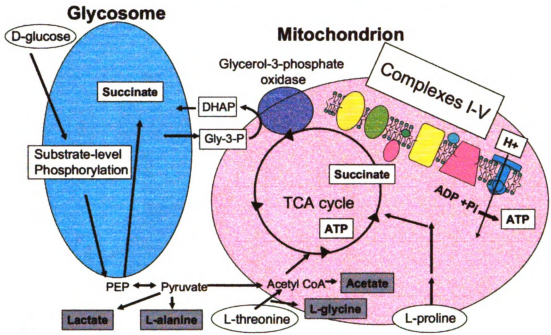

Figure 3. Diagram of energy metabolism during the procyclic stage of the life cycle. During the insect stage, the trypanosome requires a more elaborate metabolic network. The glycosome enzyme content switches to succinic fermentation similar to anaerobic organisms in order to maintain energy production in the absence of a steady glucose supply. Using the TCA cycle and respiration, the trypanosome uses amino acids (mainly proline) and any glucose available as its main energy sources. DHAP = dihydroxyacetone phosphate, Gly-3-P = glycerol 3-phosphate, PEP = phosphoenolpyruvate. Hannaert, V. *et al.* (2003) Evolution of energy metabolism and its compartmentation in Kinetoplastida. Kinetoplastid Biology and Disease. 2:11.

Figure 4

Mitochondrial Respiration Complexes
Intermembrane space
Inner mitochondrial membrane
matrix
H+
Complex I
NADH
FeS
FMN
FeS
Complex II?
?
Succinate Dehydro-genase activity
Q
Cyt c1
FeS
Cyt b_L
Cyt b_H
Complex III
Cyt c
Cyt a
Cu_A
Cyt a_3-Cu_B
Complex IV
O_2
H_2O
Alternative Oxidase
½ O_2 + 2H+
H_2O
Complex V ATP synthase
ADP +PI ⟶ ATP
Oxidative Phosphorylation

Figure 4. Diagram of the mitochondrial respiration complexes. Complexes I, III, IV, and V are present as well as the alternative oxidase. Complex II is predicted to be in trypanosome mitochondria, because a succinate dehydrogenase activity and succinate-dependent respiration are present. However, the actual proteins for the complex have not been verified. Cyt = cytochrome, Cu = copper center, H+ = proton, FeS = iron/sulfur cluster, FMN = flavin mononucleotide, NADH = Nicotinamide adenine dinucleotide in its reduced form, Q = ubiquinone. Hannaert, V. *et al.* (2003) Evolution of energy metabolism and its compartmentation in Kinetoplastida. Kinetoplastid Biology and Disease. 2:11.

structure (Lukes et al., 2002). Kinetoplast maxicircle DNA (Fig. 5A) is similar to other mitochondrial DNA in that it is circular, and encodes rRNA and some essential protein components for mitochondrial respiration. However, the majority of the mRNAs that are encoded on the maxicircle are not translatable. These mitochondrial transcripts may contain conserved frame shifts, internal stop codons, and in some cases lack start codons (Koslowsky, 2004). RNA editing in kinetoplasts is a post-transcriptional process that involves the precise insertion and deletion of uridine residues in mitochondrial messenger RNAs (mRNAs). These changes are made by several proteins that collectively form the editosome complex and are directed by a small RNA molecule called a guide RNA (gRNA). This editing process is required to make many of the mitochondrial transcripts translatable.

The first report of RNA editing showed that a frame shift in the cytochrome oxidase II gene encoded by the mitochondrial DNA was corrected in the mRNA transcript by the addition of four uridine residues (Benne et al., 1986). Uridine deletion was also found to occur (Shaw et al., 1988) during editing. Editing can repair conserved frame shifts, internal stop codons, and in some cases create the proper start codon through the precise insertion or deletion of uridines (Feagin et al., 1988b). Some mitochondrial transcripts have more than 50 percent of their reading frame added through editing (Feagin et al., 1988a).

The template for editing is provided by gRNAs that are usually encoded on minicircles (Fig. 5B) (usually 3 gRNAs per minicircle) (Sturm & Simpson, 1990). Two gRNAs are encoded on the maxicircle (Clement et al., 2004; Golden & Hajduk, 2005); one of these appears to use a novel method of *in cis* gRNA binding for RNA editing of

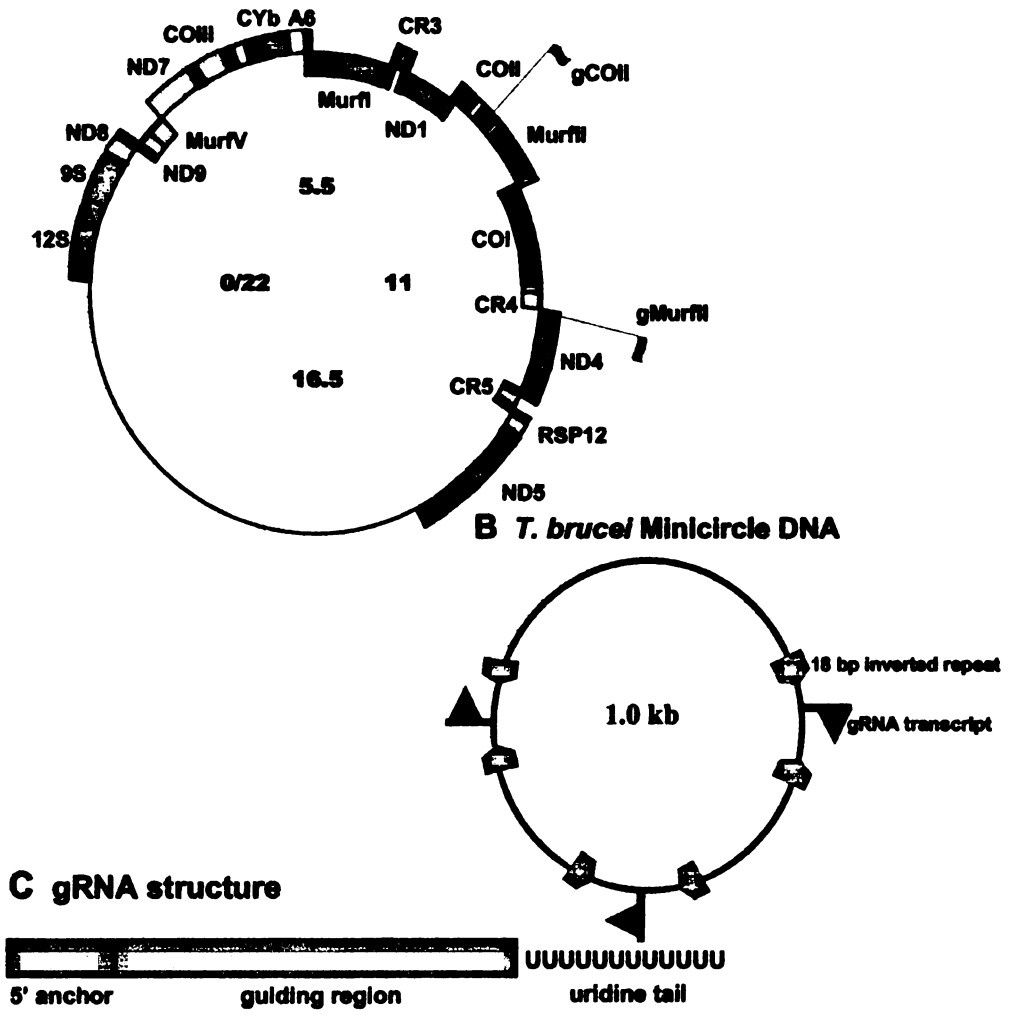

Figure 5. Maxicircle, minicircle, and gRNA diagrams. A. Maxicircle DNA resembles other eukaryotic mitochondrial DNA; it encodes rRNAs (9S and 12S) and some essential components of the mitochondrial protein respiration complexes. Many of these mitochondrial transcripts require editing before they can be translated. B. Minicircles encode ~3 gRNAs usually in between 18 bp inverted repeats. The gRNAs provide the templates for editing the mRNAs. C. A gRNA (50-70 nts) consists of 3 functional elements: an anchor sequence that is complementary to the mRNA, the guiding region provides a template for RNA editing, and a U-tail added post transcriptionally with probable multiple functions. 12S = 12S rRNA, 9S = 9S rRNA, A6 = ATPase subunit 6, CO = cytochrome oxidase, CR3 = C-rich region, CYb = apocytochrome b, Murf = Maxicircle Unidentified Reading Frame, ND = NADH dehydrogenase, RSP12 = ribosomal protein 12. Courtesy of Donna Koslowsky.

the COII transcript (Golden & Hajduk, 2005). Guide RNAs have an average length of 50-70 nts and consist of three functional elements (Fig. 5C). Contained within the 5' end of gRNAs is a short sequence known as the gRNA anchor, a 5-21 nucleotide region that base pairs with a particular mRNA just 3' of the editing domain (Blum et al., 1990). The second element, the guiding region, serves as a template for the editing process and is complementary (allowing G-U base pairs) to the mature mRNA (Blum et al., 1990). Finally, at the 3' end of the gRNA is a poly-uridylate tail (U-tail) that is added post-transcriptionally (Blum & Simpson, 1990).

Developmental Regulation of RNA Editing

Many of the proteins for energy metabolism that are made in the mitochondria are thought to be developmentally regulated by RNA editing (Table 1). Cytochrome b (CYb) and Cytochrome oxidase II (COII) are preferentially edited in the procyclic host of the *T. brucei* life cycle, while NADH dehydrogenase subunit genes 8 and 9 (ND8, ND9) are preferentially edited in the bloodstream host (Priest & Hajduk, 1994). NADH dehydrogenase subunit 7 (ND7) is fully edited in bloodstream form but only the 5' domain is edited in the insect host (Koslowsky et al., 1992). Other substrates, ATPase 6 subunit (A6) and cytochrome oxidase III (COIII), appear to have consistent levels of editing in either host (Bhat et al., 1990).

Developmental regulation of RNA editing may control mitochondrial biogenesis by only allowing production of respiratory proteins during the correct life cycle. However, very little is known concerning how editing is regulated. The gRNA transcripts, the mRNA transcripts, and the editosome protein complexes are always present

mRNA	Mitochondrial Complex/ Function	Fully Edited/Higher Levels	Higher Steady State mRNA Level
ND1	I	Never Edited	Constitutive
ND3	I	Bloodstream	Bloodstream
ND4	I	Never Edited	Bloodstream
ND5	I	Never Edited	Bloodstream
ND7	I	5'both/3'BS	Bloodstream
ND8	I	Bloodstream	Bloodstream
ND9	I	Bloodstream	Bloodstream
CYb	III	Procyclic	Procyclic
COI	IV	Never Edited	Procyclic
COII	IV	Procyclic	Procyclic
COIII	IV	Constitutive	Procyclic
A6	V	Constitutive	Constitutive
MURFI	Unknown	Never Edited	Bloodstream
MURFII	Unknown	Constitutive	Constitutive
CR3	Unknown	Bloodstream	Unknown
CR4	Unknown	Bloodstream	Unknown
RSP12	Ribosomal	Bloodstream	Bloodstream

Table 1. Regulation of the RNA editing of the *T. brucei* mRNA transcripts. Column 1: mitochondrial mRNA. Column 2: mitochondrial complex is which the protein is thought to function. Column 3: life cycle stage that the transcript is preferentially edited in. Column 4: life cycle stage where steady state level of mRNA is upregulated. The ND7 transcript is differentially edited in the two hosts; the 5' end is edited in both hosts, while the 3' end is edited in the mammalian bloodstream. 12S = 12S rRNA, 9S = 9S rRNA, A6 = ATPase subunit 6, CO = cytochrome oxidase, CR3 = C-rich region, CYb = apocytochrome b, Murf = Maxicircle Unidentified Reading Frame, ND = NADH dehydrogenase, RSP12 = ribosomal protein 12. Hajduk SL, Sabatini RS. 1998. Mitochondrial mRNA Editing in Kinetoplastid Protozoa. In: Grosjean H, Benne R, eds. Modification and Editing of RNA. Washington, D.C.: ASM Press. pp 377-411.

(Koslowsky et al., 1992; Hajduk & Sabatini, 1998). However, there may be developmentally regulated proteins that are involved in regulating RNA editing through gRNA recruitment, RNA-RNA annealing activity or chaperone activity.

Apocytochrome b

Most of my work will focus on the study of the apocytochrome b (CYb) mRNA/gRNA pair (Fig. 6). Expression of the CYb mRNA is regulated through RNA editing (Feagin et al., 1988b) and is needed for mitochondrial respiration in the insect host (Vickerman, 1965). Editing of the apocytochrome b mRNA requires the insertion of 34 uridylates at 13 sites near its 5' end (Fig. 6A). The editing process that creates the CYb initiation codon occurs preferentially during the procyclic (insect) and stumpy bloodstream stages of the trypanosome life cycle (Feagin et al., 1987; Feagin & Stuart, 1988). There are three redundant gRNAs that provide the template for initiating CYb editing (Fig. 6B) and at least one more is thought to exist for downstream editing (Riley et al., 1994). The initiating gRNA, gCYb558, directs the first seven editing events where 21 uridylates are inserted.

The Editosome

The latest model for RNA editing in trypanosomes involves >20 proteins (Table 2) that form a complex structure of proteins called the editosome around an mRNA/gRNA pair (Simpson et al., 2004; Stuart et al., 2005). The naming scheme for these 20 proteins includes kinetoplast RNA editing (KRE) at the beginning of every editosome protein name. The insertion and deletion of uridines occurs through successive rounds of enzymatic reactions. These enzymatic activities are coordinated by the editosome and

A CYb DNA aligned to edited mRNA and AA sequence:

```
     1 ---------+---------+---------+-- - -   --  - --+     -  -     42
DNA    GTTAAGAATAATGGTTATAAATTTTATATAAA A G   CG  G AGA     A  A
RNA-ed GUUAAGAAUAAUGGUUAUAAAUUUUAUAUAAAuAuGuuuCGuuGuAGAuuuuuAuuAuuu
     1 ---------+---------+---------+---------+---------+---------+  60
AA                                      M  F  R  C  R  F  L  L  F
                                      1 -  -  -  -  -  -  -  -  -     9


    43       -  -   -----   + -  --------+---------+---------+------  86
           A  A   AGAAA   G G  GTCTTTTAATGTCAGGTTGTTTATATAGAATATAT
       uuuuuAuuAuuuAGAAAuuuGuGuuGUCUUUUAAUGUCAGGUUGUUUAUAUAGAAUAUAU
    61 ---------+---------+---------+---------+---------+---------+ 120
        F  L  L  F  R  N  L  C  C  L  L  M  S  G  C  L  Y  R  I  Y
    10 +  -  -  -  -  -  -  -  -  -  -  +  -  -  -  -  -  -  -  -  -    29
```

B

CYb mRNA aligned with gCYb558:

```
5'AuAuGuuuCGuuGuAGAuuuuuAuuAuuuuuuuuAuuAuuuAGAAAuuuGuGuuGUCUUUUAAUGUCAG
                                ||:::|||||:|::||:||||||::::|||||||||||||#:|
                    gCYb-558-3'AAGGGAAAUAGUGGAUUUUUAAGUGUAACAGAAAAUUAGGG5'
```

gCYb RNA sequences aligned:

```
gCYb560A GGAGAUAGUAAAAGACAAUGUAGAUUUCUGAGUAAUGGGGAGGAUAACUACUCUCUAGGGAAGAAAAU
gCYb560B GGAGAUAGUAAAAGACAAUGUAGAUUUCUGAGUAAUAGGGAGGAUAACUACUCUCUAGGGAAGAAAAU
gCYb560C GGAGAUAGUAAAAGACAAUGUAGAUUUCUGAGUAAUGGGGGGGAUAACUACUCUCUAGGGAAGAAAAU
gCYb558  GGGAGAU--UAAAAGACAAUGUGAAUUUUUAGGUGAUAAAGGGAAUAAUUA
         .******...**************.****.*..**.**...*.*.****.**.................
```

Figure 6. A. The DNA sequence of the 5' end of the apocytochrome b gene is aligned with the 5' end of the edited RNA transcript (RNA-ed) and the amino acid sequence (AA). (A. Estevez and L. Simpson, Unpublished, http://dna.kdna.ucla.edu/trypanosome/seqs/tbcybed.map.html). The 34 uridine residues that are inserted into the 13 editing sites near the 5' end of the gene are shown in lowercase. The DNA codes for 1118 nucleotides. After editing, the mature RNA transcript is 1152 nucleotides long and codes for a protein that is 370 amino acids long. B. Part of the edited mRNA is aligned with the wild-type initiating gRNA, gCYb558. The wildtype gCYb gRNAs are aligned below the mRNA/gRNA alignment (gRNA sequences from http://biosun.bio.tu-darmstadt.de/goringer/gRNA/gRNA.html). # = mismatched sequence, ":" = GU base pair, "|" for Watson-Crick base pairing, * = matching sequence, - = gap.

Protein Name	U insertion/ deletion	Function	Functional Domains
KREPA1	Both	Interaction	1 zinc finger,1 zinc-like finger, OB fold
KREPA2	U deletion	Interaction	2 zinc finger, OB fold
KREPA3	Both	Interaction	2 zinc finger, OB fold
KREPA4	Both	Interaction	OB fold-like
KREPA5		Interaction	OB fold-like?
KREPA6	Both	Interaction	OB fold-like
KREN1	U deletion	endonuclease	U1-like zinc finger, RNaseIII, dsRBD
KREPB2	Both	endonuclease	U1-like zinc finger, RNaseIII, dsRBD
KREN2	U insertion	endonuclease	U1-like zinc finger, RNaseIII, dsRBD
KREPB4	Both	Interaction	U1-like zinc finger, RNaseIII-like, Pumilio domain
KREPB5	Both	Interaction	U1-like zinc finger, RNaseIII-like, Pumilio domain
KREPB6		Interaction	U1-like zinc finger
KREPB7	U insertion	Interaction	U1-like zinc finger
KREPB8	U deletion	Interaction	U1-like zinc finger
KREX1	U deletion	ExoUase	5'3'exonuclease, endo, exo, phosphatase
KREX2	Both?	ExoUase	5'3'exonuclease, endo, exo, phosphatase
KREL1	U deletion	RNA ligase	Ligase, tau (microtubule assoc.), kinesin light chain
KREL2	U insertion	RNA ligase	Ligase, tau (microtubule assoc.), kinesin light chain
KRET2	U insertion	TUTase	Nt. transferase domain, core, Poly(A)polymerase associated domain
KREH1	transient	helicase	Helicase
KRET1 complex			
KRET1	?	gRNA TUTase	zinc finger, poly-A polymerase catalytic and associated domains
	?		
MRP Complex			
MRP1	?	RNA matchmaking	R-rich domain
MRP2	?	RNA matchmaking	R-rich domain
Others			
RBP16	?	Interaction	cold shock domain, RGG RNA binding domain
REAP-1	?	Interaction	21 AA repeat
TbRGG1	?	Interaction	RGG RNA binding domain

Table 2. RNA editing complexes and the protein components. Column 1: name of the proteins. Column 2: involved in U insertional editing, U deletional editing, or both. Column 3: putative function. Column 4: lists the motifs found in each protein. Stuart KD, Schnaufer A, Ernst NL, Panigrahi AK. 2005. Complex management: RNA editing in trypanosomes. Trends Biochem Sci 30:97-105. Carnes J, Trotter JR, Ernst NL, Steinberg A, Stuart K. 2005. An essential RNase III insertion editing endonuclease in Trypanosoma brucei. Proc Natl Acad Sci U S A 102:16614-16619. Panigrahi AK, Ernst NL, Domingo GJ, Fleck M, Salavati R, Stuart KD. 2006. Compositionally and functionally distinct editosomes in Trypanosoma brucei. RNA 12:1038-1049.

templated by the gRNA (Blum et al., 1990; Blum & Simpson, 1990; Seiwert & Stuart, 1994; Adler & Hajduk, 1997; Simpson et al., 2004; Stuart et al., 2005). After gRNA binding, editing begins with the endonucleolytic cleavage of the pre-mRNA at the first editing site via either an insertional (KREN2) or deletional (KREN1) endonuclease containing an RNase III domain (Panigrahi et al., 2003b; Carnes et al., 2005; Trotter et al., 2005; Kang et al., 2006). Uridine residues not base paired with the gRNA are thought to be removed via an editosome U-specific 3' to 5' exonuclease (ExoUase); there are two candidate ExoUases with 5' to 3' exonuclease motifs (KREX1 and KREX2) (Aphasizhev et al., 2003a; Panigrahi et al., 2003b). KREX1 appears to be involved in U deletion; however KREX2 appears to be involved in both U insertion and U deletion and may be a "U-trimmer" (Panigrahi et al., 2006). Uridine residues are added via a terminal uridylyl transferase (TUTase) (Aphasizhev et al., 2002; Ernst et al., 2003; Panigrahi et al., 2003b). RNAi studies indicate that the most likely candidate for the editing TUTase is KRET2 (Aphasizhev et al., 2003c). A second TUTase (KRET1) is found in an independent complex and is thought to be involved in addition of the gRNA U-tail (Nebohacova et al., 2004). After uridine addition or deletion has occurred, an RNA ligase is required to ligate the two halves of the mRNA. Again, there are two RNA ligases called kinetoplast RNA editing ligase (KREL) 1 and 2 that appear to be the editing ligases (McManus et al., 2001; Panigrahi et al., 2001a; Schnaufer et al., 2001; Cruz-Reyes et al., 2002). Similar to the endonucleases and exonucleases, one ligase, KREL1, appears to be for U deletion, while the other, KREL2, appears to be for U insertion (Huang et al., 2001). However, there is some question as to how strictly these roles for the ligases in the separate U insertion or deletion complexes are upheld (Gao & Simpson, 2003). Additional protein

studies find many editosome proteins have RNA binding activities, are essential for editosome complex assembly, and appear to be involved in RNA-protein interactions and these include KREPA1-6 and KREPB4-8 (Panigrahi et al., 2001b; O'Hearn et al., 2003; Panigrahi et al., 2003a; Panigrahi et al., 2003b; Wang et al., 2003; Kang et al., 2004; Brecht et al., 2005; Salavati et al., 2006).

Significant progress has also been made in identifying proteins that appear to be accessory factors that transiently act during the editing process (Table 2) (Koller et al., 1997; Missel et al., 1997; Madison-Antenucci et al., 1998; Vanhamme et al., 1998; Hayman & Read, 1999; Aphasizhev et al., 2003b; Pelletier & Read, 2003). A few of these appear to enhance the mRNA/gRNA annealing process (Muller et al., 2001; Miller et al., 2006). The mitochondrial RNA-binding proteins (MRP), MRP1 and MRP2, are accessory factors to the editing process that are arginine rich and bind to gRNAs (Koller et al., 1997; Blom et al., 2001). Both MRP proteins co-purify in a protein complex, and when both proteins are knocked down in RNAi experiments, there are very low amounts of CYb mRNA editing (Vondruskova et al., 2005). RBP16 is a 16 kDa protein that binds U-rich sequences such as the gRNA U-tail. It contains an N-terminal cold shock domain and a C-terminal region rich in arginine and lysine residues (Hayman & Read, 1999). The *in vitro* association between RBP16 and gRNA is increased in the presence of p22, a human p32 homologue (Hayman et al., 2001). RNAi knock-down of RBP16 results in a ~98% reduction in CYb mRNA editing (Pelletier & Read, 2003).

Under electron microscopy, the editosome appears to be a structure composed of 4 protein bulges (Stuart et al., 2002). During the purification process for the editosome complex, protein complexes of various protein compositions and sizes are found to co-

exist. In 1992, Pollard et al. discovered two different complexes could be obtained through separation on glycerol gradients, a 40S complex and a 19S complex (Pollard et al., 1992). Since then, discovery of these complexes as well as others has led to new protein discoveries. These additional complexes that have been isolated by separate labs appear to have different editing capabilities, and this suggests that insertion and deletion editing could be physically and functionally separate (Goringer et al., 1994; Peris et al., 1994; Corell et al., 1996; Peris et al., 1997; Rusche et al., 1997; Cruz-Reyes et al., 1998; Stuart et al., 2002; Aphasizhev et al., 2003a; Panigrahi et al., 2003b; Schnaufer et al., 2003; Panigrahi et al., 2006). Many of the editosome proteins mentioned above appear to have evolved in pairs. It has been suggested that these pairs then insert specifically either into a U-deletion or a U-insertion complex or subcomplex. These subcomplexes may form one large complex that coordinates the entire editing process, or the editosome complexes may load and unload from the mRNA/gRNA complex during editing (Panigrahi et al., 2006).

Despite this progress, very little is known about how the editing complex is assembled onto specific RNAs. There are hundreds of different mRNA/gRNA pairs, but no conserved sequence domains have been found in mRNAs. The only conserved sequence domain shared between the gRNAs is the U-tail. Previous work in this lab suggests that different mRNA/gRNA pairs can form similar structures. Initially, computer predicted models of three separate mRNA/gRNA pairs gave three very different structures. Upon incorporating 3' crosslinking results into a secondary structure modeling program, all three mRNA/gRNA pairs formed similar structures of three helices that form around and appear to expose the first few editing sites (Leung & Koslowsky, 1999). The three

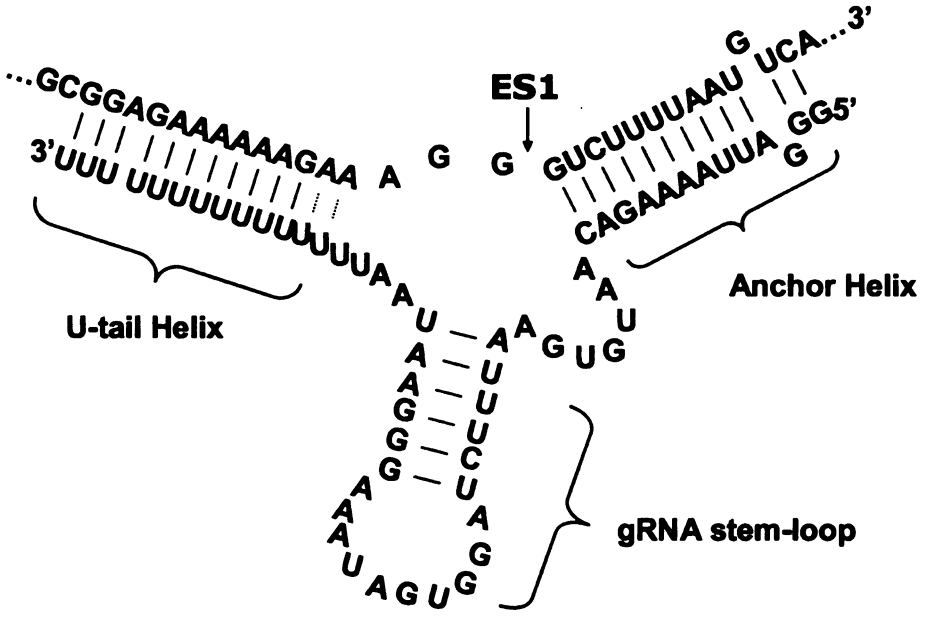

Figure 7. Diagram of the mRNA/gRNA complex. The predicted model for mRNA/gRNA complex secondary structure has three predicted helices: an mRNA/gRNA anchor helix, a gRNA stem-loop of the guiding region, and a U-tail/mRNA duplex. ES1 shows the first editing site is just 5' (mRNA) of the anchor helix.

helices consisted of a gRNA/mRNA anchor duplex, a U-tail/mRNA duplex and a gRNA stemloop (Fig. 7). Initial solution structure probing of CYb mRNA crosslinked to gCYb-558 supports this model (Leung & Koslowsky, 2001a). We believe that structure recognition of the mRNA/gRNA complex may be important for efficient editosome assembly with the mRNA/gRNA pair.

One possibility for editosome recruitment is that proteins with RNA binding sites are needed to recognize different structural elements of the mRNA/gRNA complex and that the local structure at the editing sites may determine which protein editing complex is recruited. The first step in editing is the gRNA anchor binding the mRNA anchor binding site and this anchor helix must form in order to correctly position the gRNA for efficient editing. The endonucleases of the editosome have double-stranded RNA binding domains that may target the anchor helix for binding to cleave the mRNA strand (Panigrahi et al., 2006). In addition, one of the proteins that binds RNA, KREPA4, appears to bind gRNA U-tails or U-rich sequences with a putative S1 motif similar to a cold-shock domain (Salavati et al., 2006). Proteins that prefer U-rich sequence could function as sensors to detect U's needing deletion by targeting deletion complexes to deletion sites. Additionally, there may be proteins of the editosome that bind various elements of RNA structure in order to correctly position the editosome on the complex. Discovering the structure of an mRNA/gRNA pair such as CYb may be the first step in unraveling what RNA structure attracts the editosome, and how the RNA structure changes when in contact with the editosome.

Our lab is interested in how the editosome group of proteins recognizes the mRNA/gRNA complex. There appear to be many different specialized complexes for

editing that target hundreds of different pairs of mRNA/gRNA complexes. Our lab is interested in gRNA targeting of the mRNA for binding and how this affects editing efficiency. Specifically, we are interested in the mRNA/gRNA complex interaction and understanding how the anchor sequence, U-tail, and guiding region interact with the mRNA during RNA editing. Since there appears to be no sequence homology between the many mRNAs and their gRNAs that proteins can recognize, a common structure may be what the editosome proteins recognize. We are interested in knowing what the structure of the CYb gRNA/mRNA complex is as well as what role the structure of the CYb mRNA plays in the binding affinity of the gRNA to the mRNA. We are also interested in what role the U-tail has in the mRNA/gRNA complex interaction. Additionally we would like to know what effects partial editing of the mRNA has on the gRNA/mRNA complex structure as well as the kinetics of its formation.

Other RNA-RNA Interactions

Studying other well characterized RNA-RNA interactions may aid in our understanding of this complex interaction. RNA-RNA interactions are important regulators and tools in every organism. RNA structure is critical for many RNA-RNA and RNA-protein interactions to display nucleotides in the correct orientation for efficient interaction. The versatility of RNA interactions allow organisms to control multiple processes and relies on diverse structures, mechanisms, and biological roles (Altuvia & Wagner, 2000). There appears to be some repetition in structure and method of target identification that resembles and contrasts with the gRNA/mRNA binding interaction. Here are a few well-studied examples of RNA target recognition of mRNAs that may aid in the understanding of our gRNA/mRNA interaction.

Antisense RNAs

Antisense RNA regulation in prokaryotes is one example of regulatory RNAs that use target binding to achieve post-transcriptional regulation of gene expression (Altuvia & Wagner, 2000). The studies of antisense RNAs from bacteria also elucidate ways that the structure of RNA affects target recognition and binding progression. Many antisense RNAs function as regulators of plasmid copy number in prokaryotes. Antisense RNAI binds its target RNAII to control the copy number of plasmid, ColE1. It does this by not allowing RNAII to bind the plasmid near the origin of replication where RNase H would digest RNAII to provide primers for DNA replication of ColE1 (Tomizawa et al., 1981). The RNAI-RNAII complex uses the preferred antisense target binding strategy of kissing loops. This describes the first helix nucleation event that begins when two complementary stem-loops, one or more from each RNA molecule, begin forming a helix with the two loop regions. This loop-loop interaction initiates helix formation (Tomizawa, 1984). The RNAI-RNAII kissing complex is recognized by the Rom protein that then stabilizes the complex and stops RNAII from binding the plasmid (Eguchi & Tomizawa, 1990, 1991). Most antisense RNAs present their complementary sequence in a loop structure that appears to be optimized to achieve rapid binding (Franch et al., 1999). Another antisense RNA, CopA, regulates the copy number of plasmid R1 through the translational repression of *repA*; CopA binds its target site CopT in the leader region of the *repA* mRNA. Studies of the CopA antisense RNA show that modification of loop regions and removal of bulge regions alter this RNA-RNA interaction. The bulges facilitate binding between the RNAs by acting as helix destabilizing elements in the binding intermediate structures (Hjalt & Wagner, 1995). When modifying loop regions,

disruption of a putative U-turn disrupts the structure of the loop in CopA (Slagter-Jager & Wagner, 2003) as well as sok RNA (Franch et al., 1999). The lack of U-turn inhibits binding at the nucleation site of the kissing loops, delaying formation of the stable inhibitory structure to stop translation. Rapid binding of CopA and formation of the inhibitory four helix junction is necessary to stop the ribosome from binding (Slagter-Jager & Wagner, 2003). The rate limiting step of binding of CopA to CopT is formation of the loop-loop interaction that rapidly forms an early intermediate structure. Once the kissing loops form, the probability of dissociation is small compared to conversion to the stable inhibition complex (Nordgren et al., 2001). Antisense RNAs such as ColE1, CopA, etc are efficient as inhibitors, because they have high affinity target binding (Kolb et al., 2001). These antisense RNAs do not require protein co-factors for efficient target binding. It has been postulated that the structure of these RNAs has evolved for optimal target recognition leading to plasmid copy inhibition (Kolb et al., 2001). For antisense RNAs, a fast association rate is more important than the thermodynamic stability (ΔG) between the interacting RNAs (Nordstrom & Wagner, 1994; Altuvia & Wagner, 2000). Antisense regulation requires co-transcriptional binding i.e. the antisense RNA must bind before the ribosome binds to repress translation (Altuvia & Wagner, 2000). Therefore, these antisense RNAs appear to have evolved structures that maximize the association rate.

While CopA and other antisense RNAs have been shown to bind their targets unaided, other antisense RNA interactions with their targets are mediated by a protein co-factor called Hfq. In *E. coli*, this sm-like protein was able to improve complex formation between an antisense RNA (spot42) and its mRNA target (gal) by increasing the affinity

of the anti-sense RNA for its target ~150 fold (Moller et al., 2002). It does not appear to alter the RNA structure of spot42 when bound, while it increases the affinity of the antisense RNA for its target mRNA (gal). Hfq may act as a general co-factor that facilitates RNA-RNA interactions (Moller et al., 2002). Hfq is also able to melt the structure of a target mRNA (sodB) making it accessible to RyhB, a small RNA regulator (Geissmann & Touati, 2004). Another study describes Hfq as a chaperone, because Hfq is required to facilitate the OxyS RNA-RNA interaction but is dispensable after binding has taken place (Zhang et al., 2002). There is speculation that an ancestral sm-like protein played decisive roles in the folding, binding, and functions of RNAs. Establishment of short stretches of base pairing in bimolecular RNA interactions would allow any short segment of exposed RNA to be used for target recognition (Moller et al., 2002).

miRNAs

MicroRNAs (miRNAs) also employ RNA-RNA target binding to control post-transcriptional regulation of mRNAs. Until recently, miRNAs along with other non-protein coding RNAs were considered evolutionary debris (Mattick & Makunin, 2005). However, it is becoming clear that an extensive RNA regulatory network exists in all organisms that works independently and in parallel with the protein coding system (Mattick, 2004).

MicroRNAs are ~21-25 nt RNAs made from longer hairpin precursors (primary microRNA transcripts) (Lee et al., 2003). These small RNAs target mRNAs for cleavage or translational repression (Lai, 2003) through complementarity with a ~7 bp "seed" sequence near the 5' end (Lewis et al., 2003). This seed sequence is sufficient to confer

strong regulation by the miRNA (Brennecke et al., 2005). The miRNA is separated from its complement after integration into the RNA Induced Silencing Complex (RISC) (Tomari et al., 2004; Matranga et al., 2005). The varying members of the RISC complex determine the destiny of the transcript. However, the amount of complementarity between the miRNA and the mRNA is thought to determine the fate of the mRNA through recruitment of the different RISC complexes (Hutvagner & Zamore, 2002; Tang et al., 2003).

MicroRNAs are excellent examples of mRNA regulation through target binding. The seed sequence of miRNAs is very similar to the gRNA anchor sequence. It is complementary to its target RNA and allows G-U bps. The complementarity between the gRNA and the mRNA determines the amount and type of editing of the mRNA. This correlates well with miRNAs and how the amount of miRNA complementarity to its target directs transcript cleavage or repression. The gRNA directs the editosome proteins for U addition or deletion. Studies of the editosome show that the protein content is dynamic with various editosome complexes composed of different complexes of proteins. It would appear that U addition and U deletion complexes have differing complexes of proteins (similar to RISC) suggesting alternate complexes must bind the mRNA/gRNA complex in order to complete editing (Panigrahi et al., 2006). This alternate loading of editosome complexes is directed by the gRNA; similar to the miRNA directing the loading of the proper RISC complex.

RNA-RNA conclusions

Historically, antisense RNA studies focused on RNA-RNA interactions. The studies that combine binding rate with structure changes are important first steps that laid the

groundwork for Hfq and antisense studies that were discovered later. The miRNA involvement with the mRNA mirrors the gRNA binding to its target mRNA, while loading of the RISC complexes onto the miRNA appear to be similar to the editosome complexes loading onto the mRNA/gRNA complex.

Overview

The focus of this work is on the structure and thermodynamic interaction between the CYb gRNA, gCYb-558, and its mRNA during the editing process. The many RNA-RNA examples provide ideas and templates for discovering how this interaction proceeds. The CYb interaction does not appear to copy any of these interactions, and yet elements of the interaction are similar to other RNA-RNA interactions. It will be interesting to see how this interaction compares to these examples of RNA target binding.

The structure of the CYb mRNA/gRNA pair was predicted to form three helices (Leung & Koslowsky, 1999). Solution structure probing of the unedited CYb mRNA bound to the gRNA verified two of the predicted helices (Fig. 8) (Leung & Koslowsky, 2001a). Curiously, the secondary structure predictions of two partially edited substrates, with crosslinking data incorporated, produced similar structures with the same three predicted helices. The anchor region becomes progressively longer after editing begins, and the U-tail interaction with the purine rich region becomes increasingly shorter (Fig. 8). The gRNA stem-loop was predicted to be maintained by feeding portions of the U-tail into this helix (Fig. 8) (Leung & Koslowsky, 2001b). Crosslinking data verified the 5' end (gRNA orientation) of the anchor duplex as well as the 3' position (gRNA orientation) of the U-tail. The CYb U-tail was found to interact with the same 5

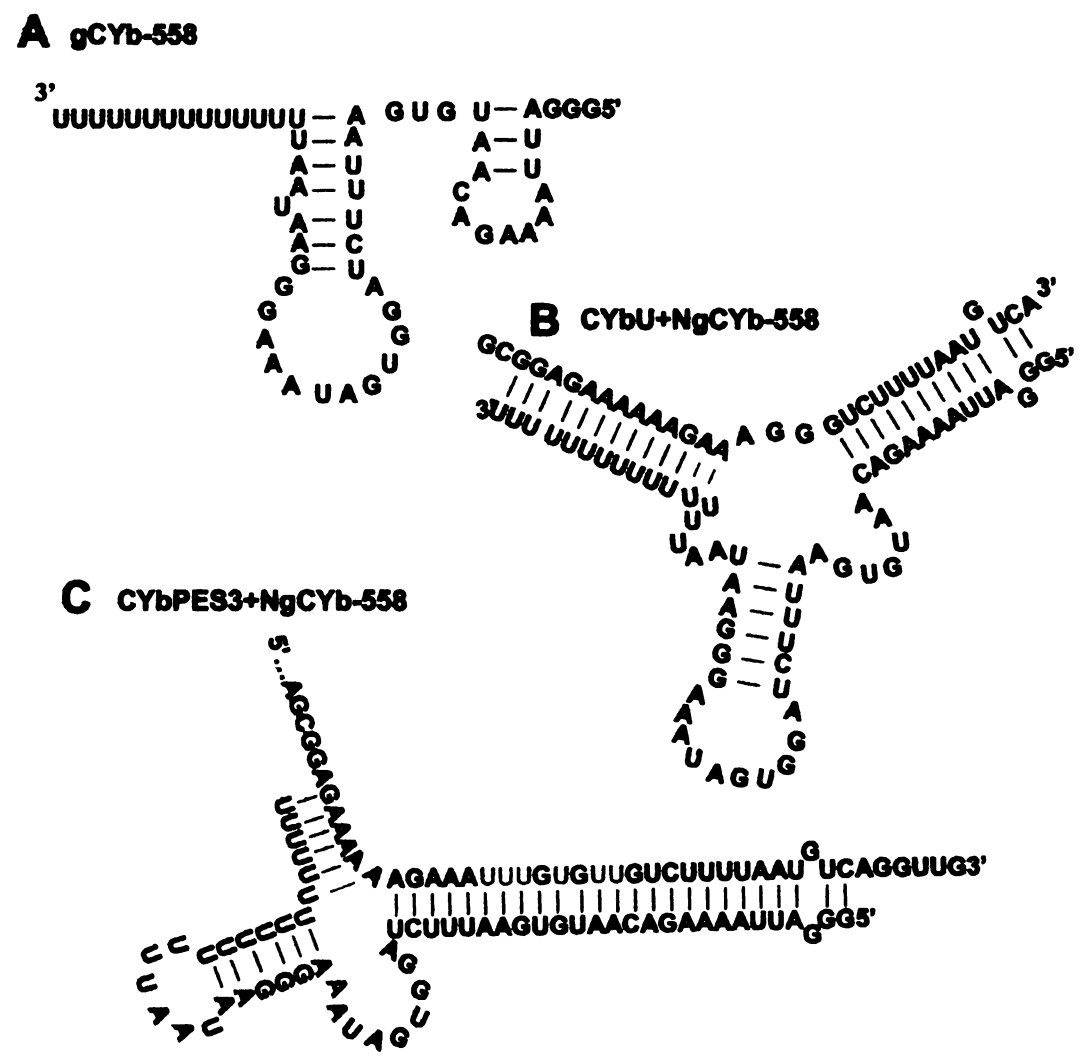

Figure 8. Predicted structures of the apocytochrome b RNAs. A. Predicted structure of gCYb-558 from Schmid, B. etal. (1995) NAR 23:3093-3102. The gRNA appears to form two loop regions. One is a small anchor loop, while the second, larger stem-loop forms in the guiding region. B. Predicted structure of 5'CYbUT+NgCYb-558 from Leung, S.S. and Koslowsky, D.J. (2001) RNA 7:1803-1816. The solution structure probing experiments prove that the mRNA is involved in two helices with the gRNA with the first few editing sites being sensitive to single-stranded specific nucleases. C. Predicted structure of 5'CYbPES3T+NgCYb-558 from Leung, S.S. and Koslowsky, D.J. (2001) NAR 29:703-709. The red U's represent uridines inserted through RNA editing and result in the anchor helix doubling in length. The 3' end of the U-tail is predicted to interact with the same region of the mRNA even after the third editing event even as the U-tail is predicted to become incorporated into the gRNA stem-loop.

nucleotides upstream of the anchor duplex when base paired with the unedited and two partially edited CYb mRNAs (Fig. 8) (Leung & Koslowsky, 1999). In chapter 2 of this thesis, the solution structure probing of the gRNA interacting with both unedited and partially edited CYb mRNAs is presented which experimentally confirms the computer predicted structures. This suggests that the formation of three helices surrounding the editing site may be an important structural feature and that the U-tail may play an important structural role. By employing an U-tail, the gRNA may increase the mRNA/gRNA complex stability, while still allowing U-tail migration within the complex during editing.

Additionally, comparisons of the thermodynamic binding affinities for two different mRNA/gRNA pairs have been investigated. The affinity of the CYb mRNA/gRNA pair was compared to the A6 mRNA/gRNA pair. The ATPase 6 subunit (A6) mRNA and its initiating gRNA, gA6-14, is used in all *in vitro* studies of editing and is constitutively edited. In contrast, the CYb mRNA is only edited in the insect and short stumpy stages of the life cycle (Feagin & Stuart, 1988) and will not undergo a full round of editing in the *in vitro* assay. The A6 mRNA/gRNA pair is predicted to have an open structure with an accessible anchor binding site, while the CYb mRNA (Fig. 9) has been shown through solution structure probing to form a stable stemloop structure that incorporates the mRNA anchor binding site within the stem (Leung & Koslowsky, 2001a). The difference in mRNA structure and accessibility of the anchor binding site is clearly reflected in the measured apparent equilibrium constants. The A6 gRNA, gA6-14, has a very high affinity for its cognate mRNA, with measured K_D's in the single digit nM range. In contrast, the CYb gRNA, gCYb-558, has a very low affinity for its cognate

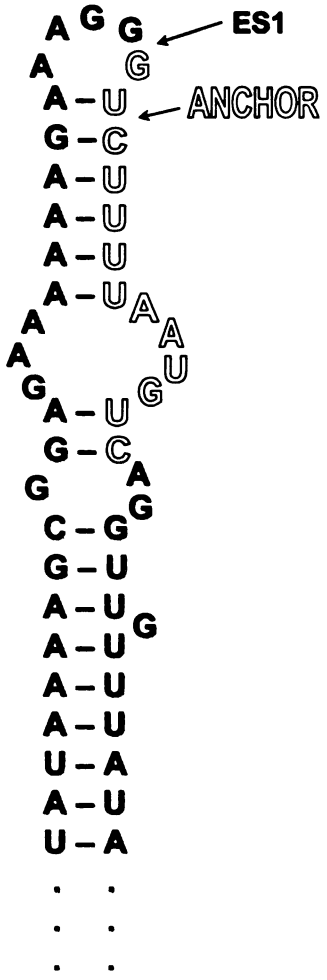

Figure 9. Predicted secondary structures of the unedited CYb mRNA. 5'CYbUT, forms a stable stem-loop with the first few editing sites positioned within the terminal loop of 5 base pairs. The hollow nucleotides represent the anchor binding site (ABS) where the gRNA anchor binds to form the mRNA/gRNA complex. ES1 = Editing site 1.

mRNA with measured K_D's in the μM range. This suggests that for efficient gRNA interaction a RNA chaperone is probably required and that the stable stem-loop formed by the CYb mRNA may be a way to regulate its editing. In chapter 3 of this dissertation, an in depth analysis using real time kinetics was used to study the thermodynamics of three different mRNA/gRNA pairs. The CYb mRNA/gRNA binding interaction is compared to two unedited mRNA/gRNA substrates that have predicted single stranded anchor binding sites (ABS) using surface plasmon resonance (SPR). The A6 and NADH dehydrogenase 7 (ND7) substrates are constitutively edited in contrast to the CYb substrate. Interestingly, the A6 and ND7 mRNAs had 2000 fold and 8400 fold higher affinity binding to their gRNAs respectively than the CYb mRNA/gRNA pair. The SPR data provides additional rate constant data. The A6 pair has a ~20 fold faster association rate and a ~20 fold slower dissociation rate than CYb. The ND7 pair has a ~90 fold faster association rate and a ~20 fold slower dissociation rate than CYb. This provides further evidence and information concerning how the mRNA structure around the immediate editing domain can strongly affect the gRNA target binding.

In chapter 4, the interaction between two partially edited CYb mRNAs and the initiating gRNA, gCYb-558, is investigated through the use of gel shift assays and surface plasmon resonance to find the dissociation constants as well as the association and dissociation rate constants. Both methods confirm that the addition of two uridines in the first editing site results in a significant decrease in the dissociation constant (K_D), while the next two editing events (+4 U's) results in an additional decrease. The binding affinity for the CYb gRNA/mRNA improves with each editing event; this suggests that with each editing event, the mRNA becomes more likely to finish editing. Surprisingly,

the presence of the U-tail appears to increase the association rate of the gRNA binding the unedited CYb mRNA. Crosslinking data shows that the U-tail binds one side of the helix that hides the anchor binding site. This suggests that the U-tail is helping disrupt the CYb mRNA stem-loop through base pairing with the upstream purine rich region. In chapter 5, I discuss the results of my research and the future directions for research on target binding between the CYb gRNA and mRNA and editosome recruitment.

Literature Cited

Adler BK, Hajduk SL. 1997. Guide RNA requirement for editing-site-specific endonucleolytic cleavage of preedited mRNA by mitochondrial ribonucleoprotein particles in Trypanosoma brucei. *Mol Cell Biol 17*:5377-5385.

Altuvia S, Wagner EG. 2000. Switching on and off with RNA. *Proc Natl Acad Sci U S A 97*:9824-9826.

Aphasizhev R, Aphasizheva I, Nelson RE, Gao G, Simpson AM, Kang X, Falick AM, Sbicego S, Simpson L. 2003a. Isolation of a U-insertion/deletion editing complex from Leishmania tarentolae mitochondria. *Embo J 22*:913-924.

Aphasizhev R, Aphasizheva I, Nelson RE, Simpson L. 2003b. A 100-kD complex of two RNA-binding proteins from mitochondria of Leishmania tarentolae catalyzes RNA annealing and interacts with several RNA editing components. *RNA 9*:62-76.

Aphasizhev R, Aphasizheva I, Simpson L. 2003c. A tale of two TUTases. *Proc Natl Acad Sci U S A.*

Aphasizhev R, Sbicego S, Peris M, Jang SH, Aphasizheva I, Simpson AM, Rivlin A, Simpson L. 2002. Trypanosome mitochondrial 3' terminal uridylyl transferase (TUTase): the key enzyme in U-insertion/deletion RNA editing. *Cell 108*:637-648.

Benne R, Van den Burg J, Brakenhoff JP, Sloof P, Van Boom JH, Tromp MC. 1986. Major transcript of the frameshifted coxII gene from trypanosome mitochondria contains four nucleotides that are not encoded in the DNA. *Cell 46*:819-826.

Bhat GJ, Koslowsky DJ, Feagin JE, Smiley BL, Stuart K. 1990. An extensively edited mitochondrial transcript in kinetoplastids encodes a protein homologous to ATPase subunit 6. *Cell 61*:885-894.

Blom D, Burg J, Breek CK, Speijer D, Muijsers AO, Benne R. 2001. Cloning and characterization of two guide RNA-binding proteins from mitochondria of Crithidia fasciculata: gBP27, a novel protein, and gBP29, the orthologue of Trypanosoma brucei gBP21. *Nucleic Acids Res 29*:2950-2962.

Blum B, Bakalara N, Simpson L. 1990. A model for RNA editing in kinetoplastid mitochondria: "guide" RNA molecules transcribed from maxicircle DNA provide the edited information. *Cell 60*:189-198.

Blum B, Simpson L. 1990. Guide RNAs in kinetoplastid mitochondria have a nonencoded 3' oligo(U) tail involved in recognition of the preedited region. *Cell 62*:391-397.

Brecht M, Niemann M, Schluter E, Muller UF, Stuart K, Goringer HU. 2005. TbMP42, a protein component of the RNA editing complex in African trypanosomes, has endo-exoribonuclease activity. *Mol Cell 17*:621-630.

Brennecke J, Stark A, Russell RB, Cohen SM. 2005. Principles of microRNA-target recognition. *PLoS Biol 3*:e85.

Brown HW, Neva FA. 1983. Ch. 4: Blood and Tissue Protozoa of Man. *Basic Clinical Parasitology*. Norwalk, CT: Appleton Century Croft. pp 45-53.

Brown RC, Evans DA, Vickerman K. 1973. Changes in oxidative metabolism and ultrastructure accompanying differentiation of the mitochondrion in Trypanosoma brucei. *Int J Parasitol 3*:691-704.

Carnes J, Trotter JR, Ernst NL, Steinberg A, Stuart K. 2005. An essential RNase III insertion editing endonuclease in Trypanosoma brucei. *Proc Natl Acad Sci U S A 102*:16614-16619.

Clement SL, Mingler MK, Koslowsky DJ. 2004. An intragenic guide RNA location suggests a complex mechanism for mitochondrial gene expression in Trypanosoma brucei. *Eukaryot Cell 3*:862-869.

Corell RA, Read LK, Riley GR, Nellissery JK, Allen TE, Kable ML, Wachal MD, Seiwert SD, Myler PJ, Stuart KD. 1996. Complexes from Trypanosoma brucei that exhibit deletion editing and other editing-associated properties. *Mol Cell Biol 16*:1410-1418.

Coustou V, Besteiro S, Riviere L, Biran M, Biteau N, Franconi JM, Boshart M, Baltz T, Bringaud F. 2005. A mitochondrial NADH-dependent fumarate reductase involved in the production of succinate excreted by procyclic Trypanosoma brucei. *J Biol Chem 280*:16559-16570.

Cruz-Reyes J, Rusche LN, Sollner-Webb B. 1998. Trypanosoma brucei U insertion and U deletion activities co-purify with an enzymatic editing complex but are differentially optimized. *Nucleic Acids Res 26*:3634-3639.

Cruz-Reyes J, Zhelonkina AG, Huang CE, Sollner-Webb B. 2002. Distinct functions of two RNA ligases in active Trypanosoma brucei RNA editing complexes. *Mol Cell Biol 22*:4652-4660.

Eguchi Y, Tomizawa J. 1990. Complex formed by complementary RNA stem-loops and its stabilization by a protein: function of ColE1 Rom protein. *Cell 60*:199-209.

Eguchi Y, Tomizawa J. 1991. Complexes formed by complementary RNA stem-loops. Their formations, structures and interaction with ColE1 Rom protein. *J Mol Biol 220*:831-842.

Ernst NL, Panicucci B, Igo RP, Jr., Panigrahi AK, Salavati R, Stuart K. 2003. TbMP57 is a 3' terminal uridylyl transferase (TUTase) of the Trypanosoma brucei editosome. *Mol Cell 11*:1525-1536.

Feagin JE, Abraham JM, Stuart K. 1988a. Extensive editing of the cytochrome c oxidase III transcript in Trypanosoma brucei. *Cell 53*:413-422.

Feagin JE, Jasmer DP, Stuart K. 1987. Developmentally regulated addition of nucleotides within apocytochrome b transcripts in Trypanosoma brucei. *Cell 49*:337-345.

Feagin JE, Shaw JM, Simpson L, Stuart K. 1988b. Creation of AUG initiation codons by addition of uridines within cytochrome b transcripts of kinetoplastids. *Proc Natl Acad Sci U S A 85*:539-543.

Feagin JE, Stuart K. 1988. Developmental aspects of uridine addition within mitochondrial transcripts of Trypanosoma brucei. *Mol Cell Biol 8*:1259-1265.

Franch T, Petersen M, Wagner EG, Jacobsen JP, Gerdes K. 1999. Antisense RNA regulation in prokaryotes: rapid RNA/RNA interaction facilitated by a general U-turn loop structure. *J Mol Biol 294*:1115-1125.

Gao G, Simpson L. 2003. Is the Trypanosoma brucei REL1 RNA ligase specific for U-deletion RNA editing, and is the REL2 RNA ligase specific for U-insertion editing? *J Biol Chem 278*:27570-27574.

Geissmann TA, Touati D. 2004. Hfq, a new chaperoning role: binding to messenger RNA determines access for small RNA regulator. *Embo J 23*:396-405.

Golden DE, Hajduk SL. 2005. The 3'-untranslated region of cytochrome oxidase II mRNA functions in RNA editing of African trypanosomes exclusively as a cis guide RNA. *RNA 11*:29-37.

Goringer HU, Koslowsky DJ, Morales TH, Stuart K. 1994. The formation of mitochondrial ribonucleoprotein complexes involving guide RNA molecules in Trypanosoma brucei. *Proc Natl Acad Sci U S A 91*:1776-1780.

Hajduk SL, Sabatini RS. 1998. Mitochondrial mRNA Editing in Kinetoplastid Protozoa. In: Grosjean H, Benne R, eds. *Modification and Editing of RNA*. Washington, D.C.: ASM Press. pp 377-411.

Hannaert V, Bringaud F, Opperdoes FR, Michels PA. 2003. Evolution of energy metabolism and its compartmentation in Kinetoplastida. *Kinetoplastid Biol Dis 2*:11.

Hayman ML, Miller MM, Chandler DM, Goulah CC, Read LK. 2001. The trypanosome homolog of human p32 interacts with RBP16 and stimulates its gRNA binding activity. *Nucleic Acids Res 29*:5216-5225.

Hayman ML, Read LK. 1999. Trypanosoma brucei RBP16 is a mitochondrial Y-box family protein with guide RNA binding activity. *J Biol Chem 274*:12067-12074.

Hjalt TA, Wagner EG. 1995. Bulged-out nucleotides in an antisense RNA are required for rapid target RNA binding in vitro and inhibition in vivo. *Nucleic Acids Res 23*:580-587.

Huang CE, Cruz-Reyes J, Zhelonkina AG, O'Hearn S, Wirtz E, Sollner-Webb B. 2001. Roles for ligases in the RNA editing complex of Trypanosoma brucei: band IV is needed for U-deletion and RNA repair. *Embo J 20*:4694-4703.

Hutvagner G, Zamore PD. 2002. A microRNA in a multiple-turnover RNAi enzyme complex. *Science 297*:2056-2060.

Kang X, Falick AM, Nelson RE, Gao G, Rogers K, Aphasizhev R, Simpson L. 2004. Disruption of the zinc finger motifs in the Leishmania tarentolae LC-4 (=TbMP63) L-complex editing protein affects the stability of the L-complex. *J Biol Chem 279*:3893-3899.

Kang X, Gao G, Rogers K, Falick AM, Zhou S, Simpson L. 2006. Reconstitution of full-round uridine-deletion RNA editing with three recombinant proteins. *Proc Natl Acad Sci U S A*.

Kolb FA, Westhof E, Ehresmann C, Ehresmann B, Wagner EG, Romby P. 2001. Bulged residues promote the progression of a loop-loop interaction to a stable and inhibitory antisense-target RNA complex. *Nucleic Acids Res 29*:3145-3153.

Koller J, Muller UF, Schmid B, Missel A, Kruft V, Stuart K, Goringer HU. 1997. Trypanosoma brucei gBP21. An arginine-rich mitochondrial protein that binds to guide RNA with high affinity. *J Biol Chem 272*:3749-3757.

Koslowsky DJ. 2004. A historical perspective on RNA editing: how the peculiar and bizarre became mainstream. *Methods Mol Biol 265*:161-197.

Koslowsky DJ, Riley GR, Feagin JE, Stuart K. 1992. Guide RNAs for transcripts with developmentally regulated RNA editing are present in both life cycle stages of Trypanosoma brucei. *Mol Cell Biol 12*:2043-2049.

Kuzoe FAS, Schofield CJ. 2004. Strategic review of traps and targets for tsetse and African trypanosomiasis control. *Special programme for research and training in tropical diseases (TDR)*. Geneva: UNICEF/UNDP/World Bank/WHO, http://www.who.int/tdr/publications/publications/tsetse_traps.htm.

Lai EC. 2003. microRNAs: runts of the genome assert themselves. *Curr Biol 13*:R925-936.

Lamour N, Riviere L, Coustou V, Coombs GH, Barrett MP, Bringaud F. 2005. Proline metabolism in procyclic Trypanosoma brucei is down-regulated in the presence of glucose. *J Biol Chem 280*:11902-11910.

Lee Y, Ahn C, Han J, Choi H, Kim J, Yim J, Lee J, Provost P, Radmark O, Kim S, Kim VN. 2003. The nuclear RNase III Drosha initiates microRNA processing. *Nature 425*:415-419.

Leung SS, Koslowsky DJ. 1999. Mapping contacts between gRNA and mRNA in trypanosome RNA editing. *Nucleic Acids Res 27*:778-787.

Leung SS, Koslowsky DJ. 2001a. Interactions of mRNAs and gRNAs involved in trypanosome mitochondrial RNA editing: structure probing of an mRNA bound to its cognate gRNA. *RNA 7*:1803-1816.

Leung SS, Koslowsky DJ. 2001b. RNA editing in Trypanosoma brucei: characterization of gRNA U-tail interactions with partially edited mRNA substrates. *Nucleic Acids Res 29*:703-709.

Lewis BP, Shih IH, Jones-Rhoades MW, Bartel DP, Burge CB. 2003. Prediction of mammalian microRNA targets. *Cell 115*:787-798.

Lukes J, Guilbride DL, Votypka J, Zikova A, Benne R, Englund PT. 2002. Kinetoplast DNA network: evolution of an improbable structure. *Eukaryot Cell 1*:495-502.

Madison-Antenucci S, Sabatini RS, Pollard VW, Hajduk SL. 1998. Kinetoplastid RNA-editing-associated protein 1 (REAP-1): a novel editing complex protein with repetitive domains. *Embo J 17*:6368-6376.

Matranga C, Tomari Y, Shin C, Bartel DP, Zamore PD. 2005. Passenger-strand cleavage facilitates assembly of siRNA into Ago2-containing RNAi enzyme complexes. *Cell 123*:607-620.

Matthews KR. 2005. The developmental cell biology of Trypanosoma brucei. *J Cell Sci 118*:283-290.

Mattick JS. 2004. RNA regulation: a new genetics? *Nat Rev Genet 5*:316-323.

Mattick JS, Makunin IV. 2005. Small regulatory RNAs in mammals. *Hum Mol Genet 14 Spec No 1*:R121-132.

Mattock N, Pink R. 2003-2004. Making health research work for poor people. *WHO Tropical Disease Research 17th Annual Progress Report.*
Geneva: UNICEF/UNDP/World Bank/WHO,
http://www.who.int/tdr/publications/publications/pr17.htm.

McManus MT, Shimamura M, Grams J, Hajduk SL. 2001. Identification of candidate mitochondrial RNA editing ligases from Trypanosoma brucei. *RNA 7*:167-175.

Michels PA, Hannaert V, Bringaud F. 2000. Metabolic aspects of glycosomes in trypanosomatidae - new data and views. *Parasitol Today 16*:482-489.

Miller MM, Halbig K, Cruz-Reyes J, Read LK. 2006. RBP16 stimulates trypanosome RNA editing in vitro at an early step in the editing reaction. *RNA 12*:1292-1303.

Missel A, Souza AE, Norskau G, Goringer HU. 1997. Disruption of a gene encoding a novel mitochondrial DEAD-box protein in Trypanosoma brucei affects edited mRNAs. *Mol Cell Biol 17*:4895-4903.

Moller T, Franch T, Hojrup P, Keene DR, Bachinger HP, Brennan RG, Valentin-Hansen P. 2002. Hfq: a bacterial Sm-like protein that mediates RNA-RNA interaction. *Mol Cell 9*:23-30.

Muller UF, Lambert L, Goringer HU. 2001. Annealing of RNA editing substrates facilitated by guide RNA-binding protein gBP21. *Embo J 20*:1394-1404.

Nebohacova M, Maslov DA, Falick AM, Simpson L. 2004. The effect of RNA interference Down-regulation of RNA editing 3'-terminal uridylyl transferase (TUTase) 1 on mitochondrial de novo protein synthesis and stability of respiratory complexes in Trypanosoma brucei. *J Biol Chem 279*:7819-7825.

Nolan DP, Voorheis HP. 1992. The mitochondrion in bloodstream forms of Trypanosoma brucei is energized by the electrogenic pumping of protons catalysed by the F1F0-ATPase. *Eur J Biochem 209*:207-216.

Nordgren S, Slagter-Jager JG, Wagner GH. 2001. Real time kinetic studies of the interaction between folded antisense and target RNAs using surface plasmon resonance. *J Mol Biol 310*:1125-1134.

Nordstrom K, Wagner EG. 1994. Kinetic aspects of control of plasmid replication by antisense RNA. *Trends Biochem Sci 19*:294-300.

O'Hearn SF, Huang CE, Hemann M, Zhelonkina A, Sollner-Webb B. 2003. Trypanosoma brucei RNA editing complex: band II is structurally critical and maintains band V ligase, which is nonessential. *Mol Cell Biol 23*:7909-7919.

Panigrahi AK, Allen TE, Stuart K, Haynes PA, Gygi SP. 2003a. Mass spectrometric analysis of the editosome and other multiprotein complexes in Trypanosoma brucei. *J Am Soc Mass Spectrom 14*:728-735.

Panigrahi AK, Ernst NL, Domingo GJ, Fleck M, Salavati R, Stuart KD. 2006. Compositionally and functionally distinct editosomes in Trypanosoma brucei. *RNA 12*:1038-1049.

Panigrahi AK, Gygi SP, Ernst NL, Igo RP, Jr., Palazzo SS, Schnaufer A, Weston DS, Carmean N, Salavati R, Aebersold R, Stuart KD. 2001a. Association of two novel

proteins, TbMP52 and TbMP48, with the Trypanosoma brucei RNA editing complex. *Mol Cell Biol 21*:380-389.

Panigrahi AK, Schnaufer A, Carmean N, Igo RP, Jr., Gygi SP, Ernst NL, Palazzo SS, Weston DS, Aebersold R, Salavati R, Stuart KD. 2001b. Four related proteins of the Trypanosoma brucei RNA editing complex. *Mol Cell Biol 21*:6833-6840.

Panigrahi AK, Schnaufer A, Ernst NL, Wang B, Carmean N, Salavati R, Stuart K. 2003b. Identification of novel components of Trypanosoma brucei editosomes. *RNA 9*:484-492.

Pelletier M, Read LK. 2003. RBP16 is a multifunctional gene regulatory protein involved in editing and stabilization of specific mitochondrial mRNAs in Trypanosoma brucei. *RNA 9*:457-468.

Peris M, Frech GC, Simpson AM, Bringaud F, Byrne E, Bakker A, Simpson L. 1994. Characterization of two classes of ribonucleoprotein complexes possibly involved in RNA editing from Leishmania tarentolae mitochondria. *Embo J 13*:1664-1672.

Peris M, Simpson AM, Grunstein J, Liliental JE, Frech GC, Simpson L. 1997. Native gel analysis of ribonucleoprotein complexes from a Leishmania tarentolae mitochondrial extract. *Mol Biochem Parasitol 85*:9-24.

Pollard VW, Harris ME, Hajduk SL. 1992. Native mRNA editing complexes from Trypanosoma brucei mitochondria. *Embo J 11*:4429-4438.

Priest JW, Hajduk SL. 1994. Developmental regulation of Trypanosoma brucei cytochrome c reductase during bloodstream to procyclic differentiation. *Mol Biochem Parasitol 65*:291-304.

Riley GR, Corell RA, Stuart K. 1994. Multiple guide RNAs for identical editing of Trypanosoma brucei apocytochrome b mRNA have an unusual minicircle location and are developmentally regulated. *J Biol Chem 269*:6101-6108.

Rusche LN, Cruz-Reyes J, Piller KJ, Sollner-Webb B. 1997. Purification of a functional enzymatic editing complex from Trypanosoma brucei mitochondria. *Embo J 16*:4069-4081.

Salavati R, Ernst NL, O'Rear J, Gilliam T, Tarun S, Jr., Stuart K. 2006. KREPA4, an RNA binding protein essential for editosome integrity and survival of Trypanosoma brucei. *RNA 12*:819-831.

Schnaufer A, Clark-Walker GD, Steinberg AG, Stuart K. 2005. The F1-ATP synthase complex in bloodstream stage trypanosomes has an unusual and essential function. *Embo J 24*:4029-4040.

Schnaufer A, Ernst NL, Palazzo SS, O'Rear J, Salavati R, Stuart K. 2003. Separate insertion and deletion subcomplexes of the Trypanosoma brucei RNA editing complex. *Mol Cell 12*:307-319.

Schnaufer A, Panigrahi AK, Panicucci B, Igo RP, Jr., Wirtz E, Salavati R, Stuart K. 2001. An RNA ligase essential for RNA editing and survival of the bloodstream form of Trypanosoma brucei. *Science 291*:2159-2162.

Seiwert SD, Stuart K. 1994. RNA editing: transfer of genetic information from gRNA to precursor mRNA in vitro. *Science 266*:114-117.

Shaw JM, Feagin JE, Stuart K, Simpson L. 1988. Editing of kinetoplastid mitochondrial mRNAs by uridine addition and deletion generates conserved amino acid sequences and AUG initiation codons. *Cell 53*:401-411.

Simpson L, Aphasizhev R, Gao G, Kang X. 2004. Mitochondrial proteins and complexes in Leishmania and Trypanosoma involved in U-insertion/deletion RNA editing. *RNA 10*:159-170.

Slagter-Jager JG, Wagner EG. 2003. Loop swapping in an antisense RNA/target RNA pair changes directionality of helix progression. *J Biol Chem 278*:35558-35563.

Stuart K, Panigrahi AK, Schnaufer A, Drozdz M, Clayton C, Salavati R. 2002. Composition of the editing complex of Trypanosoma brucei. *Philos Trans R Soc Lond B Biol Sci 357*:71-79.

Stuart KD, Schnaufer A, Ernst NL, Panigrahi AK. 2005. Complex management: RNA editing in trypanosomes. *Trends Biochem Sci 30*:97-105.

Sturm NR, Simpson L. 1990. Kinetoplast DNA minicircles encode guide RNAs for editing of cytochrome oxidase subunit III mRNA. *Cell 61*:879-884.

Tang G, Reinhart BJ, Bartel DP, Zamore PD. 2003. A biochemical framework for RNA silencing in plants. *Genes Dev 17*:49-63.

Tomari Y, Matranga C, Haley B, Martinez N, Zamore PD. 2004. A protein sensor for siRNA asymmetry. *Science 306*:1377-1380.

Tomizawa J. 1984. Control of ColE1 plasmid replication: the process of binding of RNA I to the primer transcript. *Cell 38*:861-870.

Tomizawa J, Itoh T, Selzer G, Som T. 1981. Inhibition of ColE1 RNA primer formation by a plasmid-specified small RNA. *Proc Natl Acad Sci U S A 78*:1421-1425.

Trotter JR, Ernst NL, Carnes J, Panicucci B, Stuart K. 2005. A deletion site editing endonuclease in Trypanosoma brucei. *Mol Cell 20*:403-412.

Unisci. 2001. Artificial cow helps to eradicate sleeping sickness. In: Radler D, ed. *Daily University Science News*: UniScience News Net, Inc.

Vanhamme L, Perez-Morga D, Marchal C, Speijer D, Lambert L, Geuskens M, Alexandre S, Ismaili N, Goringer U, Benne R, Pays E. 1998. Trypanosoma brucei TBRGG1, a mitochondrial oligo(U)-binding protein that co-localizes with an in vitro RNA editing activity. *J Biol Chem 273*:21825-21833.

Vickerman K. 1965. Polymorphism and mitochondrial activity in sleeping sickness trypanosomes. *Nature 208*:762-766.

Vickerman K. 1985. Developmental cycles and biology of pathogenic trypanosomes. *Br Med Bull 41*:105-114.

Vondruskova E, van den Burg J, Zikova A, Ernst NL, Stuart K, Benne R, Lukes J. 2005. RNA interference analyses suggest a transcript-specific regulatory role for mitochondrial RNA-binding proteins MRP1 and MRP2 in RNA editing and other RNA processing in Trypanosoma brucei. *J Biol Chem 280*:2429-2438.

Wang B, Ernst NL, Palazzo SS, Panigrahi AK, Salavati R, Stuart K. 2003. TbMP44 Is Essential for RNA Editing and Structural Integrity of the Editosome in Trypanosoma brucei. *Eukaryot Cell 2*:578-587.

WHO. 2001. African trypanosomiasis or sleeping sickness. *Fact Sheet 259*: World Health Organization.

Zhang A, Wassarman KM, Ortega J, Steven AC, Storz G. 2002. The Sm-like Hfq protein increases OxyS RNA interaction with target mRNAs. *Mol Cell 9*:11-22.

CHAPTER 2
INTERACTIONS OF MRNAS AND GRNAS INVOLVED IN TRYPANOSOME MITOCHONDRIAL RNA EDITING: STRUCTURE PROBING OF A GRNA BOUND TO ITS COGNATE MRNA

(Portions of this chapter were previously published in RNA (2006) 12:1-11.)

Introduction

In kinetoplastid protozoa, guide RNAs (gRNAs) serve as templates for the precise insertion and deletion of uridylates during RNA editing of the mitochondrial mRNA transcripts. This post-transcriptional process produces translatable mRNAs by creating the open reading frames as well as initiation and termination signals. In addition, there is a transcript-specific mechanism that regulates editing during the life cycle of the parasite. The gRNAs are key components of the reaction as they provide the information for the nucleotide (nt) alterations and direct the cleavage and ligation events (Simpson et al., 2004; Stuart et al., 2005). Guide RNAs have an average length of 50-70 nts and consist of three functional elements. Contained within the 5' end of gRNAs is a short sequence known as the gRNA anchor, a 5-21 nucleotide region that base pairs with a particular mRNA just 3' of the editing domain. The second element, the guiding region, serves as a template for the editing process and is complementary (allowing G-U base pairs) to the mature mRNA. Finally, at the 3' end of the gRNA is a poly-uridylate tail (U-tail) that is added post-transcriptionally (Blum et al., 1990; Blum & Simpson, 1990).

The latest model for RNA editing in trypanosomes involves >20 proteins that form a complex structure called the editosome around an mRNA/gRNA pair (Simpson et al., 2004; Stuart et al., 2005). The insertion and deletion of uridines occur through successive rounds of enzymatic reactions coordinated by the editosome and templated by the gRNA (Blum et al., 1990; Blum & Simpson, 1990; Seiwert & Stuart, 1994; Adler & Hajduk, 1997). Significant progress has been made in identifying proteins involved in the editing reaction, including both proteins in the complex as well as proteins that appear to be accessory factors that transiently act during the editing process (Koller et al., 1997;

Missel et al., 1997; Madison-Antenucci et al., 1998; Vanhamme et al., 1998; Hayman & Read, 1999; Aphasizhev & Simpson, 2001; McManus et al., 2001; Panigrahi et al., 2001a; Panigrahi et al., 2001b; Rusche et al., 2001; Schnaufer et al., 2001; Aphasizhev et al., 2003a; Aphasizhev et al., 2003b; Panigrahi et al., 2003a; Panigrahi et al., 2003b; Pelletier & Read, 2003). However, despite this progress, very little is known about how the editing complex is assembled onto specific RNAs. No conserved sequence domains have been found in mRNAs, and the only conserved sequence domain shared between the gRNAs is the U-tail. Previous work in this lab suggests that different mRNA/gRNA pairs can form similar structures (Leung & Koslowsky, 1999), and we believe that structure recognition may be important for efficient editosome assembly with the mRNA/gRNA pair.

In previous studies, we used a RNA folding program to look for conserved structures between three different mRNA/gRNA pairs. The predicted secondary structures for these mRNA/gRNA pairings incorporated a distance constraint based on photoaffinity crosslinks (Leung & Koslowsky, 1999). Further structure analyses for the *apocytochrome b* mRNA/gRNA complex were undertaken to look at mRNA/gRNA structure as editing progresses up through the third editing site. The predicted secondary structures for these mRNA/gRNA pairings are based on photoaffinity crosslinking studies of the 5' and 3' ends of NgCYb-558 that were mapped along 5'CYbUT (first 88 nts. of CYb mRNA), 5'CYbPES1T (edited through site 1), and 5' CYbPES3T (edited through site 3) (Leung & Koslowsky, 2001b). In addition, a solution structure probing study of 5'CYbUT while paired with NgCYb-558 or NgCYb-558sU (no U-tail) was done (Leung & Koslowsky, 2001a). With the data from these studies, we proposed a secondary

structure model that includes the following features: a gRNA/mRNA anchor helix, a U-tail/mRNA helix, and a gRNA stem-loop (Fig. 11A) (Leung & Koslowsky, 1999, 2001a, b). The predicted structure of the gRNA interaction with the partially edited mRNA was particularly interesting because it suggests that the U-tail could function to maintain the gRNA stem-loop during the first few editing events (Fig. 11B). The focus of this paper is on the solution structure probing of the secondary structure of the gRNA, NgCYb-558, paired with unedited and partially edited mRNAs, as we would like to understand how the gRNA structure may be changing during the early steps of the editing process. In addition, we have also probed the structure of the partially edited mRNA, CYbPES3, to corroborate our gRNA structure data. Our data indicate that the stem-loop formed by the guiding region of the gRNA alone is maintained in its interaction with the pre-edited message as predicted in the computer models. In addition, our data support the predicted structure for the gRNA interaction with its partially edited mRNA in that the gRNA stem-loop structure appears to be maintained through the first few editing events by the use of alternative base pairing with the U-tail.

Results and Discussion

Crosslinked RNAs used for Solution Structure Probing

Editing of the *apocytochrome b* mRNA is developmentally regulated with the insertion of 34 uridylates at 13 sites near its 5' end. The editing process that creates the CYb initiation codon occurs preferentially during the procyclic (insect) and stumpy bloodstream stages of the trypanosome life cycle (Feagin et al., 1987; Feagin & Stuart, 1988). In these experiments, we used modified versions of 5'CYbUT (Koslowsky et al., 1992; Koslowsky et al., 1996). CYbU (U = unedited) is identical in sequence to

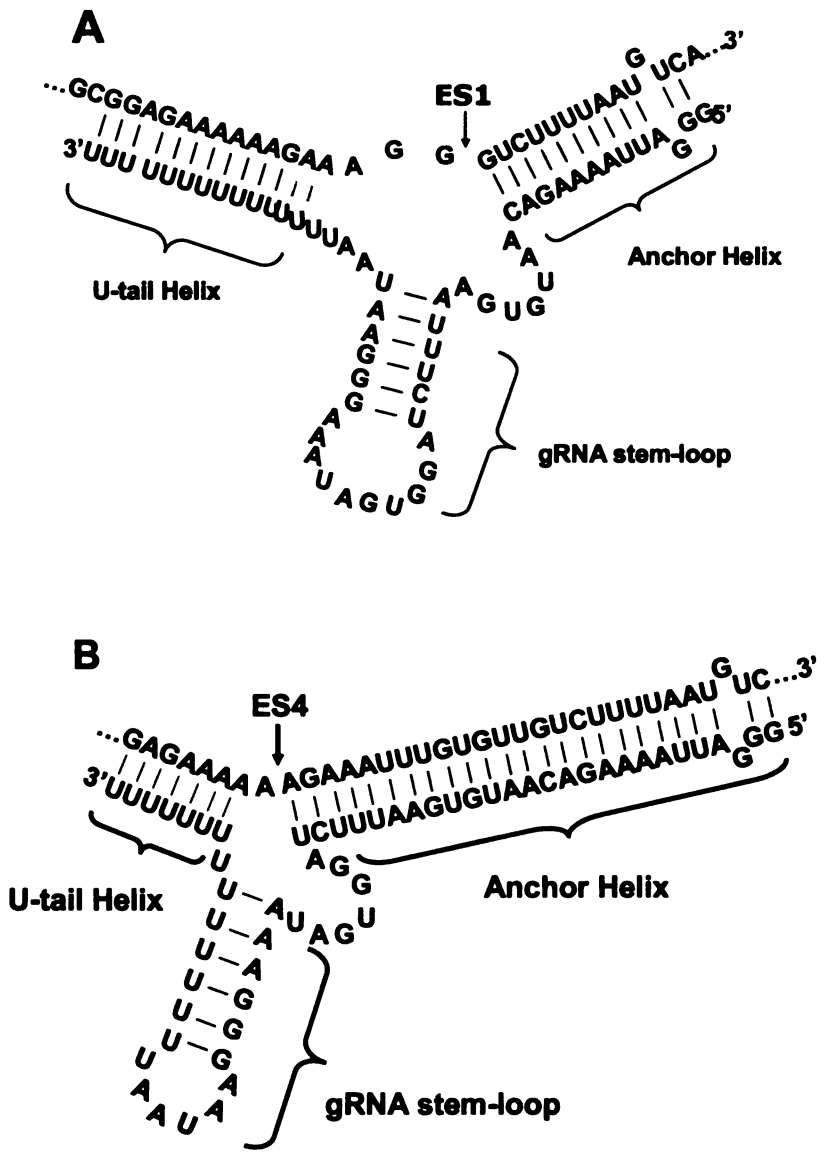

Figure 10. The predicted models for mRNA/gRNA complex secondary structure have three helices: a mRNA/gRNA anchor helix, a gRNA stem-loop within the guiding region, and an U-tail/mRNA duplex. A. CYbU-NgCYb-558 pair with the first editing site just 5' (mRNA) of the anchor indicated by ES1. B. CYbPES3-NgCYb-558 pair with the fourth editing site just 5' (mRNA) of the anchor indicated by ES4.

5'CYbUT except for the deletion of 12 nts at the 5'most end (Fig. 11A) and is composed of 88 nts from the 5' end of the *apocytochrome b* mRNA (beginning at +13) including all 13 editing sites as well as a 24 nt vector tag at the 3' end. The partially edited substrate, CYbPES3 (PES = Partially Edited through Site 3), is identical to CYbU except for the 6 uridines added so that the first 3 editing sites are fully edited (Fig. 11B). Our gRNA construct NgCYb-558 (Fig. 11C) is very similar to wildtype gCYb-558 and two other redundant gRNAs, gCYb560A, B. All three gRNAs can act as the editing initiating gRNA that direct the editing of the first seven editing sites (Riley et al., 1994). NgCYb-558 is 59 nucleotides long including a 15 nt uridylate-tail (U-tail) that is added via ligation with T4 DNA ligase and a bridging deoxyoligonucleotide (Moore & Sharp, 1992; Leung & Koslowsky, 2001a).

The secondary structure of gCYb-558 was reported by Schmid et al. (1995) and described as two thermodynamically unstable hairpin loops separated by a single-stranded region. The smaller hairpin at the 5' end contains the anchor binding sequence that selects the mRNA for editing. The guiding region forms a longer stem-loop and the U-tail appears to be single-stranded (Schmid et al., 1995). The sequence of the gRNA used in this study differs slightly from the gCYb-558 used in the Schmid et al. study. One significant difference is that a cytosine residue replaces a uridine at position 25, a nucleotide change also seen in wild type gCYb-560A, B (Fig. 11C). This U to C change creates a strong G-C base pair within the guiding region that appears to stabilize a single gRNA stem-loop that differs slightly from the Schmid et al. (1995) report.

In order to determine the structure of the gRNA in its interaction with its cognate mRNA, we used solution structure probing techniques and 3' end labeled gRNAs that

A

5'CYbUSh Sequence (mRNA transcript):

GGUUAUAAAUUUUAUAUAAAAGCGGAGAAAAAAGAAAGGGUCUUUUAAUGUCAGGUUGUUUAUAUAGAAUAUAUGG*auccacuaguucua gagcggcc*

5'CYbUSh aligned to NgCYb-558:

```
----------------GGUUAUAAAUUUUAUAUAAAAGCGGAGAAAAAAGAAAGGGUCUUUUAAUGUCAGGUUGUUUAUAUAGAAUAUAUGG
-------------------------------------------------------||||||||||#:|
NgCYb-558UUUUUUUUUUUUUUUUAAUAAGGGAAAUAGUGGAUCUUUAAGUGUAACAGAAAAUUAGGG
```

B

5'CYbPES3Sh Sequence (mRNA transcript):

GGUUAUAAAUUUUAUAUAAAAGCGGAGAAAAAAGAAAuuuGuGuuGUCUUUUAAUGUCAGGUUGUUUAUAUAGAAUAUAUGG*auccacua guucuagagcggcc*

5'CYbPES3Sh aligned to NgCYb-558:

```
----------GGUUAUAAAUUUUAUAUAAAAGCGGAGAAAAAAGAAAuuuGuGuuGUCUUUUAAUGUCAGGUUGUUUAUAUAGAAUAUAUGG
-----------------------------------------|||||||::::|||||||||||||#:|
NgCYb-558-UUUUUUUUUUUUUUUUAAUAAGGGAAAUAGUGGAUCUUUAAGUGUAACAGAAAAUUAGGG
```

C

New-gCYb558 sequence:

```
New-gCYb558-5'GGG--AUUAAAAGACAAUGUGAAUUUCUAGGUGAUAAAGGGAAUAAUUAUUUUUUUUUUUUUUU
gCYb558-----5'GGGAGAUUAAAAGACAAUGUGAAUUUUUAGGUGAUAAAGGGAAUAA---UUUUUUUUUUUUUUU
gCYb[560A]-5'GGAGAUAGUAAAAGACAAUGUAGAUUUCUGAGUAAUGGGGAGGAUAACUACUCUCUAGGGAAGAAAAUUUUUUUUUUUUUUUU
           .*.**...**************..****.*..**.**...*.*.****.....................
```

Figure 11. Sequence and alignment of the gRNA/mRNA substrate pairs. **A.** The full CYbU (U = unedited) transcript and CYbU aligned to NgCYb-558 is shown. CYbU is composed of 88 nts from the 5' end of the *apocytochrome b* mRNA (beginning at +13) including all 13 editing sites as well as a 24 nt vector tag at the 3' end. **B.** The CYbPES3 (PES = Partially Edited through Site 3) transcript and CYbPES3 aligned to NgCYb-558 is shown. The partially edited mRNA, CYbPES3, is identical to CYbU except for the 6 uridines (lowercase u's) added so that the first 3 editing sites are fully edited. The complementarity between the gRNA and mRNA in the anchor duplex (bold) is shown with # = mismatched sequence, ":" = GU base pair, "|" for Watson-Crick base pairing. Arrow indicates the position of the introduced crosslink. **C.** The NgCYb-558 sequence aligned with wild type initiating CYb gRNAs, gCYb-558 and gCYb[560A] sequences. NgCYb-558 is 59 nucleotides long including a 15 nt uridylate-tail (U-tail) and has 4 nt differences compared to wild type gCYb-558. * = matching sequence, - = gap. C_{25}, according to NgCYb-558, is bold and underlined in all the gRNAs.

had been crosslinked to the cognate mRNA at the 3' end of the anchor duplex (mRNA orientation). It has been previously shown that these structures can assemble with enzymatically-active editing proteins and are biologically relevant (Leung & Koslowsky, 2001a).

Crosslinked substrates were generated by transcribing gRNAs in the presence of guanosine 5'-monophosphorothioate (GMPS) (Burgin & Pace, 1990; Harris & Christian, 1999). The gRNAs were 3'end labeled using T4 RNA ligase and [5'-^{32}P] cytidine 3', 5'-bisphosphate (pCp) when probing the gRNA; the mRNAs were 5' end labeled using T4 Kinase and [γ ^{32}P] rATP, when probing the mRNA structure. After labeling, the thiol group of GMPS at the 5' end of the gRNA was coupled to azidophenacyl bromide (APA) and UV crosslinked as previously described (Burgin & Pace, 1990; Leung & Koslowsky, 1999). The resultant crosslink is covalently linked to the mRNA at the 3' end (mRNA orientation) of the gRNA/mRNA anchor duplex (Fig. 11A, B). Therefore, these crosslinked RNAs maintain the anchor duplex, an element required for the process of editing. The higher order structure of NgCYb-558 crosslinked to its cognate mRNA was probed using ribonuclease accessibility experiments (Fig. 12). Single-stranded, non-stacked conformations were monitored using ribonucleases T1 (G specific), T2 (slight preference for A), and Mung Bean Nuclease (MBN) (slight preference for A). RNase V1 was used to determine nucleotides involved in base paired helical interactions or in stacked, structured elements (Lowman & Draper, 1986). For comparative purposes, an analysis of the structure of the free NgCYb-558 was compared to the structure of the

Figure 12

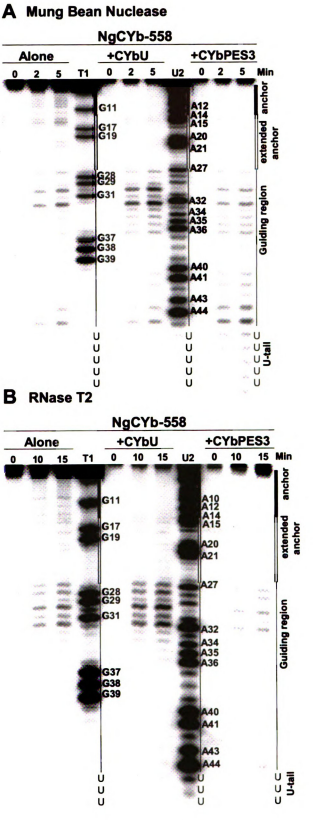
A Mung Bean Nuclease
NgCYb-558
Alone
+CYbU
+CYbPES3
0 2 5 T1 0 2 5 U2 0 2 5 Min
G11
G17
G19
G28
G29
G31
G37
G38
G39
A12
A14
A15
A20
A21
A27
A32
A34
A35
A36
A40
A41
A43
A44
extended anchor
anchor
Guiding region
U-tail
B RNase T2
NgCYb-558
Alone
+CYbU
+CYbPES3
0 10 15 T1 0 10 15 U2 0 10 15 Min
G11
G17
G19
G28
G29
G31
G37
G38
G39
A10
A12
A14
A15
A20
A21
A27
A32
A34
A35
A36
A40
A41
A43
A44
anchor
extended anchor
Guiding region
U-tail

Figure 12 continued

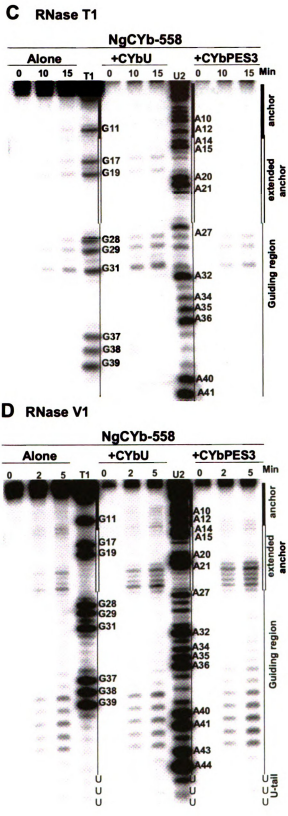

Figure 12. Structure Probing of the gRNA, NgCYb-558. Each solution structure probing gel has three sections showing the digestion pattern of NgCYb-558 alone, NgCYb-558 crosslinked to CYbU (+CYbU), and NgCYb-558 crosslinked to CYbPES3 (+CYbPES3). Digestion times in minutes are shown at the top. RNase T1 and U2 ladders with nt numbers are indicated. A line diagram indicating the anchor (bold line), extended anchor (double line), guiding region (thin line), and U-tail of the gRNA is shown next to each digestion pattern. **A**. Mung Bean Nuclease gel, single-strand specific. **B**. RNase T2, single-strand. **C**. RNase T1, single-strand guanosine specific. **D**. RNase V1, double-strand specific.

gRNA crosslinked to either unedited CYb (CYbU) or to a partially edited CYb (CYbPES3). In addition, to complement the gRNA data, the structure of CYbPES3 crosslinked to both NgCYb-558 and NgCYb-558sU (NgCYb-558 lacking a U-tail) was also examined. The mRNA secondary structure was probed by both ribonuclease accessibility and chemical reactivity (diethyl pyrocarbonate (A, N7)) (Fig. 13, 14). The data were used to construct secondary structure models with the data summarized in Figure 15. In the summary figures the intensity of the cut is represented by large or small symbols for each enzyme or chemical. The high intensity cleavages (large symbols) represent hot spots that are unprotected by secondary and tertiary interactions. Cleavages of medium and low intensity were harder to classify and may include both sites where tertiary structure incompletely blocks access and some secondary cuts that are not reflective of the native structure (small symbols). In addition, the lower intensity cleavages could be due to alternative structures formed by a small percentage of the RNA population. However these cleavages appeared consistently in all gels.

Structure of the NgCYb-558 anchor region

Structure probing of unpaired NgCYb-558 by single-strand specific nucleases indicates that the anchor region (G1-C13) is mostly single-stranded (Fig. 12). Under our conditions (100 mM KCl and 1mM $MgCl_2$) distinct cleavage products were clearly visible in the anchor region using Mung Bean Nuclease (MBN), RNase T2 (T2), and RNase T1 (T1). As expected, when the gRNA was crosslinked to its cognate mRNA (+CYbU and +CYbPES3), the anchor-duplex formed and was no longer sensitive to the single-strand specific RNases. The RNase V1 (V1) sensitivity pattern generally complemented these data. We did observe two V1 cleavages in the unpaired gRNA at

Figure 13

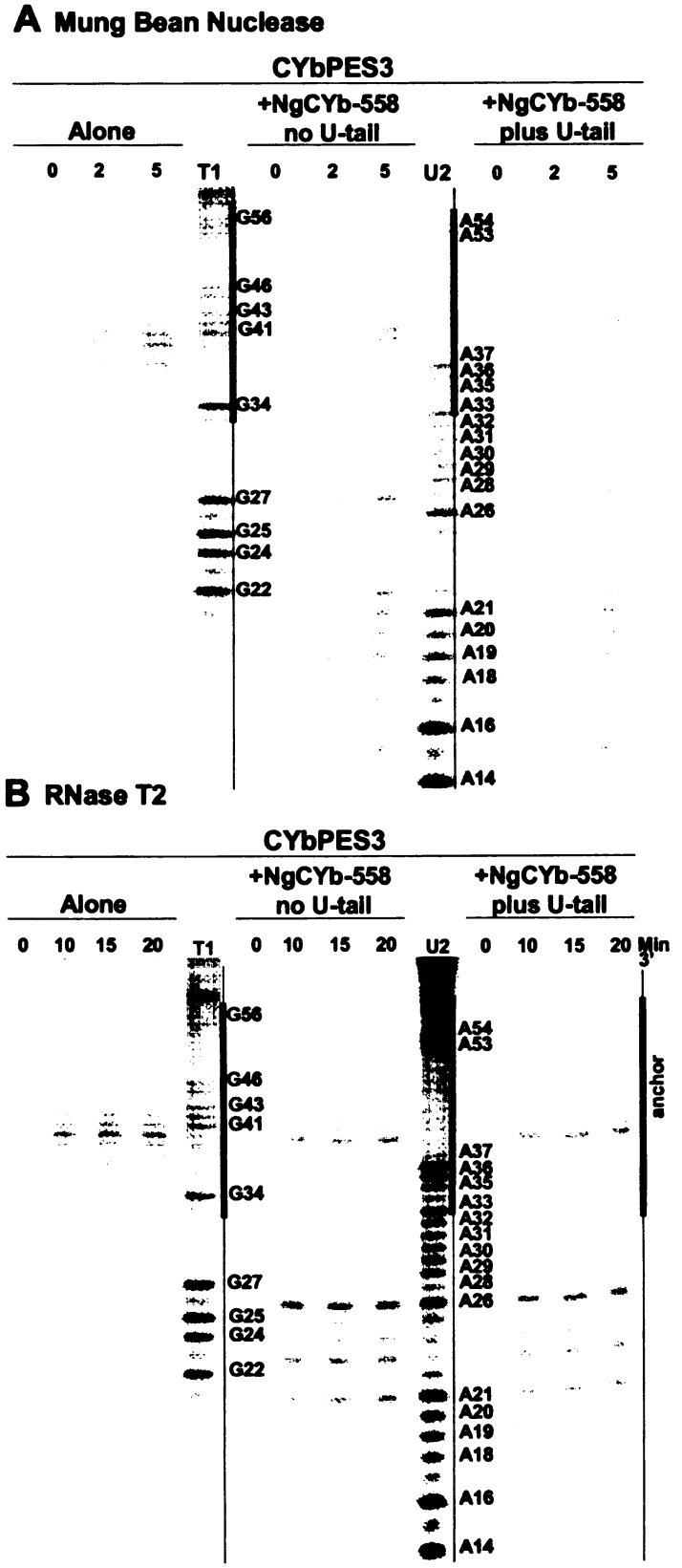
A Mung Bean Nuclease
CYbPES3
Alone
+NgCYb-558 no U-tail
+NgCYb-558 plus U-tail
0 2 5
T1
0 2 5
U2
0 2 5
G56
G46
G43
G41
G34
G27
G25
G24
G22
A54
A53
A37
A36
A35
A33
A32
A31
A30
A29
A28
A26
A21
A20
A19
A18
A16
A14
B RNase T2
CYbPES3
Alone
+NgCYb-558 no U-tail
+NgCYb-558 plus U-tail
0 10 15 20
T1
0 10 15 20
U2
0 10 15 20 Min
3'
anchor
G56
G46
G43
G41
G34
G27
G25
G24
G22
A54
A53
A37
A36
A35
A33
A32
A31
A30
A29
A28
A26
A21
A20
A19
A18
A16
A14

Figure 13 continued

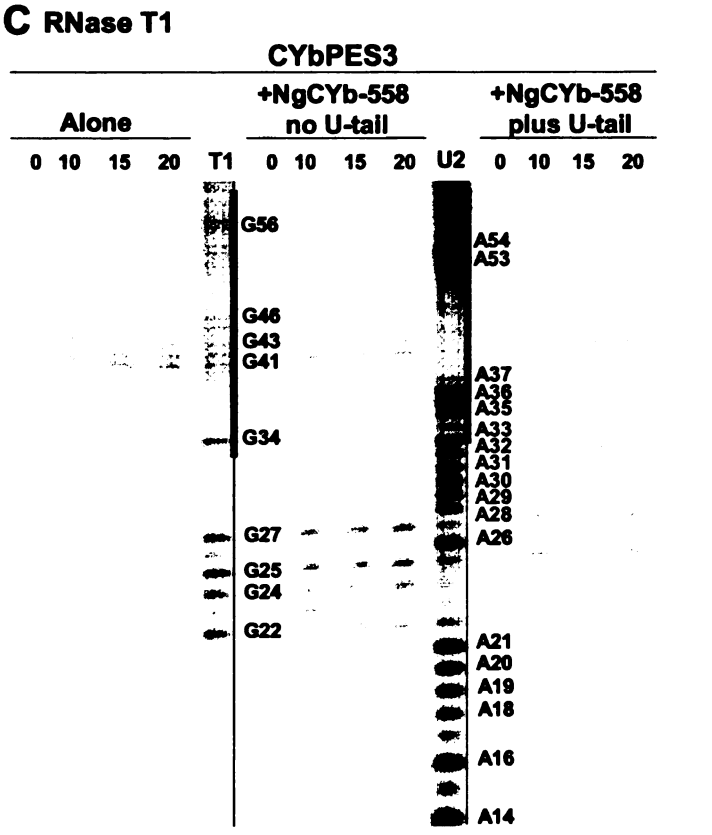

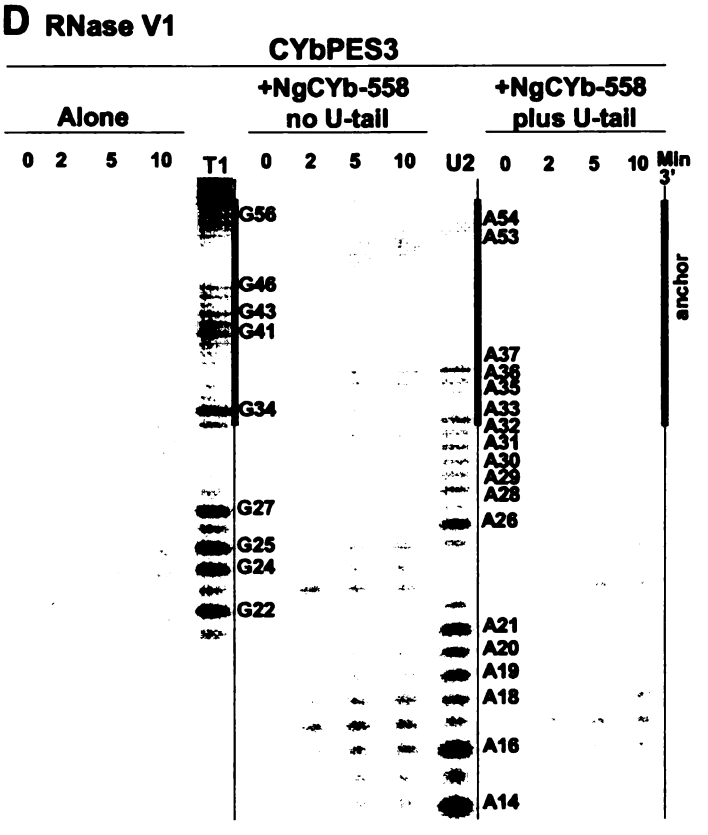

Figure 13. Structure Probing of the partially edited CYb mRNA, CYbPES3. Each solution structure probing gel has three sections showing the digestion pattern of CYbPES3 alone, CYbPES3 crosslinked to NgCYb-558sU (no U-tail), and CYbPES3 crosslinked to NgCYb-558. Digestion times in minutes are shown at the top. RNase T1 and U2 ladders with nt numbers are indicated. A diagram of the mRNA is next to each digestion pattern showing the orientation 3' to 5' with the extended anchor (bold line). **A.** Mung Bean Nuclease gel, single-strand specific **B.** RNase T2, single-strand. **C.** RNase T1, single-strand guanosine specific. **D.** RNase V1, double-strand specific.

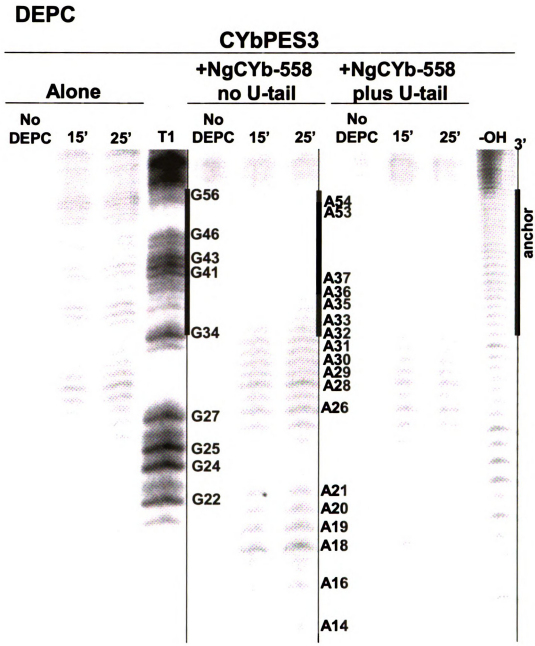

Figure 14. Chemical structure probing of the partially edited CYb mRNA, CYbPES3. The diethyl pyrocarbonate (DEPC) chemical structure probing gel has three sections showing the difference in digestion pattern of CYbPES3 alone, CYbPES3 crosslinked to NgCYb-558sU (no U-tail), and CYbPES3 crosslinked to NgCYb-558. Digestion times in minutes are shown at the top. RNase T1 and U2 ladders with nt numbers are indicated; an alkaline hydrolysis ladder (OH-) was included as well. A diagram of the mRNA is next to each digestion pattern showing the orientation 3' to 5' with the extended anchor (bold line).

Figure 15

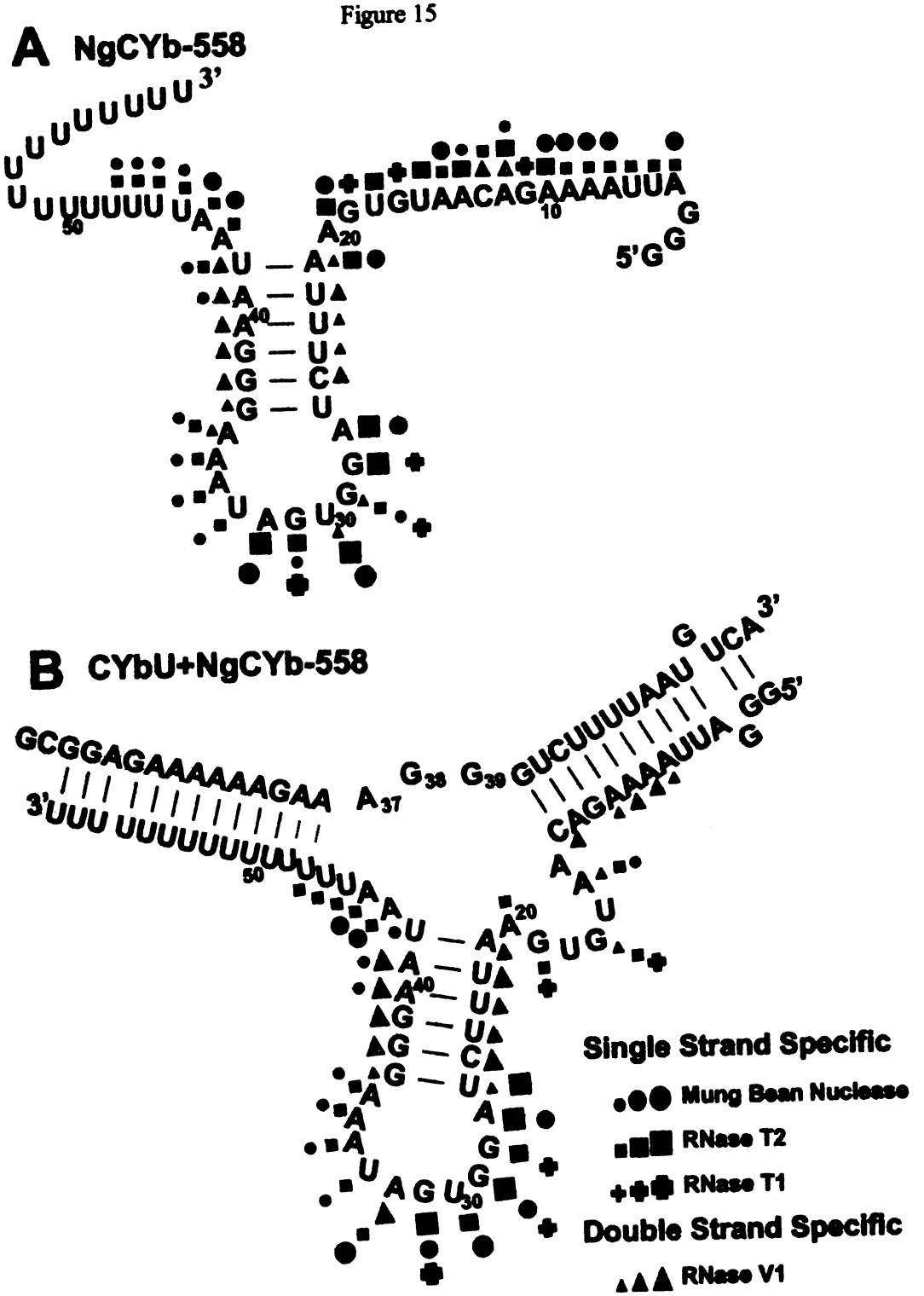
A NgCYb-558
B CYbU+NgCYb-558
Single Strand Specific
Mung Bean Nuclease
RNase T2
RNase T1
Double Strand Specific
RNase V1

Figure 15 continued

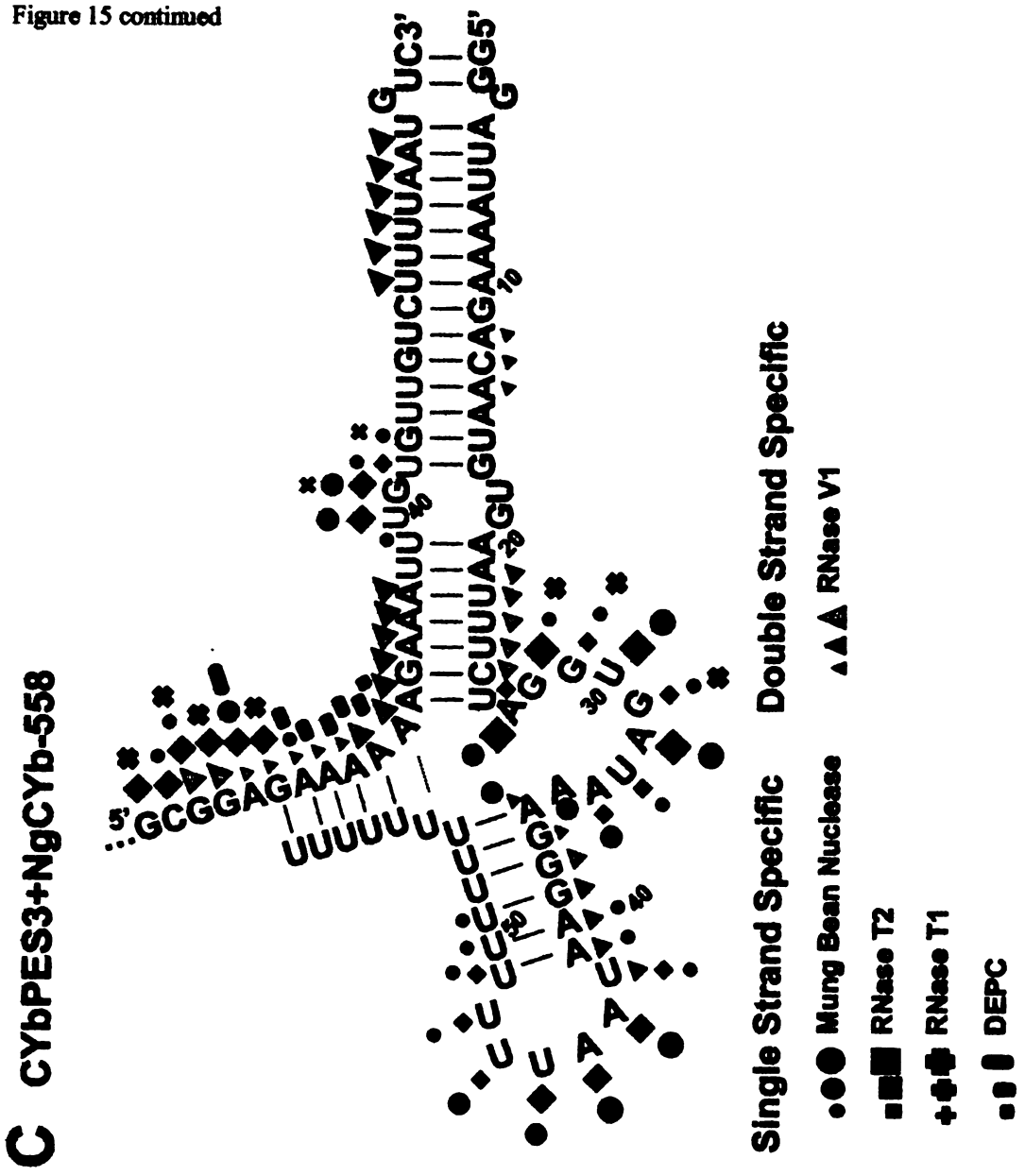

Figure 15. Summary figures from solution structure probing gels that show predicted secondary structures with cleavages from all 4 nucleases and DEPC chemical. Three sizes of symbols indicate the intensity of cleavage. Circles indicate mung bean nuclease (single-strand specific) cleavages, squares indicate RNase T2 (single-strand specific) cleavages, crosses indicate RNase T1 (single-strand guanosine specific) cleavages, cylinders indicate DEPC (single-strand adenosine specific), and triangles indicate RNase V1 (double-strand specific) cleavages. **A.** NgCYb-558 alone **B.** CYbU/NgCYb-558 complex **C.** CYbPES3/NgCYb-558 complex. The red U's represent the uridylates added during editing.

positions A12 and C13 (Fig. 12D), located near the end of the anchor region that were also sensitive to the single-strand specific nucleases.

While V1 sensitive cleavages were clearly visible within the anchor duplex of the paired gRNA (+CYbU, Fig. 12) and within the extended anchor duplex (+CYbPES3, Fig. 12), it was interesting that the cleavages were concentrated in the 5' half (mRNA orientation) of the anchor duplex. Lack of cleavage in the G1-A7 region may be due to the presence of the crosslink. For NgCYb-558 paired with CYbU, V1 cleavages within the anchor were surprisingly weak and limited to A8-C13 (Fig. 12D). This region was also very poorly cleaved in the NgCYb-558/CYbPES3 pairing, where the anchor is extended to U26. In this extended anchor, strong V1 cleavages were observed in the 3' most end of the duplex (A21-U26, Fig. 12D). The limitation of strong RNase V1 cleavage to the A21-U26 region of the extended anchor duplex was unexpected and suggests that most of the anchor duplex may be protected by tertiary interactions.

Structure of NgCYb-558 guiding region

Secondary structure analyses of several unpaired gRNAs indicate that the guiding regions (nucleotides between the 5' anchor and 3' U-tail) form a gRNA stem-loop element (Schmid et al., 1995). In our digests of unpaired NgCYb-558, we also observe the presence of a gRNA stem-loop (Fig. 15). Weak but consistent single-strand specific cleavages at nts A14-A20 indicate that the area adjacent to the anchor (containing the template for the first few editing sites) is single-stranded until nt A21 (Fig. 12). Distinct cleavages using the single-strand specific RNases were also observed for nts A27-A36. The lack of single-stranded specific cleavages in the U22-U26 and G37-G39 flanking regions and weak cleavages of A41 to U42 suggested that the U22-U42 region base pairs

to the G37-U42 region and forms a stem with a large 10 nt terminal loop (A27-A36) (Fig. 12). The presence of this stem-loop is confirmed by the pattern of V1 sensitive cleavages of nts U22-26 and nts G37-U42 (Fig. 12D). When the gRNA was paired with the unedited mRNA (+CYbU) or the partially edited CYbPES3, the patterns of nuclease cleavages for the guiding region were almost identical to those observed in the gRNA alone (Fig. 12). This was particularly surprising for the NgCYb-558/CYbPES3 pair, as the anchor duplex has doubled in length (26 bp vs 13 bp) and has incorporated the U22-U26 5'-stem region from our gRNA stem-loop. All three gRNA structures (gRNA alone, paired with CYbU and paired with CYbPES3) showed a pattern of single-strand RNase sensitivity in the A27-A36 region flanked by RNase V1 sensitivity in the A21-U26 and G38-A42 regions (Figs. 12, 15). While the RNase cleavage patterns of the guiding region were very similar, we did see some consistent differences. For the NgCYb-558/CYbU pair, weak but consistent MBN and RNase T2 cleavage sensitivity could be seen in the A15 to U18. In addition, both G17 and G19 are accessible to RNase T1, suggesting the presence of a 5-6 nt bulge between the anchor duplex and the gRNA guiding region stem (Fig. 12A, B, C). The corresponding region is completely protected when the gRNA is paired with CYbPES3 as would be expected with the extension of the anchor duplex to U26. The NgCYb-558 paired to CYbPES3 also showed a subtle difference in the pattern of RNase V1 cleavage in the A21-U26 region (Fig. 12). Both the gRNA alone and gRNA paired with unedited CYb had stronger RNase V1 cleavages at U22 and C25 when these nts are forming the initial gRNA stem-loop. When the gRNA is paired with CYbPES3 and nts U22 and C25 have become part of the anchor duplex, the U22 V1 cleavage appears to be intense, while the other sites in this region had

relatively equal cleavage intensities (Fig. 12D). We also observed a slight increase in the RNase V1 sensitivity in the U33-G37 region for the gRNA when paired to CYbPES3 (Fig. 12D, panel 3). In addition, the single-strand specific cleavages in the A27-A36 region were consistently less intense for the gRNA when paired with CYbPES3 (Fig. 12). The cleavage patterns of the gRNA were incorporated into summary figures based on computer modeling of the predicted secondary structure of the gRNA alone (Fig. 15A) as well as the mRNA/gRNA complex with both unedited and partially edited mRNA (Fig 15B, C). Our cleavage patterns support the computer predicted models and illustrate the change in gRNA structure produced by editing of the mRNA. The unpaired gRNA forms a gRNA stem-loop that is maintained when the gRNA pairs with the pre-edited mRNA (Fig. 15A, B). Editing of the first three sites extends the anchor duplex by 13 bp, incorporating one side of the gRNA stem into the anchor helix. The nucleotides that were located within the terminal loop remain single-stranded, but are now located within a bulge region between the anchor duplex and the new gRNA stem-loop. However, a new gRNA stem-loop is formed by alternative base pairing of A36-A41 with part of the U-tail (Fig. 15C).

Structure of CYbPES3

In order to corroborate the structure of the gRNA interaction with the partially edited CYbPES3, we also probed the secondary structure of CYbPES3. For comparative purposes, we investigated the structure of CYbPES3 alone as well as its structure when paired with NgCYb-558 with and without the U-tail. In previous work, the structure of the unedited CYb mRNA alone was found to be a strongly base paired stem-loop with the first three editing sites contained in a terminal 5 nt loop (A35-U41) (Leung &

Koslowsky, 2001a). Editing of the first three sites, appears to add an additional 6 uridines to the terminal loop, but otherwise does not significantly change the structure found within the stem region (Figs. 13, 14, 16). This is shown (Figs. 13, 14) by MBN (U42-A36), T2 (U42-U38), and T1 (G41, G43) cleavages within the terminal loop (Fig. 13, 16). RNase V1 data complements the data from the single-stranded nucleases (Fig.13D, 16).

The structure of CYbPES3 crosslinked to its cognate gRNA (NgCYb-558) was much more difficult to interpret. Pairing of the partially edited mRNA with its gRNA clearly changed the structure of the mRNA, making it much more susceptible to the single-strand specific nucleases (Fig. 13). Interestingly, while the anchor duplex region was mostly protected, we did observe distinct cleavages in the U39-G43 regions for all three single-strand specific nucleases (Fig. 13). This corresponds to a run of four G:U base pairs within the anchor duplex created by the second and third RNA editing events. Within this region, the RNase V1 analyses did complement the single-strand specific nucleases with distinct V1 cleavages localized in two regions flanking the U39-G43 region; A33-A37 and U47-A54. No corresponding single-strand nuclease sensitivity was observed when probing the gRNA; however, this region was also protected in our RNase V1 analyses suggesting that tertiary interactions may be restricting nuclease access. It has been proposed that G-U base pairs may locally destabilize helical regions widening the major groove (Chow et al., 1992).

Upstream of the anchor duplex, nts A14-G27, were also much more sensitive to the single-stranded nucleases, indicating that interaction with the gRNA opens up the stable stem-loop structure of the mRNA (Fig. 13, 15C). Surprisingly, the run of six adenosine

Figure 16

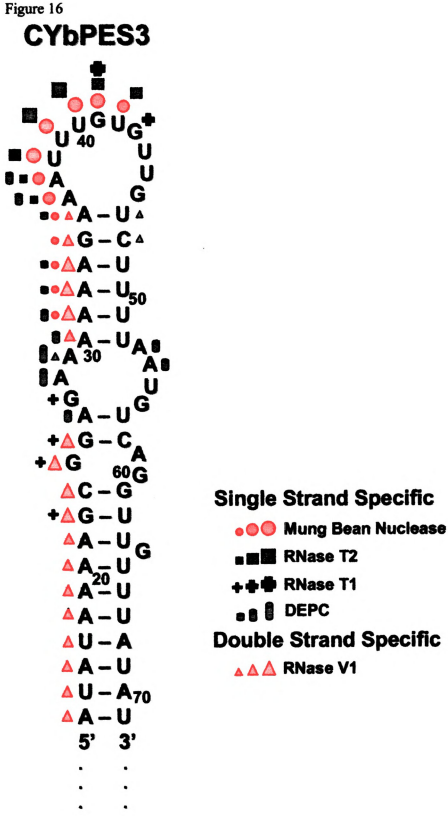
CYbPES3
Single Strand Specific
Mung Bean Nuclease
RNase T2
RNase T1
DEPC
Double Strand Specific
RNase V1
5'
3'

Figure 16. Summary figure of CYbPES3 alone from solution structure probing gels that show predicted secondary structure with cleavages from all 4 nucleases and DEPC using three sizes of symbols to indicate intensity of cleavage. Circles indicate mung bean nuclease (single-strand specific) cleavages, squares indicate RNase T2 (single-strand specific) cleavages, crosses indicate RNase T1 (single-strand guanosine specific) cleavages, cylinders indicate DEPC (single-strand adenosine specific), and triangles indicate RNase V1 (double-strand specific) cleavages.

residues (A28-A32), located just 5' of the anchor duplex were clearly protected from cleavage by both MBN and RNase T2 (Fig. 13). RNase V1 cleavages were observed within this region. However, RNase V1 cleavages were also observed for nts A14-G27, which also show distinct sensitivity to the single stranded nucleases (Fig. 13D). The ability of RNase V1 to cleave stacked, highly structured regions and junctions found between two helices may explain some of the overlapping nuclease sensitivity (Lowman & Draper, 1986). In an effort to resolve our conflicting nuclease results, additional structure probing experiments, using diethyl pyrocarbonate (DEPC), were performed (Fig. 14). This chemical was chosen because it is reactive with purines and because their reactivity can be monitored via chain scission, a necessity with our crosslinked substrates. DEPC is very sensitive to the stacking of base rings; therefore, adenines within a helix are not reactive. In these experiments, while the anchor is clearly protected, nts A26-A32 are reactive with DEPC suggesting that this region is in fact single-stranded and is not highly structured (Figs. 14, 15C). Adenosine residues located further upstream (A14-A21) are not reactive suggesting that this region is helical in nature (Figs. 14, 15C).

In comparing the cleavage patterns when CYbPES3 was paired to its gRNA with and without (NgCYb-558sU) a U-tail, we saw very little difference. Previous crosslinking experiments indicate that the U-tail does interact with the purine rich region around G25; however, in these experiments the crosslinking efficiency was low indicating that this interaction is not stable.

Conclusions

In this study, we investigated the structure of NgCYb-558 alone and its structure when paired with its cognate unedited mRNA or partially edited mRNA. From our previous

structure studies (Leung & Koslowsky, 1999), the computer predicted models suggested that the gRNA stem-loop (A29-U42) is maintained when the initial mRNA/gRNA complex is formed (Fig. 15B). In addition, 3' crosslinking studies with partially edited substrates suggested that a gRNA stem-loop structure is preserved as editing proceeds through the third editing site via interaction with the U-tail (A36-U53)(Fig. 15C). The results of this study support the predicted models and suggest that the gRNA stem-loop may be an important structural component of the initial editing complex. We hypothesize that the formation of multiple helices surrounding the first few editing sites may allow for tertiary interactions that help stabilize the initial gRNA/mRNA interaction. Increasing the amount of editing increases the number of base pairs within the anchor duplex, and this may negate the need for tertiary interactions during the later stages of the gRNA interaction. Alternatively, the multiple helices may limit the number of potential gRNA/mRNA interaction sites, and this may help increase the accuracy of the editing process. This suggests that the U-tail may enhance the editing process in a number of ways. The U-tail is added post-transcriptionally and has been shown to be unnecessary for *in vitro* cleavage of editing substrates (Kable et al., 1996; Seiwert et al., 1996; Burgess et al., 1999). However, sequence modifications that disrupt upstream base pairing interactions severely diminish formation of edited product. Likewise, sequence modifications that increase the stability of the upstream duplex are known to increase the efficiency of *in vitro* editing, suggesting that the upstream gRNA/mRNA interaction is important (Burgess et al., 1999; Kapushoc & Simpson, 1999; Igo et al., 2000; Cruz-Reyes et al., 2001). Previous work in our lab using gel shift analyses indicates that the U-tail is very important for stabilization of the interaction of some mRNA/gRNA pairs

(Koslowsky et al., 2004). RNAi studies have also shown that when the RNA editing terminal uridylyl transferase (RET1), responsible for adding the U-tail to gRNAs is down regulated, there is a decrease in edited mRNAs and inhibited growth of the trypanosome (Aphasizhev et al., 2002). This suggests that the U-tail is necessary for in vivo editing (Gott, 2003; Nebohacova et al., 2004). We know that the RNA editing process must involve the formation and disruption of intramolecular helices to form a number of intermediate complexes (Nordgren et al., 2001). Guide RNAs appear to be able to take advantage of U-tail flexibility through the ability of uridines to base pair with both purine bases. By employing an uridylate tail, the gRNA may increase mRNA/gRNA complex stability without hampering the U-tail migration needed within the complex during the editing process. In addition, the editing process may take advantage of the special properties of G-U base pairs. The G-U base pair has a distinctly different geometry and may locally destabilize helical regions creating protein recognition elements (Chow et al., 1992; Batey & Williamson, 1996). Editing also creates G-U base pairs raising interesting possibilities for protein recognition of the edited mRNA/gRNA complex, and the recruitment of RNA helicases necessary for multiple gRNA utilization.

Recent work on the editing accessory factors MRP1 and MRP2 (Koller et al., 1997; Blom et al., 2001; Aphasizhev et al., 2003b) provide a crystal structure for the matchmaking proteins MRP1 and 2 binding a gRNA (Fig. 17). Both MRP1 and 2 are required for a stable MRP complex to form and knockdown of this complex through RNAi results in a reduction of CYb editing (Vondruskova et al., 2005). MRP1 was found to have a RNA annealing activity that increases gRNA/mRNA complex formation

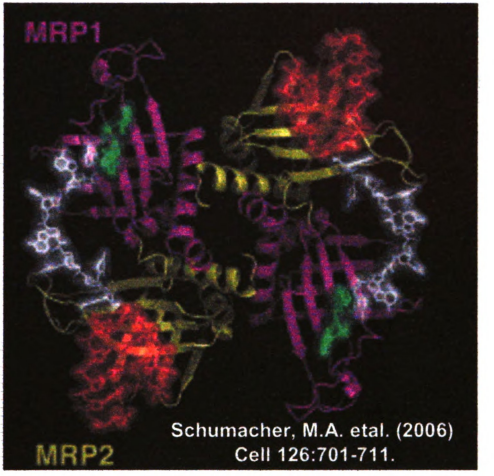

Figure 17. The structure of the MRP1/MRP2 heterotetramer binding two gND7-506 gRNAs. This is a ribbon diagram of the MRP1/MRP2-gND7-506 complex. MRP1 is colored magenta, while MRP2 is yellow. The gRNA nucleotides for the anchor region include green nucleotides representing a small stem-loop as well as white nucleotides representing the region between the anchor helix and the guiding region stem-loop. Red nucleotides represent the gRNA stem-loop of the guiding region. MRP = mitochondrial RNA binding proteins. ND7 = NADH dehydrogenase subunit 7. This figure is from Schumacher, M.A. et al. (2006) Cell 126:701-711.

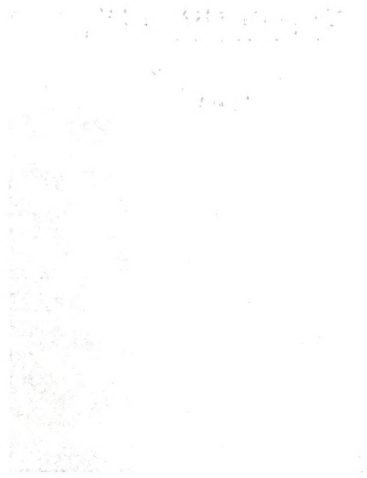

(Muller et al., 2001) through a putative charge reduction function between the mRNA/gRNA anchor helix (Muller & Goringer, 2002). MRP1 and 2 form a heterotetramer potentially binding two gRNAs. MRP1 binds the gRNA anchor and holds it in a single stranded conformation similar to our CYb gRNA anchor structure, while MRP2 binds the predicted gRNA stem-loop (Fig. 17) (Schumacher et al., 2006). The structure data for the gRNA in this complex correlates well with our gRNA alone structure for NgCYb-558 providing evidence that the RNA structures are relevant, and that the gRNA anchor region is most likely in a single stranded conformation during anchor helix formation. MRP1 presents the anchor sequence with the bases exposed and ready for binding, while providing charge neutralization for the anchor phosphate backbone. In addition, these accessory factors appear to recognize structure not sequence as the protein/RNA binding interaction occurs primarily through electrostatic-phosphate contacts. This appears to verify our hypothesis that the structure and not the sequence of the mRNA/gRNA complex is recognized by the editosome proteins as it is known that MRP1 and MRP2 are transient members of the editosome complex (Allen et al., 1998). Interestingly, the structure of the gRNA is not altered by the MRP complex (Hermann et al., 1997; Schumacher et al., 2006), and the gRNA guiding region stem-loop is maintained providing additional evidence that the gRNA stem-loop appears to be an important structure for the editing process.

We have reported here the structure of the naked RNA for the dynamic CYb mRNA/gRNA complex. It will be interesting to discover in future studies how much these RNA structures and dynamics change or are maintained in the presence not only of

the accessory factors but also with the editosome proteins assembling and disassembling from the mRNA/gRNA complex.

MATERIALS AND METHODS

Oligodeoxyribonucleotides:

All oligodeoxynucleotides (Table 3) were ordered from Integrated DNA Technologies, Inc. (Coralville, IA).

Oligoribonucleotide:

Oligoribonucleotide was ordered from Dharmacon Research, Inc. (Lafayette, CO). U_{15}-tail: 5'UUUUUUUUUUUUUU3', 15 nt.

DNA templates and RNA synthesis:

DNA templates of the partial mRNAs: CYbU and CYbPES3 templates were created by ligating two oligodeoxyribonucleotides, the 5' (5'ShortCYb and 5'CYbPES3Short, Table 3) and 3' (3'ShortCYb and 3'CYbPES3Short, Table 3) halves of the molecules using T4 DNA ligase (Roche) and a complementary DNA bridge (ShortCYb bridge and CYbPES3ShortDNAbridge, Table 3) (Moore & Sharp, 1992). The ligated templates were then PCR amplified with T7 and Big SK oligonucleotides (Table 3) and Taq polymerase (Promega) as per the manufacturer's directions. The gRNA constructs (NgCYb558 and NgCYb558(sU), Table 3) have been previously described (Leung & Koslowsky, 2001b). The mRNA transcripts were synthesized either by T7 RNA polymerase (Ribomax, Promega) according to the manufacturer's directions or in the presence of 5 mM guanosine as described previously (Leung & Koslowsky, 2001a). NgCYb-558 and NgCYb-558sU were synthesized using a T7 RNA polymerase using a Ribomax kit (Promega) in the presence (Burgin & Pace, 1990; Harris & Christian, 1999)

Name	Sequence	Length (nts.)
Big SK	5'-GGCCGCTCTAGAACTAGTGG-3'	20
T7	5'- AATTAATACGACTCACTATAG-3'	22
NgCYb558(sU)	5'-TTATTCCCTTTATCACCTAGAAAT TCACATTGTCTTTTAATCCCTATAGT GAGTCGTATTAAATT-3'	65
NgCYb558	5'-AAAAAAAAAAAAAAAATTATTCCCTT TATCACCTAGAAATTCACATTGTCTTTT AATCCCTATAGTGAGTCGTATTAAATT-3'	80
gCYb558(sU) bridge	5'-AAAAAAAAAAAAAAAATTATTCCC TTTATCACC-3'	32
5'ShortCYb	5'-CTTTCTTTTTTCTCCGCTTTTATA TAAAATTTATAACCTATAGTGAGTC GTATTAAATT-3'	59
3'ShortCYb	5'-CCGCTCTAGAACTAGTGGATCCA TATATTCTATATAAACAACCTGACAT TAAAAGACC-3'	58
ShortCYb bridge	5'-GGAGAAAAAAGAAAGGGTCTTTT AATGTCAG-3'	31
5'CYbPES3Short	5'-CAAATTTCTTTTTTCTCCGCTTTTA TATAAAATTTATAACCCTATAGTGAG TCGTATTAAATT-3'	63
3'CYbPES3Short	5'-CCGCTCTAGAACTAGTGGATCCAT ATATTCTATATAAACAACCTGACATTA AAAGACAACA-3'	61
CYbPES3ShortDNAbridge	5'-GGAGAAAAAAGAAATTTGTGTTGT CTTTTAATGTCAG-3'	37

Table 3. List of oligodeoxyribonucleotides

or absence of Guanosine 5'-monophosphorothioate (GMPS)(Biolog Life Science Institutes, Germany or Harris Lab). If GMPS was incorporated at the 5' end of the NgCYb-558 transcripts (with and without U-tail), then 20 μCi of [^{32}αP] rATP (Perkin-Elmer) was added for visualization, the rGTP was reduced to 80 nmols, and 8 μl of 100 mM $MgCl_2$ was added per 80 μl reaction. The mRNAs and gRNAs were gel purified on 6% and 15% 7 M urea acrylamide gels respectively (Leung & Koslowsky, 2001a). The oligoribonucleotide U_{15}-tail was phosphorylated using T4 kinase (Invitrogen) and ligated to NgCYb-558sU using 25 U T4 DNA ligase (Roche) and the NgCYb-558(sU) bridge (Table 3) (Moore & Sharp, 1992; Leung & Koslowsky, 2001a).

RNA crosslinking and end-labeling:

Attachment of p-azidophenacyl bromide (Sigma) to GMPS NgCYb-558 and GMPS NgCYb-558sU transcripts as well as crosslinking of gRNAs and mRNAs was done as described previously (Leung & Koslowsky, 1999, 2001a, b). The mRNA (50 pmols of free and 5 pmols of crosslinked mRNA) was 5' end labeled using 50-100 μCi of [γ ^{32}P] rATP (Perkin-Elmer) and T4 Kinase (Invitrogen) as per the manufacturers' directions and gel purified as above. The gRNA was 3' end labeled by ligating 0.5 nmols of U_{15}-tail to 130 μCi of [5'-^{32}P] cytidine 3',5'-bisphosphate (pCp) (Perkin-Elmer) using T4 RNA ligase (New England Biolabs) as per the manufacturer's directions. The labeled U_{15}-tail was ethanol precipitated, 5' phosphorylated with T4 Kinase (Invitrogen) according to the manufacturer's directions, and ligated to NgCYb-558sU (no U-tail) using 25 U high concentration T4 DNA Ligase (Roche) and the NgCYb558(sU) bridge (Table 3) as previously described.

Structure specific enzymatic probing:

In these experiments, 150-200 kcpm of labeled RNA sample and 10 μg of tRNA were heated to 50°C, cooled slowly, and incubated at 27°C for 20 minutes. Enzyme was then added to the sample (0.1 U RNase T1 (Industrial Research, LTD), 0.18 U RNase V1 Cobra Venom ($Pierce_{MB}$), 0.4 U RNase T2 (Invitrogen), 1 U Mung Bean Nuclease(GibcoBRL)). For RNases T1 and T2, aliquots were taken at 5, 10, and 15 minutes of digestion, and for RNase V1 and Mung Bean Nuclease aliquots were taken at 2, 5, and 10 minutes. The aliquots were immediately phenol/chloroform extracted, ethanol precipitated, and then loaded on 12 or 15% denaturing acrylamide gels. Reactions were performed in 10 mM Tris pH 7.5, 100 mM KCl, 1 mM $MgCl_2$ for all enzymes except MBN. MBN had buffer conditions of 10 mM Tris pH 7.5, 10 mM NaOAc pH 5.0, 0.1 mM ZnOAc, 50 mM NaCl, 1 mM L-cysteine, 5% glycerol, 1 mM $MgCl_2$. RNA sequence ladders were made by denaturing 150 kcpm of labeled RNA and 2 ug of tRNA and digesting with 0.07 U RNase T1 and 0.2 U RNase U2 (Industrial Research, LTD) for 10 minutes at 55°C in the following buffers: [1 X Buffer I(T1):19.8 mM NaCitrate pH 5.0, 1 mM EDTA, 4.2 M Urea, 0.02% Xylene Cyanol, 0.05% Bromophenol blue], [1 X Buffer II(U2): same as above except NaCitrate pH 3.5](buffer recipes courtesy of Dr. Brenda Peculis, NIH, personal communication). The gels were fixed, dried, and exposed on a phosphorimaging screen overnight.

Solution Structure Probing with Chemicals:

For chemical modification and cleavage, the 5' end labeled mRNA was annealed to the gRNA by heating to 50°C and cooling slowly to 27°C where they were held for 30 minutes in 50ul of 1 X HE buffer (25 mM Hepes pH 7.5, 2 mM MgOAc, 50 mM KCl, 0.5 mM DTT, and 0.1 mM EDTA) and then crosslinked along with controls as above.

The mRNA alone samples as well as untreated samples were treated as above without crosslinking. Ten μg of tRNA plus 40U of rRNAsin (Promega) were added to all samples and a no chemical control aliquot (10μl) was taken. Four μl of 97% diethyl pyrocarbonate (DEPC, Aldrich) was added and the samples incubated at room temperature (Brunel & Romby, 2000). A 20μl aliquot was taken from each reaction at 15 and 25 minutes. The aliquots were immediately ethanol precipitated twice in the presence of 0.2 M NaOAc pH 7.0, followed by a 70% ethanol rinse. Crosslinks and controls were then gel purified on 6% acrylamide, 7 M urea gels as described above (Leung & Koslowsky, 1999, 2001a, b). Strand scission of all chemical samples was accomplished by incubating samples in 20 μl of 1 M Aniline (Sigma-Aldrich) pH 4.5 for 10 minutes at 55°C, ethanol precipitating as above (Brunel & Romby, 2000), and analyzed on 15% denaturing acrylamide gels. T1 RNA sequencing ladders were made as described above. An alkaline hydrolysis ladder of mRNA was generated by incubating 100 kcpm of RNA and 10 μg tRNA in 50 mM $NaHCO_3/Na_2CO_3$ pH 9.0, 1mM EDTA pH 8.0 at 90°C for 5 minutes.

Acknowledgements

This work was supported by National Institutes of Health Grant AI34155 to D.K. We'd like to thank Dr. Ron Patterson, Dr. Charles Hoogstraten, Dr. John Wang, Dr. Sandra Clement, Larissa Reifur, and Melissa Mingler and all other members of the MSU RNA Journal Club for critical reading of the manuscript and helpful discussions as well as to Dr. Brenda Peculis at NIH for sharing her buffer recipes and digestion conditions. We would also like to thank Dr. Michael Harris from Case Western University for samples of GMPS and technical advice.

Literature Cited

Adler BK, Hajduk SL. 1997. Guide RNA requirement for editing-site-specific endonucleolytic cleavage of preedited mRNA by mitochondrial ribonucleoprotein particles in Trypanosoma brucei. *Mol Cell Biol 17*:5377-5385.

Allen TE, Heidmann S, Reed R, Myler PJ, Goringer HU, Stuart KD. 1998. Association of guide RNA binding protein gBP21 with active RNA editing complexes in Trypanosoma brucei. *Mol Cell Biol 18*:6014-6022.

Aphasizhev R, Aphasizheva I, Nelson RE, Gao G, Simpson AM, Kang X, Falick AM, Sbicego S, Simpson L. 2003a. Isolation of a U-insertion/deletion editing complex from Leishmania tarentolae mitochondria. *Embo J 22*:913-924.

Aphasizhev R, Aphasizheva I, Nelson RE, Simpson L. 2003b. A 100-kD complex of two RNA-binding proteins from mitochondria of Leishmania tarentolae catalyzes RNA annealing and interacts with several RNA editing components. *Rna 9*:62-76.

Aphasizhev R, Sbicego S, Peris M, Jang SH, Aphasizheva I, Simpson AM, Rivlin A, Simpson L. 2002. Trypanosome mitochondrial 3' terminal uridylyl transferase (TUTase): the key enzyme in U-insertion/deletion RNA editing. *Cell 108*:637-648.

Aphasizhev R, Simpson L. 2001. Isolation and characterization of a U-specific 3'-5'-exonuclease from mitochondria of Leishmania tarentolae. *J Biol Chem 276*:21280-21284.

Batey RT, Williamson JR. 1996. Interaction of the Bacillus stearothermophilus ribosomal protein S15 with 16 S rRNA: II. Specificity determinants of RNA-protein recognition. *J Mol Biol 261*:550-567.

Blom D, Burg J, Breek CK, Speijer D, Muijsers AO, Benne R. 2001. Cloning and characterization of two guide RNA-binding proteins from mitochondria of Crithidia fasciculata: gBP27, a novel protein, and gBP29, the orthologue of Trypanosoma brucei gBP21. *Nucleic Acids Res 29*:2950-2962.

Blum B, Bakalara N, Simpson L. 1990. A model for RNA editing in kinetoplastid mitochondria: "guide" RNA molecules transcribed from maxicircle DNA provide the edited information. *Cell 60*:189-198.

Blum B, Simpson L. 1990. Guide RNAs in kinetoplastid mitochondria have a nonencoded 3' oligo(U) tail involved in recognition of the preedited region. *Cell 62*:391-397.

Brunel C, Romby R. 2000. Probing RNA Structure and RNA-Ligand Complexes with Chemical Probes. In: Abelson JN, Simon MI, eds. *Methods in Enzymology: RNA-Ligand Interactions*. San Diego: Academic Press. pp 3-21.

Burgess ML, Heidmann S, Stuart K. 1999. Kinetoplastid RNA editing does not require the terminal 3' hydroxyl of guide RNA, but modifications to the guide RNA terminus can inhibit in vitro U insertion. *Rna 5*:883-892.

Burgin AB, Pace NR. 1990. Mapping the active site of ribonuclease P RNA using a substrate containing a photoaffinity agent. *Embo J 9*:4111-4118.

Chow CS, Behlen LS, Uhlenbeck OC, Barton JK. 1992. Recognition of tertiary structure in tRNAs by Rh(phen)2phi3+, a new reagent for RNA structure-function mapping. *Biochemistry 31*:972-982.

Cruz-Reyes J, Zhelonkina A, Rusche L, Sollner-Webb B. 2001. Trypanosome RNA editing: simple guide RNA features enhance U deletion 100-fold. *Mol Cell Biol 21*:884-892.

Feagin JE, Jasmer DP, Stuart K. 1987. Developmentally regulated addition of nucleotides within apocytochrome b transcripts in Trypanosoma brucei. *Cell 49*:337-345.

Feagin JE, Stuart K. 1988. Developmental aspects of uridine addition within mitochondrial transcripts of Trypanosoma brucei. *Mol Cell Biol 8*:1259-1265.

Gott JM. 2003. Two distinct roles for terminal uridylyl transferases in RNA editing. *Proc Natl Acad Sci U S A 100*:10583-10584.

Harris ME, Christian EL. 1999. Use of circular permutation and end modification to position photoaffinity probes for analysis of RNA structure. *Methods 18*:51-59.

Hayman ML, Read LK. 1999. Trypanosoma brucei RBP16 is a mitochondrial Y-box family protein with guide RNA binding activity. *J Biol Chem 274*:12067-12074.

Hermann T, Schmid B, Heumann H, Goringer HU. 1997. A three-dimensional working model for a guide RNA from Trypanosoma brucei. *Nucleic Acids Res 25*:2311-2318.

Igo RP, Jr., Palazzo SS, Burgess ML, Panigrahi AK, Stuart K. 2000. Uridylate addition and RNA ligation contribute to the specificity of kinetoplastid insertion RNA editing. *Mol Cell Biol 20*:8447-8457.

Kable ML, Seiwert SD, Heidmann S, Stuart K. 1996. RNA editing: a mechanism for gRNA-specified uridylate insertion into precursor mRNA. *Science 273*:1189-1195.

Kapushoc ST, Simpson L. 1999. In vitro uridine insertion RNA editing mediated by cis-acting guide RNAs. *RNA 5*:656-669.

Koller J, Muller UF, Schmid B, Missel A, Kruft V, Stuart K, Goringer HU. 1997. Trypanosoma brucei gBP21. An arginine-rich mitochondrial protein that binds to guide RNA with high affinity. *J Biol Chem 272*:3749-3757.

Koslowsky DJ, Goringer HU, Morales TH, Stuart K. 1992. In vitro guide RNA/mRNA chimaera formation in Trypanosoma brucei RNA editing. *Nature 356*:807-809.

Koslowsky DJ, Kutas SM, Stuart K. 1996. Distinct differences in the requirements for ribonucleoprotein complex formation on differentially regulated pre-edited mRNAs in Trypanosoma brucei. *Mol Biochem Parasitol 80*:1-14.

Koslowsky DJ, Reifur L, Yu LE, Chen W. 2004. Evidence for U-Tail Stabilization of gRNA/mRNA Interactions in Kinetoplastid RNA Editing. *RNA Biology 1*:28-34.

Leung SS, Koslowsky DJ. 1999. Mapping contacts between gRNA and mRNA in trypanosome RNA editing. *Nucleic Acids Res 27*:778-787.

Leung SS, Koslowsky DJ. 2001a. Interactions of mRNAs and gRNAs involved in trypanosome mitochondrial RNA editing: structure probing of an mRNA bound to its cognate gRNA. *RNA 7*:1803-1816.

Leung SS, Koslowsky DJ. 2001b. RNA editing in Trypanosoma brucei: characterization of gRNA U-tail interactions with partially edited mRNA substrates. *Nucleic Acids Res 29*:703-709.

Lowman HB, Draper DE. 1986. On the recognition of helical RNA by cobra venom V1 nuclease. *J Biol Chem 261*:5396-5403.

Madison-Antenucci S, Sabatini RS, Pollard VW, Hajduk SL. 1998. Kinetoplastid RNA-editing-associated protein 1 (REAP-1): a novel editing complex protein with repetitive domains. *Embo J 17*:6368-6376.

McManus MT, Shimamura M, Grams J, Hajduk SL. 2001. Identification of candidate mitochondrial RNA editing ligases from Trypanosoma brucei. *Rna 7*:167-175.

Missel A, Souza AE, Norskau G, Goringer HU. 1997. Disruption of a gene encoding a novel mitochondrial DEAD-box protein in Trypanosoma brucei affects edited mRNAs. *Mol Cell Biol 17*:4895-4903.

Moore MJ, Sharp PA. 1992. Site-specific modification of pre-mRNA: the 2'-hydroxyl groups at the splice sites. *Science 256*:992-997.

Muller UF, Goringer HU. 2002. Mechanism of the gBP21-mediated RNA/RNA annealing reaction: matchmaking and charge reduction. *Nucleic Acids Res 30*:447-455.

Muller UF, Lambert L, Goringer HU. 2001. Annealing of RNA editing substrates facilitated by guide RNA-binding protein gBP21. *Embo J 20*:1394-1404.

Nebohacova M, Maslov DA, Falick AM, Simpson L. 2004. The effect of RNA interference Down-regulation of RNA editing 3'-terminal uridylyl transferase

(TUTase) 1 on mitochondrial de novo protein synthesis and stability of respiratory complexes in Trypanosoma brucei. *J Biol Chem 279*:7819-7825.

Nordgren S, Slagter-Jager JG, Wagner GH. 2001. Real time kinetic studies of the interaction between folded antisense and target RNAs using surface plasmon resonance. *J Mol Biol 310*:1125-1134.

Panigrahi AK, Allen TE, Stuart K, Haynes PA, Gygi SP. 2003a. Mass spectrometric analysis of the editosome and other multiprotein complexes in Trypanosoma brucei. *J Am Soc Mass Spectrom 14*:728-735.

Panigrahi AK, Gygi SP, Ernst NL, Igo RP, Jr., Palazzo SS, Schnaufer A, Weston DS, Carmean N, Salavati R, Aebersold R, Stuart KD. 2001a. Association of two novel proteins, TbMP52 and TbMP48, with the Trypanosoma brucei RNA editing complex. *Mol Cell Biol 21*:380-389.

Panigrahi AK, Schnaufer A, Carmean N, Igo RP, Jr., Gygi SP, Ernst NL, Palazzo SS, Weston DS, Aebersold R, Salavati R, Stuart KD. 2001b. Four related proteins of the Trypanosoma brucei RNA editing complex. *Mol Cell Biol 21*:6833-6840.

Panigrahi AK, Schnaufer A, Ernst NL, Wang B, Carmean N, Salavati R, Stuart K. 2003b. Identification of novel components of Trypanosoma brucei editosomes. *Rna 9*:484-492.

Pelletier M, Read LK. 2003. RBP16 is a multifunctional gene regulatory protein involved in editing and stabilization of specific mitochondrial mRNAs in Trypanosoma brucei. *RNA 9*:457-468.

Riley GR, Corell RA, Stuart K. 1994. Multiple guide RNAs for identical editing of Trypanosoma brucei apocytochrome b mRNA have an unusual minicircle location and are developmentally regulated. *J Biol Chem 269*:6101-6108.

Rusche LN, Huang CE, Piller KJ, Hemann M, Wirtz E, Sollner-Webb B. 2001. The two RNA ligases of the Trypanosoma brucei RNA editing complex: cloning the essential band IV gene and identifying the band V gene. *Mol Cell Biol 21*:979-989.

Schmid B, Riley GR, Stuart K, Goringer HU. 1995. The secondary structure of guide RNA molecules from Trypanosoma brucei. *Nucleic Acids Res 23*:3093-3102.

Schnaufer A, Panigrahi AK, Panicucci B, Igo RP, Jr., Wirtz E, Salavati R, Stuart K. 2001. An RNA ligase essential for RNA editing and survival of the bloodstream form of Trypanosoma brucei. *Science 291*:2159-2162.

Schumacher MA, Karamooz E, Zikova A, Trantirek L, Lukes J. 2006. Crystal Structures of T. brucei MRP1/MRP2 Guide-RNA Binding Complex Reveal RNA Matchmaking Mechanism. *Cell 126*:701-711.

Seiwert SD, Heidmann S, Stuart K. 1996. Direct visualization of uridylate deletion in vitro suggests a mechanism for kinetoplastid RNA editing. *Cell 84*:831-841.

Seiwert SD, Stuart K. 1994. RNA editing: transfer of genetic information from gRNA to precursor mRNA in vitro. *Science 266*:114-117.

Simpson L, Aphasizhev R, Gao G, Kang X. 2004. Mitochondrial proteins and complexes in Leishmania and Trypanosoma involved in U-insertion/deletion RNA editing. *RNA 10*:159-170.

Stuart KD, Schnaufer A, Ernst NL, Panigrahi AK. 2005. Complex management: RNA editing in trypanosomes. *Trends Biochem Sci 30*:97-105.

Vanhamme L, Perez-Morga D, Marchal C, Speijer D, Lambert L, Geuskens M, Alexandre S, Ismaili N, Goringer U, Benne R, Pays E. 1998. Trypanosoma brucei TBRGG1, a mitochondrial oligo(U)-binding protein that co-localizes with an in vitro RNA editing activity. *J Biol Chem 273*:21825-21833.

Vondruskova E, van den Burg J, Zikova A, Ernst NL, Stuart K, Benne R, Lukes J. 2005. RNA interference analyses suggest a transcript-specific regulatory role for mitochondrial RNA-binding proteins MRP1 and MRP2 in RNA editing and other RNA processing in Trypanosoma brucei. *J Biol Chem 280*:2429-2438.

CHAPTER 3
INTERACTIONS OF MRNAS AND GRNAS INVOLVED IN TRYPANOSOME MITOCHONDRIAL RNA EDITING: MEASUREMENTS OF THE REAL TIME KINETICS OF BINDING FOR THREE MRNAS BOUND TO THEIR GRNAS

(The ND7 experiments were run by Aimee B. Ogden, a former undergraduate, under my supervision.)

Introduction

RNA editing in kinetoplasts is a post-transcriptional process that involves the precise insertion and deletion of uridine residues in mitochondrial mRNAs. These changes are made by more than twenty proteins collectively known as the editosome and are directed by a small RNA called a guide RNA (gRNA). The gRNA plays key roles in the template directed cleavage, uridylate insertion or deletion and finally religation of the transcript (Simpson et al., 2004; Stuart et al., 2005). Therefore, the ability of the gRNAs to target their cognate substrates efficiently is an important part of the editing process. The gRNAs that direct the editing process are short RNA molecules (~50-70 nucleotides) made of three functional elements. At the 5' end of the gRNA is a 5-21 nucleotide region known as the anchor that is complementary to the mRNA just 3' of the editing domain. The second element is known as the guiding region and serves as the template for proper editing of the mRNA. The guiding region is complementary to the mature mRNA (allowing G-U base pairs). The poly-uridylate tail (~15 nts) is the third element, and it is added post-transcriptionally (Blum et al., 1990; Blum & Simpson, 1990).

Little is known about how fast editing occurs, so it is unknown if the gRNA/mRNA complex requires additional protein factors for a faster association rate. However, the stability of the mRNA/gRNA complex may be important for the editing process. In previous work, different mRNA/gRNA pairs were investigated to find the difference in the binding interaction each gRNA had for its cognate mRNA: the unedited ATPase 6 subunit (A6) mRNA and its initiating gRNA, gA6-14, and the unedited apocytochrome b (CYb) mRNA with its initiating gRNA, gCYb-558 (Koslowsky et al., 2004). The A6 mRNA is constitutively edited and is used for the *in vitro* studies of the editing process.

The apparent K_D (K_{Dapp}) for the gA6-14/A6UENDSh interaction is in the nM range indicating that this guide RNA has high affinity for its cognate message. Editing of the CYb mRNA is developmentally regulated occurring preferentially in the insect host (procyclic) (Feagin et al., 1985). In contrast to gA6-14, the interaction between gCYb-558 and its cognate unedited mRNA is very weak with apparent K_D's in the μM range. Solution structure probing indicates that the CYb mRNA forms a stable stem-loop structure, with the anchor binding site (ABS) found within the double-stranded stem (Fig. 20A) (Leung & Koslowsky, 2001a). Our hypothesis is that the stable secondary structure of the CYb mRNA plays an important role in the regulation of the editing process for this transcript. The stability of the CYb mRNA stem-loop suggests that a RNA helicase is probably required for effective gRNA interaction. RNA structure is critical for many RNA-RNA and RNA-protein interactions to display nucleotides in the correct orientation for efficient interaction. It is clear that the structure of the immediate editing domain can profoundly affect the efficiency of the interaction between the gRNA and the target mRNA. To gain a better understanding of how structure surrounding the anchor binding site may affect gRNA targeting, we analyzed the kinetic parameters of binding for three different mRNA/gRNA pairs using surface plasmon resonance technology. The dissociation rate constants (k_{off}), the association rate constants (k_{on}), and the dissociation equilibrium constants (K_D) are compared at 2 mM magnesium for the unedited apocytochrome b (CYb) mRNA/gRNA interaction as well as two other initiating mRNA/gRNA pairs, ATPase 6 (A6) and NADH

Figure 18 **A CYbU**

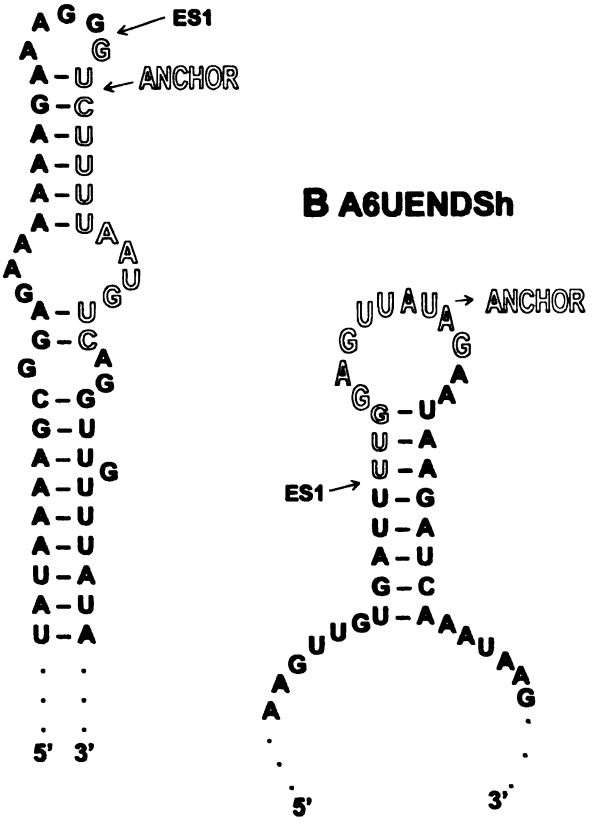

B A6UENDSh

C mND7550

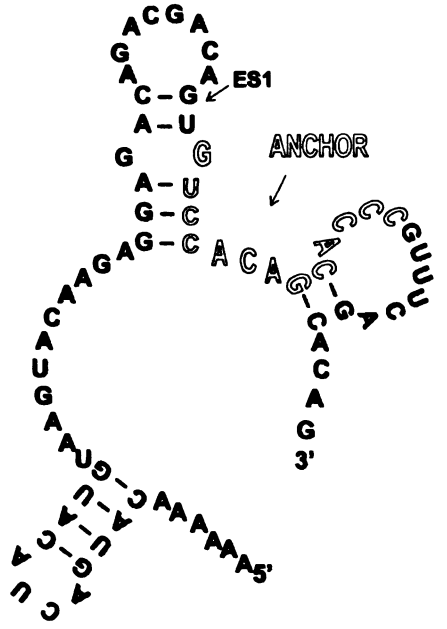

Figure 18 continued **D NgCYb-558**

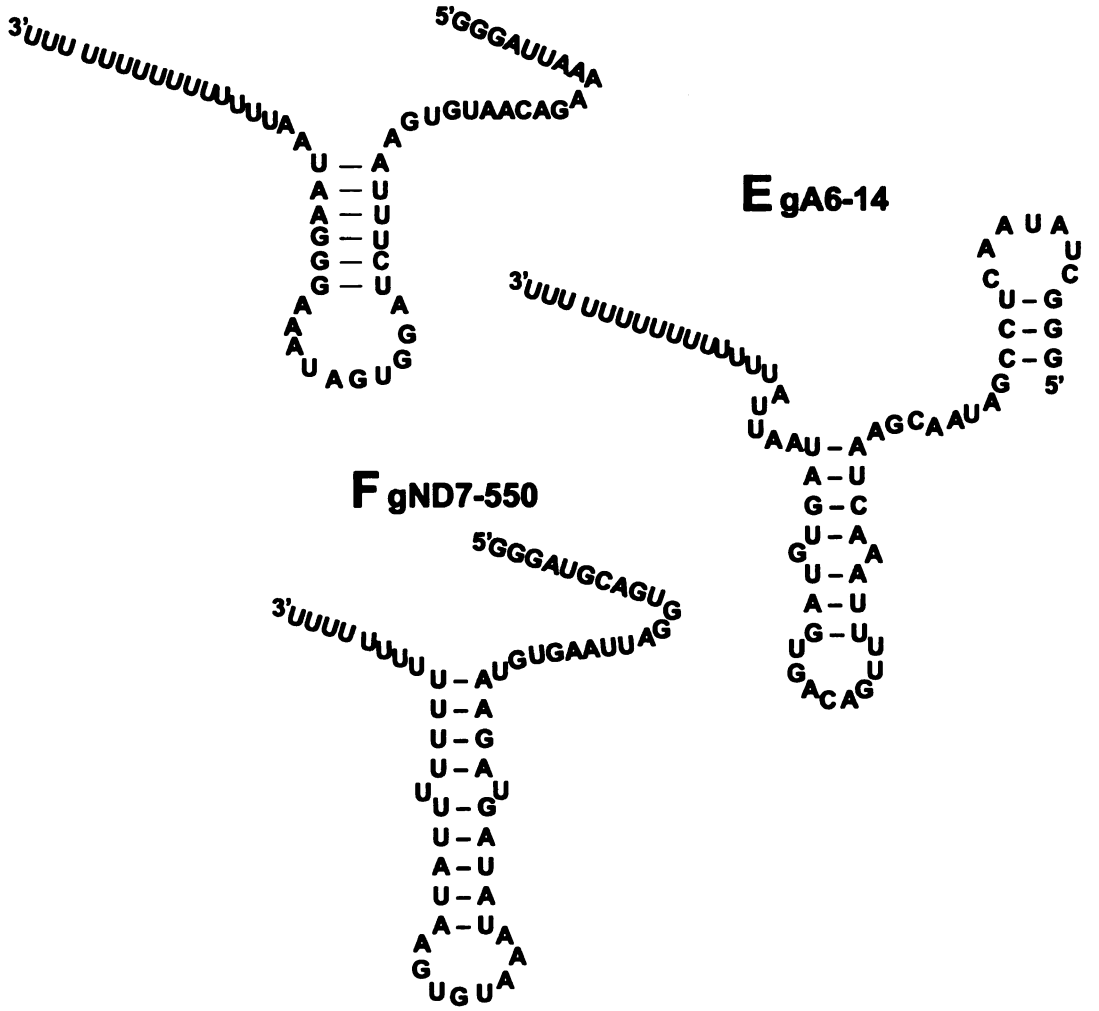

Figure 18 continued

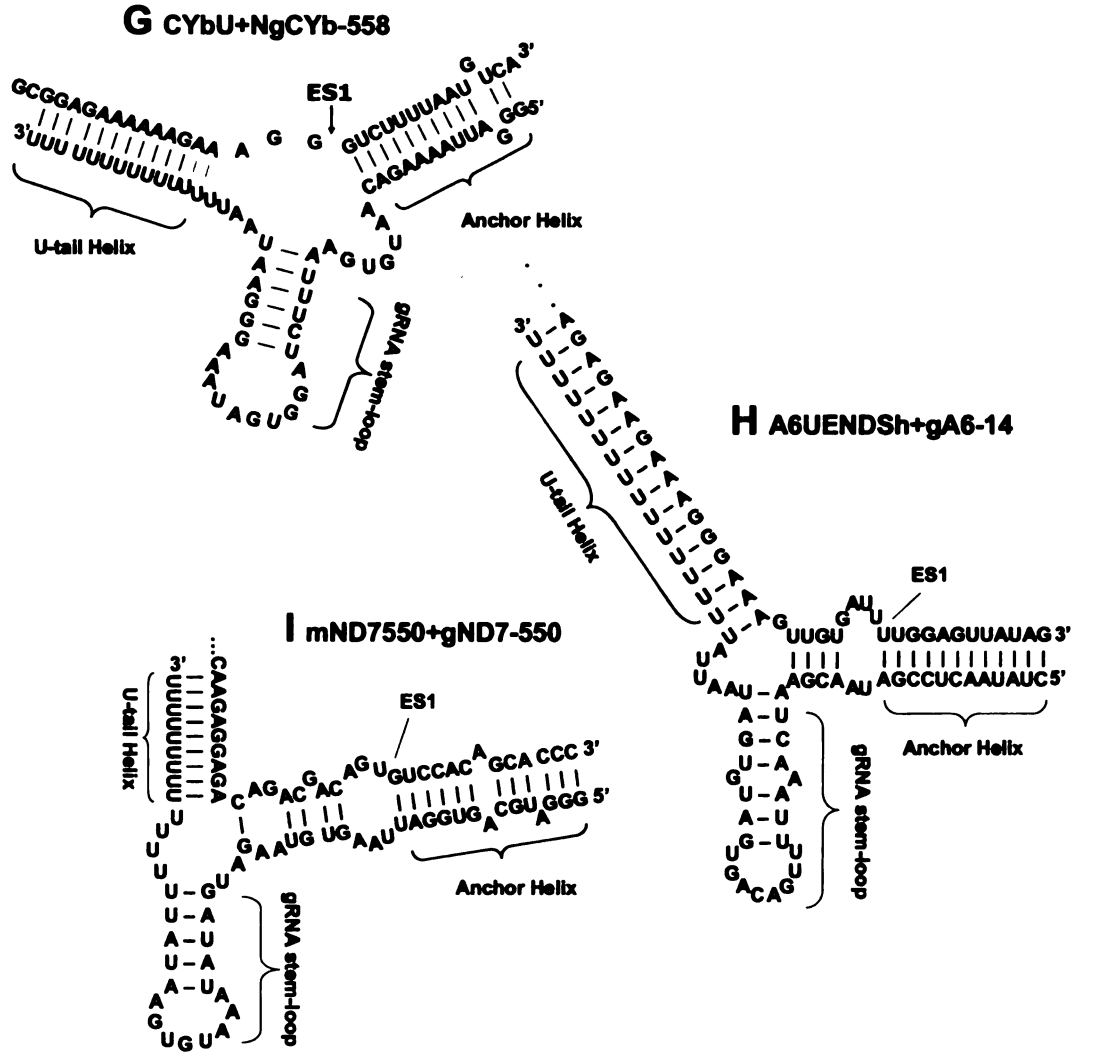

Figure 18. Predicted secondary structures of the A6, CYb, and ND7 RNAs. A. CYbU, the unedited mRNA, forms a stable stem-loop (5 bases) with the first few editing sites positioned within the terminal loop and most of the anchor binding site is base paired. B. A6UENDSh, an unedited mRNA with a loose open structure and part of the anchor region in a loop. C. mND7550, another unedited mRNA, has a loose open structure with a mostly single-stranded anchor binding site. The hollow letters represent nucleotides that are part of the anchor binding site. ES1 = editing site 1. D. NgCYb-558 gRNA secondary structure. E. gA6-14 gRNA secondary structure. F. gND7-550 gRNA secondary structure. All gRNAs are predicted to have a mostly single stranded anchor sequence, a gRNA stem-loop, and a single stranded U-tail. G. CYbUSh+NgCYb-558 mRNA/gRNA complex secondary structure. H. A6UENDSh+gA6-14 mRNA/gRNA complex predicted secondary structure. I. mND7-550+gND7-550 mRNA/gRNA complex predicted secondary structure. All three mRNA/gRNA complexes contain mRNA/gRNA anchor helices, a gRNA stem-loop, and a mRNA/U-tail helix.

dehydrogenase 7 (ND7). In contrast to the CYb substrate, the A6 and ND7 mRNAs are constitutively edited and predicted to have relatively little structure surrounding their single stranded anchor binding sites.

In this study, the CYb mRNA/gRNA interaction appears to be severely affected by the structure of the mRNA. The association rate for CYb is unusually slow compared to the other mRNA/gRNA substrates. In addition, the dissociation rate is considerably faster, resulting in a calculated equilibrium dissociation constant (K_D) in the micromolar range. The A6 and ND7 substrates show that in the absence of significant mRNA structure (such as the CYb mRNA) and when compared to other RNA-RNA binding interactions, the mRNA/gRNA interaction appears to have a relatively normal association rate coupled with a much slower dissociation rate. This study allows us to begin to dissect what elements of the mRNA and gRNA, sequence and structure, are important to achieve stable duplex formation. The high affinity observed in the A6 and ND7 mRNA/gRNA interactions is the result of a very slow dissociation rate. This complex stability may be required for editing to occur.

Results

mRNA/gRNA pairs examined using surface plasmon resonance

CYbU-NgCYb-558

The CYbU and NgCYb-558 RNAs used in this study have been previously described (Yu & Koslowsky, 2006). CYbU is composed of the first 88 nts from the CYb mRNA 5' end. Editing of this mRNA is developmentally regulated with the insertion of 34 uridylates at 13 sites occurring preferentially during the procyclic stage of the life cycle (Feagin et al., 1987; Feagin & Stuart, 1988). The gRNA construct, NgCYb-558, is 59

nucleotides long including a 15 nt. uridylate tail (U-tail) (Table 4) (Leung & Koslowsky, 2001b). NgCYb-558 is almost identical to wild type and directs 21 uridylate insertions at the first 7 editing sites. The secondary structures for NgCYb-558, the CYbU mRNA substrate, and the gRNA/mRNA complex have been determined using both solution structure probing and UV-crosslinking techniques (Schmid et al., 1995; Leung & Koslowsky, 1999, 2001a, b; Yu & Koslowsky, 2006). The CYbU mRNA substrate alone folds into a stable stem-loop (ΔG = -24.47 kCal/mol) (Reifur et al., 2006), with the terminal loop containing the first three editing sites (Fig. 18A). The anchor binding site (ABS) of the unedited CYb mRNA is composed of 13 nts and is found sequestered within the stable mRNA stem (Leung & Koslowsky, 2001a). The CYb gRNA has a mostly single-stranded anchor. The guiding region is contained within a stem-loop that forms before editing begins whereas the U-tail appears to have a single-stranded conformation (Fig. 18D) (Schmid et al., 1995; Yu & Koslowsky, 2006). Duplex formation between the gRNA and mRNA results in the formation of a three helical structure surrounding the first few editing sites. These include a gRNA/mRNA anchor helix, gRNA stem-loop, and U-tail/mRNA helix (Fig. 18G) (Leung & Koslowsky, 2001a; Yu & Koslowsky, 2006). The anchor helix formed between the gRNA and mRNA involves 12 base pairs composed of eight A-U bps, three G-C bps, and one G-U bp (Fig. 19A)

A6UENDSh-gA6-14

ATPase 6 subunit (A6) mRNA appears to have consistent levels of editing in either host (Bhat et al., 1990) and is extensively edited with multiple gRNAs. The A6UENDSh substrate used in this study represents 80 nts from the 3' end of the ATPase 6 subunit

RNA	Analyte or Ligand	Sequence	No. of nts.
CYbU+BigSK	Ligand	5'GGUUAUAAAUUUUAUAUAAAAGCGG AGAAAAAAGAAAGGGUCUUUUAAUGUC AGGUUGUUUAUAUAGAAUAUAUGGAUC atatggaagtaattagaagga-biotin3'	100
CYbU+ Biatag1	Ligand	5'GGUUAUAAAUUUUAUAUAAAAGCGGA GAAAAAAGAAAGGGUCUUUUAAUGUCAG GUUGUUUAUAUAGAAUAUAUGGAUCcacua guucuagagcggcc-biotin3'	98
NgCYb-558	Analyte	5'GGGAUUAAAAGACAAUGUGAAUUUCUA GGUGAUAAAGGGAAUAAUUUUUUUUUUU UUUU3'	59
mND7550+Bi gSK	Ligand	5'AAAAACAUGACUACAUGAUAAGUACAAG AGGAGACAGACGACAGUGUCCACAGCACC CGUUUCAGCACAGatatggaagtaattagaagga-biotin3'	91
gND7-550	Analyte	5'GGGAUGCAGUGGAUUAAGUGUAAGAUGA UAUAAAUGUGAAUAUUUUUUUUUUUUU3'	57
A6UENDSh+ BigSK	Ligand	5'GGAAAGGUUAGGGGGAGGAGAGAAGAAA GGGAAAGUUGUGAUUUUGGAGUUAUAGAA UAAGAUCAAAUAAGUUAAUAAUAcactagttcta gagcggcc-biotin3'	99
gA6-14	Analyte	5'AUAUACUAUAACUCCGAUAACGAAUCAG AUUUUGACAGUGAUAUGAUAAUUAUUUUU UUUUUUUUUUU3'	68

Table 4. List of all Biacore substrates used in Biacore experiments. The biotinylated DNA tags were ligated on using DNA bridges (listed in Table 6) and are indicated by lowercase letters. Column 1: RNA name. Column 2: Ligands were biotinylated and attached to streptavidin coated SA chips (Biacore, Uppsala, Sweden) and Analytes were injected in running buffer and flowed across the surface of the chip to bind the Ligand. Column 3: Sequence of the Biacore substrates. Column 4: number of nucleotides.

A

CYbU aligned to NgCYb-558:

```
----------------GGUUAUAAAUUUUAUAUAAAAGCGGAGAAAAAAGAAAGGGUCUUUUAAUGUCAGGUUGUUUAUAUAGAAUAUAUGG
-------------------------------------------------------||||||||||#:|
NgCYb-558UUUUUUUUUUUUUUUUAAUAAGGGAAAUAGUGGAUCUUUAAGUGUAACAGAAAAUUAGGG
```

B

A6UENDsh aligned to gA6-14:

```
--GGAAAGGUUAGGGGGAGGAGAGAAGAAAGGGAAAGUUGUGAUUUUGGAGUUAUAGAAUAAGAUCAAAUAAGUUAAUAAUA
-------------------------------------------|:||||||||||##:
NgA6-14-U15AUUAAUAGUAUAGUGACAGUUUUAGACUAAGCAAUAGCCUCAAUAUCGGG
```

C

mND7550 (Dharm)aligned to gND7-550:

```
AAAAACAUGACUACAUGAUAAGUACAAGAGGAGACAGACGACAGUGUCCACAGCACCCGUUUCAGCACAG
-----------------------------------------:||#|||#||#\\\
gND7-550UUUUUUUUUUUUUUUUAUAAGUGUAAAUAUAGUAGAAUUAGGUGACGUAGGG
```

Figure 19. The anchor helices of the RNAs. Lowercase, italic letters = vector sequence, # = mismatched sequence, : = GU base pair, | = complementary sequence, the aligned anchors are bold. A. The CYbU transcript aligned to NgCYb-558 at the anchors. B. The A6UENDSh transcript aligned to gA6-14 at the anchors. C. The mND7-550 transcript aligned to gND7-550 at the anchors.

mRNA. There are 26 editing sites within this substrate. Solution structure probing of the mRNA alone indicates that the A6UENDSh substrate forms a short stem-loop structure (stem = 8 bps, ΔG = -8.00 kCal/mol) (Reifur et al., 2006). However, in contrast to the CYb mRNA, the ABS for the A6 mRNA is mostly located within the single stranded loop region (Fig. 18B) (Reifur & Koslowsky, 2006). The initiating gRNA, gA6-14, directs insertion of 57 uridines in 23 sites and deletion of 6 uridines at 3 sites (Table 4). Solution structure probing of the A6 gRNA suggests that it forms a structure similar to NgCYb-558 with a mostly single-stranded anchor, a modified gRNA stem-loop, and a single-stranded U-tail (Fig. 18E) (Schmid et al., 1995; Reifur & Koslowsky, 2006). UV crosslinking analyses combined with computer modeling indicate that the A6 mRNA/gRNA complex also forms a three helical structure including an anchor helix, gRNA stem-loop, and U-tail/mRNA helix (Leung & Koslowsky, 1999). However, between the anchor helix and the gRNA stem-loop, there is a bulge as well as an additional short helical region (Fig. 18H). This bulge 5' (mRNA) of the anchor helix contains the first editing site, and the upstream short helical region is composed of 4 consecutive bps (1 G-C, 2 A-U, and 1 G-U) that may contribute to complex stability (Reifur & Koslowsky, 2006).

mND7550-gND7-550

Editing of the NADH dehydrogenase subunit 7 mRNA (ND7) is unusual in that editing occurs within two distinct domains separated by 59 nts (homology region 3 (HR3)) that are not edited (Koslowsky et al., 1990). The mND7-550 mRNA substrate (Table 4) used in this study consists of the 5' most 70 nts of the ND7 transcript. It contains the anchor binding site for gND7-550; a span of 14 nts that are not edited in the

mature transcript. The computer predicted structure for mND7550 suggests that this substrate has very little structure surrounding the ABS (ΔG = -10.83 kCal/mol) (Reifur et al., 2006). While the ΔG suggests that mND7550 is slightly more stable than A6UENDSh, it is characterized by multiple short helices. The mND7550 ABS is predicted to be mostly single stranded, spanning the region between two short helices (Fig. 18C). The gND7-550 gRNA directs 33 uridine insertions into 12 editing sites and appears to initiate editing (Koslowsky et al., 1990; Corell et al., 1993). The gND7-550 gRNA is composed of 57 nts and is predicted to have a single-stranded anchor sequence, a modified gRNA stem-loop that incorporates six uridylates from the U-tail, and additional single-stranded uridylates in the U-tail (Fig. 18F) similar to the general predicted structure for most gRNAs (Schmid et al., 1995). The mND7550/gND7-550 anchor helix is composed of 3 A-U bps, 8 G-C bps, 2 mismatches, and 1 G-U bp (Fig. 19C). The ND7 mRNA/gRNA complex is also predicted to form a three helical structure composed of an anchor helix, gRNA stem-loop, and U-tail/mRNA helix. Between the anchor helix and the gRNA stem-loop there are two predicted bulges, a mismatch, and a short helical region (Fig. 18I). The first predicted bulge 5' (mRNA) of the anchor helix contains the first editing site, and further editing would disrupt the upstream short helical regions. However, the additional bps upstream of the anchor contain 3 G-C and 2 A-U bps, and these would have additional stabilizing effects for complex formation. The ND7 anchor helix contains more G-C bps than A6 and CYb; however, there are also 2 internal mismatches.

Surface Plasmon Resonance Studies

The association and dissociation rate constants of the gRNA/mRNA interactions were measured using surface plasmon resonance (SPR). The BIACORE 2000 (Biacore, Uppsala, Sweden) monitors intermolecular interactions through SPR that arises when incident light is reflected from a thin gold film between two layers. A change of the refractive index changes the angle of light which is recorded by the detector as a change in resonance units (RU). The change in refractive index depends on the material close to the non-illuminated side of the gold surface where a binding reaction takes place and is closely correlated to a change in mass near the gold surface. The rate at which this change occurs provides information about the association and dissociation rates of the molecules (Katsamba et al., 2002).

In these experiments, a deoxyoligonucleotide tag with a 3' biotin label was ligated onto the 3' ends of the target mRNAs (Moore & Sharp, 1992). The biotin labeled mRNA was then immobilized to the streptavidin covered surface of the SA chip (Biacore, Uppsala, Sweden) in two of the four channels of a BIACORE 2000 (Biacore, Uppsala, Sweden). One channel remained empty and was used as a reference surface and one contained the biotinylated tag as a control for background binding. When gRNA was injected over the channels and bound mRNA, there was a change in refractive index which was displayed as a sensogram. A continuous flow of gRNA solution at various concentrations (30 to 1500 nM) was injected over the immobilized mRNAs to monitor the gRNA association with its target mRNA. The dissociation phase was monitored by chasing the gRNAs with buffer alone.

In order to see reliable gRNA binding to the mRNA, 50 to 350 resonance units of mRNA was attached to the chip surface. For the CYb substrate, binding did not come to

equilibrium even with high gRNA concentrations and long injection times. In addition, the long injection times and the regeneration procedure used between two binding assays at different RNA concentrations progressively affected the mRNA integrity during the experiments (von der Haar & McCarthy, 2003). These limitations make it difficult to generate curves amenable to simple Scatchard-type analyses and thermodynamically valid rate constants for the different mRNA/gRNA pairs under similar conditions. The CYb interaction has a very slow association rate and appears to be at the limit of detection for the Biacore machine for the on-rate; however, it is within the range of the off-rate. In addition, line fitting using global analysis requires extremely high quality experimental data. Since CYbU kinetics is at the detection limit for the machine, this method of analysis proved impractical (Myszka, 1997). However, using the separate fits function of Biaevaluation 3.0 (Biacore, Uppsala, Sweden) with a global analysis for each association and dissociation curve separately allowed an analysis of the individual rate constants. The individual rate constants were averaged and the equilibrium dissociation constant was calculated from the rate constants. The errors reported were based on the variances of all curves obtained (Nordgren et al., 2001).

The NgCYb-558/5'CYbUT Interaction

For the binding of NgCYb-558 to its cognate mRNA target, CYbU, 150-250 µl of 2 mM magnesium buffer containing 200 to 1500 nM gCYb-558 were injected, at a flow rate of 10 µl/min over the surface of the sensor chip. After each injection of gRNA, buffer was allowed to flow for 15-20 minutes at 10 µl/min for dissociation rate information. A one minute injection of 8 M Urea or 10 mM EDTA was run between every cycle to strip the gRNA from the mRNA.

Using surface plasmon resonance (SPR), for CYbU+NgCYb-558 (Table 4) we saw an association rate constant (k_{on}) for CYbU+NgCYb-558 of 570 $M^{-1}s^{-1}$ (5.7 x 10^2 $M^{-1}s^{-1}$). The dissociation rate constant (k_{off}) for the CYb complex was 2.7 x 10^{-3} s^{-1} (Table 5). These numbers were calculated from separate line fits of the association and dissociation curves from the Biacore sensograms in BIAevaluation 3.0 (Biacore, Uppsala, Sweden) (Fig. 20A). The dissociation equilibrium constant (K_D) of 4.7 μM (4.7 x 10^{-6} M) was calculated from the rate constants above (Table 5) using the equation $K_D = k_{off}/k_{on}$. This K_D is ten fold higher than the apparent K_D found for CYb using gel shift assays (Koslowsky et al., 2004).

The association rate for CYbU is very slow compared to loop-loop RNA-RNA interactions such as TAR-TAR* and CopA-CopT; however, the dissociation rate is comparable to these RNA-RNA interactions (Persson et al., 1988; Nair et al., 2000; Nordgren et al., 2001). The antisense RNAs such as CopA-CopT are diffusion-controlled relying on a rapid association in conjunction with high antisense concentrations in order to achieve post-transcriptional control of plasmid propagation (Nordgren et al., 2001). The CYb mRNA stem-loop does not allow complex formation to be diffusion-controlled (i.e. mRNA and gRNA do not bind every time they come into contact). The slowness of the CYb association rate suggests that the CYbU complex probably rarely forms *in vivo* without help from an annealing factor.

The gA6-14 /A6ENDSh Interaction

For the binding of gA6-14 to its cognate mRNA target, A6UENDSh, 100-300 μl of 2 mM magnesium buffer containing 50 to 200 nM gA6-14 were injected, at a flow rate of 5 μl/min over the surface of the sensor chip. After each injection of gRNA, buffer was

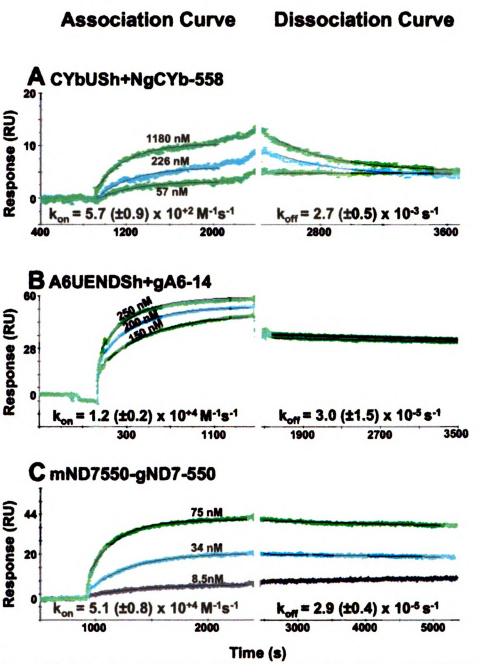

Figure 20. Separate association and dissociation line fits of the unedited CYb, A6, and ND7 Biacore sensograms. The concentration of gRNA is indicated on each graph above each line. A. Sensogram of CYbU + NgCYb-558 with first the association line fit and then the dissociation line fit. B. Sensogram of A6UENDSh + gA6-14 with first the association line fit and then the dissociation line fit. C. Sensogram of mND7550 + gND7-550 with first the association line fit and then the dissociation line fit. Each association rate constant (k_{on}) and dissociation rate constant (k_{off}) is listed with the error in parentheses. RU = resonance units and s = seconds.

mRNA	gRNA	K_D (M)	k_{on} ($M^{-1}s^{-1}$)	k_{off} (s^{-1})
CYbU	NgCYb-558	4.7×10^{-6}	$5.7 (\pm 0.9) \times 10^{+2}$	$2.7 (\pm 0.5) \times 10^{-3}$
A6UENDSh	gA6-14	2.5×10^{-9}	$1.2 (\pm 0.2) \times 10^{+4}$	$3.0 (\pm 1.5) \times 10^{-5}$
mND7550	gND7-550	5.6×10^{-10}	$5.1 (\pm 0.8) \times 10^{+4}$	$2.9 (\pm 0.4) \times 10^{-5}$

Table 5. Table of rate constants and dissociation constants calculated from CYbU, A6UENDSh, and mND7550 Biacore data from a global analysis of separate line fits. Column 1: mRNA, Column 2: gRNA, Column 3: dissociation equilibrium constants, Column 4: association rate constants, and Column 5: dissociation rate constants from surface plasmon resonance experiments run at 2 mM magnesium.

allowed to flow for 30 minutes at 5 μl/min for dissociation rate information. A one minute injection of 8 M Urea was run between every cycle to strip the gRNA from the mRNA.

Using SPR, the dissociation rate constant (k_{off}) was found to be 3.0×10^{-5} s^{-1}, and the association rate constant (k_{on}) was 12000 $M^{-1}s^{-1}$ (1.2×10^{4} $M^{-1}s^{-1}$) (Fig 20B, Table 5). The equilibrium dissociation constant (K_D) at 2 mM magnesium was calculated to be 2.5 nM (2.5×10^{-9} M) (Fig. 18B, Table 5). The A6 mRNA/gRNA complex had ~2000 fold higher affinity binding than CYbU. The single stranded, unstructured ABS allowed a ~20 fold faster association rate coupled with a dissociation rate being ~20 fold slower (Fig. 20A, B). When compared to the TAR-TAR* and CopA-CopT RNA-RNA interactions, the association rate of the A6 mRNA/gRNA complex is eighteen fold slower. The dissociation rate of A6 is 90 fold slower than these loop-loop interactions (Persson et al., 1988; Nair et al., 2000; Nordgren et al., 2001). When studying aptamers targeting the TAR RNA, the kinetic analysis of mutants showed that the stability of the complex formation is controlled by the off-rate (k_{off}) and not the on-rate (k_{on}) (Duconge et al., 2000). This appears to be true for the A6 mRNA/gRNA complex. This slow dissociation rate suggests that once the mRNA/gRNA complex forms it may be stable enough to allow formation of the editosome complex.

The gND7-550/mND7-550 Interaction

For the binding of gND7-550 to its cognate mRNA target, mND7550, 150-250 μl of 2 mM magnesium buffer containing 8.5 to 270 nM gND7-550 were injected, at a flow rate of 10 μl/min over the surface of the sensor chip. After each injection of gRNA, buffer was allowed to flow for 60 minutes at 10 μl/min for dissociation rate information. A one

minute injection of 8 M Urea was run between every cycle to strip the gRNA from the mRNA.

Using SPR, the dissociation rate constant (k_{off}) was found to be 2.9×10^{-5} s^{-1}, and the association rate constant (k_{on}) was 51000 $M^{-1}s^{-1}$ (5.1×10^{4} $M^{-1}s^{-1}$) (Fig. 18C, Table 5). Surprisingly, while the dissociation rate was almost identical to that determined for the gA6-14/A6UENDSh interation, the ND7 association rate was ~5 fold faster than A6 and ~90 fold faster than CYbU. The faster association rate resulted in a calculated equilibrium dissociation constant (K_D) of 0.56 nM (5.6×10^{-10} M) (Table 5), this was significantly lower than the K_D calculated for A6 (Table 5).

Discussion

Substantial differences are seen in both association rate and dissociation rates for all three substrates. The A6 and ND7 mRNA substrates bind with their initiating gRNAs with ~2000 and 8400 fold higher affinity respectively than the CYb mRNA binds its gRNA. It is interesting that the ND7 substrate binds its gRNA with a five fold faster association rate than the A6 substrate even though they are both predicted to have single stranded anchor binding sites. One possibility for this difference could be the G-C content of the anchor binding sites. The ND7 ABS contains 7 G-C base pairs (Fig 19C), while the A6 ABS contains only 4 G-C pairs (Fig. 19B). The CYb ABS contains 3 G-C pairs; however, two of the three residues are already in G-C bps in the mRNA stem-loop so the gRNA must compete for anchor binding (Fig. 19A, 18A). The G-C rich ABS appears to be an advantage for ND7, but may be a disadvantage for the CYb stem-loop resulting in a slower anchor binding association rate. The dissociation rate constants for A6 and ND7 are ~20 fold slower than the CYb rate. When compared to the kinetically

favorable loop-loop interaction, CYb has a similar dissociation rate, while A6 and ND7 have significantly slower dissociation rates. This suggests that in the absence of the competition of inhibitory RNA structures (such as the CYb stem-loop) the mRNA/gRNA complex is fairly stable and this stability may allow editing to occur. In addition, the A6 and ND7 mRNA/gRNA complexes have longer anchor helices than CYb. There are additional bps predicted after the editing bulge that may increase the stability of the complex that could result in a slower dissociation rate. A baseline study like this gives tentative insights into how different aspects of the two interacting RNA molecules contribute to formation of the binary complex. The mRNA structure can have a profound effect on the interaction of the gRNAs and their mRNAs. In addition, the three helix junction formed by the mRNA/gRNA complex may contribute to the stability of the complex resulting in the very slow dissociation rate.

RNA-RNA interactions are important regulators and tools in every organism. The kissing loop-loop interaction is a well characterized RNA-RNA interaction that appears to occur in all organisms. It is a kinetically favored base pairing intermediate (Chang & Tinoco, 1997) that appears to have evolved RNA structures optimized for rapid RNA-RNA interaction (Franch et al., 1999). Binding of the TAT protein to the TAR RNA is required for HIV replication and results in transcriptional activation. The TAR loop can be targeted by a complementary hairpin, TAR*, and has a very fast association rate of 10^5 $M^{-1}s^{-1}$ coupled with a dissociation rate of 10^{-3} s^{-1}. TAR-TAR* binding results in the inhibition of TAT binding as well as transcription (Nair et al., 2000). Another well characterized RNA-RNA interaction is the CopA-CopT antisense RNA that forms a stable loop-loop intermediate with its target RNA resulting in transcriptional inhibition of

the RepA protein; the RepA protein is required for plasmid replication, so CopA-CopT formation blocks plasmid replication. The CopA-CopT interaction also has a fast association rate of 10^5-10^6 $M^{-1}s^{-1}$ coupled with a dissociation rate of 10^{-3} s^{-1} (Persson et al., 1988; Nordgren et al., 2001). The TAR-TAR* interaction and the CopA-CopT binding interaction both result in transcriptional inactivation.

The mRNA/gRNA interaction appears to be different from these loop-loop RNA-RNA interactions. When compared to the mRNA/gRNA complexes, the TAR-TAR* and CopA-CopT complexes have a 370 fold faster association rate than CYbU, eighteen fold faster than A6, and four fold faster than ND7. The TAR-TAR and CopA-CopT complexes dissociate at a rate similar to CYbU and 90 fold faster than A6 and ND7. Interestingly, the dissociation rate of the complex for A6 and ND7 appears to be significantly slower than the loop-loop interactions. This suggests that formation of the anchor helix does not require a fast association rate but higher complex stability to achieve editing and may have evolved to dissociate slowly to allow editing to begin.

The CYb mRNA is edited preferentially in the insect host. The developmental nature of CYb editing (Feagin et al., 1988) is one way that trypanosomes regulate the formation of the respiration complexes when occupying different hosts (Feagin & Stuart, 1988). One of the ways that editing of CYb is developmentally controlled may be the formation of a stable mRNA stem-loop that the gRNA must invade in order to bind the mRNA.

The CYb unedited mRNA has a slower kinetic interaction between the mRNA and gRNA than A6 or ND7. The CYb mRNA/gRNA interaction likely requires a protein co-factor to initiate the intermolecular base pairing event of the unedited mRNA/gRNA complex as the binding interaction is very slow and unstable. This appears to be a

common requirement in other organisms. In *E. coli*, a sm-like protein, Hfq, was able to improve complex formation between an anti-sense RNA and its mRNA target by increasing the affinity of the anti-sense RNA for its target ~150 fold (Moller et al., 2002). A developmentally regulated protein co-factor such as Hfq could control CYb editing by selectively increasing the binding rate of the mRNA to the gRNA whether through chaperone binding activity (encourage helix formation) or helicase activity (alter RNA structure). Some mRNA/gRNA pairs already have relatively fast and stable kinetics of complex formation on their own (such as A6 and ND7) and might be less affected by regulation of this co-factor during trypanosome mitochondrial development. These RNAs could continue to be edited; although, the rate of editing might be slightly reduced in the absence of the initiating co-factor. However, the CYb mRNA editing would be severely reduced in the absence of this co-factor. There are trypanosome protein co-factors that are RNA binding proteins and may be involved in editing. One possibility is RBP16 (Hayman & Read, 1999); it has an RGG RNA-binding motif as well as a cold shock domain and binds the U-tails of gRNAs with the help of p22 (Pelletier et al., 2000; Hayman et al., 2001; Miller & Read, 2003). Another interesting possibility is the MRP1 (Koller et al., 1997) and MRP2 (Blom et al., 2001) protein complex that also binds poly U tracts and is transiently associated with the proteins of the editing complex by binding the RNAs for editing (Allen et al., 1998; Lambert et al., 1999). MRP1 has been shown to accelerate the anchor formation of annealing mRNAs and gRNAs (Muller et al., 2001) and is expected to be released once hybridization of the anchors has occurred (Muller & Goringer, 2002). RNAi knockdown of both RBP16/p22 and MRP1/MRP2 have been shown to disrupt CYb mRNA editing (Pelletier & Read, 2003; Vondruskova et al., 2005).

It will be interesting to see if these proteins are developmentally regulated in the different hosts of the life cycle. One or both of these proteins may facilitate the mRNA/gRNA complex formation and be released once the editosome binds the RNA complex.

Constitutively edited substrates such as A6 and the 5' end of the ND7 mRNAs have an easily accessible ABS that may encourage editing. A better understanding of gRNA hybridization to the mRNA ABS and the effects caused by secondary structure may provide a better understanding of the formation of mRNA/gRNA complexes during the editing process (Schwille et al., 1996). Currently, there is no data reporting how fast the rate of editing occurs, so it is unknown if an acceleration of these rate constants is necessary for *in vivo* editing.

The mND7550+gND7-550 pair has a faster mRNA/gRNA association rate than A6, but it is not edited in vitro (Reifur et al., 2006). Apparently, the structure of the mRNA and the ease of the gRNA binding are not the only factors controlling RNA editing (Reifur et al., 2006). Previous gel shift assays have shown multiple bands of migration of the mRNA/gRNA complex suggesting multiple conformations (Koslowsky et al., 2004; Reifur et al., 2006). In the hepatitis delta virus, the secondary structure of its RNA controls editing of this RNA by its host. Only RNAs with a branched secondary structure are edited (Linnstaedt et al., 2006). Perhaps only mRNA/gRNA complexes that adopt the correct tertiary structure can be recognized by the editing machinery *in vitro*. Of the mRNA/gRNA complexes studied to date, it appears that A6 is the only mRNA/gRNA complex that folds into the correct tertiary complex in the absence of chaperones. So while editing of CYb appears to be controlled kinetically, editing of other mRNAs such as ND7 may be controlled structurally.

Other RNAs, such as ribozymes, containing three helix junctions similar to the mRNA/gRNA complex can exist in the inactive extended conformations for long periods of time and may require regulatory ligands to transition to the correct tertiary structure (Klostermeier & Millar, 2000). In the same manner, the mRNA/gRNA complex may require a chaperone to transition to the correct tertiary structure for editing. In addition, some RNA binding proteins may be required to stabilize the RNA structure; however, in the absence of proper folding these proteins may exacerbate kinetic traps (Mohr et al., 2002) instead of stabilizing the correct structure for editing.

Surface plasmon resonance (SPR) is a label free method capable of determining the kinetics of binding of the mRNA/gRNA complex formation. The equilibrium dissociation constants (K_D) calculated using BIACORE are similar to those calculated using gel shift assays for ND7 and A6 mRNA/gRNA complexes (Reifur et al., 2006), whereas the CYb BIACORE determined K_D is ten fold higher than that previously reported using gel shift assays (Koslowsky et al., 2004). Previous reports of SPR suggest that, although SPR works well for some RNA-RNA substrates, the k_{on} values measured for some substrates are lower when compared to other methods (Slagter-Jäger, 2003). This will be discussed in more depth in Chapter four.

In conclusion, editing may be controlled on many different levels. Substrates such as the CYb mRNA appear to be regulated kinetically with a slow on-rate and a fast off-rate, while substrates such as ND7 and A6 are not kinetically regulated as shown by the relatively fast on-rate and very slow off-rate. The slow dissociation rates of the A6 and ND7 substrates may have evolved to allow the correct editosome complex to assemble on a stable mRNA/gRNA complex. This study provides information on how the

mRNA/gRNA complexes interact; future studies using proteins will show how these interactions differ in the presence of proteins.

MATERIALS AND METHODS

Oligodeoxyribonucleotides

All oligodeoxyribonucleotides (Table 6) were ordered from Integrated DNA Technologies, Inc. (Coralville, IA).

RNA Synthesis and Labeling

The templates and sequences for CYbU have been previously described and were amplified using primers, CYb(-BigSK) and T7CYbShort, listed in Table 6 (Yu & Koslowsky, 2006). The template for A6UENDSh (5'-AATTTAATACGACTCACTATAGGAAAGGTTAGGGGGAGGAGAGAAGAA AGGGAAAGTTGTGATTTTGGAGTTATAGAATAAGATCAAATAAGTTAATAAT A-3') was amplified using primers, T7A6short and 3'A6END-4, listed in Table 6. NgCYb-558 (Leung & Koslowsky, 1999, 2001a, b) as well as gA6-14 and gND7-550 (Table 4) were synthesized using the Uhlenbeck single-stranded T7 transcription method (Milligan et al., 1987) with the oligonucleotides described in Table 6. All RNAs were synthesized by T7 RNA polymerase using a Ribomax Large Scale RNA production kit (Promega) according to the manufacturer's directions. RNAs were gel purified as described previously (Koslowsky et al., 2004). The mND7550 transcript (Table 7) was purchased from Dharmacon (Boulder, CO).

Name	Sequence	Length (nts.)
T7 22mer	5'-AATTTAATACGACTCACTATAG-3'	22
NgCYb-558	5'-AAAAAAAAAAAAAAATTATTCCCTT TATCACCTAGAAATTCACATTGTCTTTT AATCCCTATAGTGAGTCGTATTAAATT-3'	80
NgA6-14	5'-AAAAAAAAAAAAAAATAATTATCATATC ACTGTCAAAATCTGATTCGTTATCGGAGTTA TAGCCCTATAGTGAGTCGTATTAAATT-3'	86
gND7-550	5'-AAAAAAAAAAAAAAATATTCACATTTA TATCATCTTACACTTAATCCACTGCATCCC TATAGTGAGTCGTATTAAATT-3'	78
T7CYbShort	5'-AATTTAATACGACTCACTATAGGGT TATAAAT-3'	32
CYb(-BigSK)	5'-GATCCATATATTCTATATAAACAA CCTGACATT-3'	33
T7A6short	5'-AATTTAATACGACTCACTATAGGAAA GG-3'	28
3'A6END-4	5'-TATTATTAACTTATTTGATCTTATTCT ATAACTCCAA-3'	37
3'BigSK-biotin	5'-CACTAGTTCTAGAGCGGCC-biotin-3'	19
CYbbigskBIAbridge	5'-GCTCTAGAACTAGTGGATCCATATAT TCTA-3'	30
A6bigskBIAbridge	5'-GCTCTAGAACTAGTGTATTATTAAC TTATTTG-3'	32
ND7550BigSKBIA bridge	5'GCTCTAGAACTAGTGCTGTGCTGAAAC GGG3'	30
Biatag1	5'-ATATGAGTAGGTAATTAGTA-biotin-3'	20
Biatag1CYbbridge	5'-ATTACCTACTCATATGATCCATATA TTCTA-3'	30

Table 6. List of oligodeoxyribonucleotides ordered from Integrated DNA Technologies (Coralville, IA).

Name	Sequence	Lengt h(nts.)
mND7550	5'-AAAAACAUGACUACAUGAUAAGUACAAGAGG AGACAGACGACAGUGUCCACAGCACCCGUUUCAGCACA G-3'	70

Table 7. Oligoribonucleotide ordered from Dharmacon (Boulder, CO).

Surface Plasmon Resonance Studies

All Biacore mRNA and gRNA substrates are listed in Table 4. All the bridging oligonucleotides are listed in Table 6. Measurements of the association and dissociation rate constants were performed in a BIACORE 2000 instrument (BIACORE, Uppsala, Sweden). All the solutions used in the binding studies were filtered through a 0.22 μm polyethersulfone membrane (Corning) or a 0.22 μm Millex-GS membrane (Millipore) and degassed. The CYbU, A6, and ND7 mRNAs were ligated to the BigSK-biotin DNA tag. CYbU was also ligated to Biatag1, a different biotinylated DNA tag; the measurements of CYbU were similar regardless of the DNA tag that was attached. BigSK-biotin or Biatag1 was annealed to the 3' end of the appropriate RNA using DNA bridging oligonucleotides (Table 6) as described previously (Yu & Koslowsky, 2006). The biotinylated mRNAs were gel extracted without phenol and purified using ultra-free MC membranes (Millipore) and microcon tubes (YM-50, Millipore) according to the manufacturer's directions. The gRNAs were transcribed as described above and purified using Ultra-free MC and the microcon tubes (YM-10, 30) (Millipore) as above. The RNA samples were then diluted in running buffer (100 mM Tris pH 7.5, 0.1 mM EDTA, 2 mM $MgCl_2$, and 100 mM KCl). The biotinylated mRNA was diluted to 10 nM and between 50-400 resonance units (RU) of mRNA was attached at 5 μl/min to a streptavidin coated SA sensor chip (BIACORE, Uppsala, Sweden); the better the

mRNA/gRNA interaction the less mRNA was attached. Two cells were immobilized with mRNA, one was left unmodified to serve as a reference cell, and one cell was immobilized with the biotinylated DNA tag as a control cell. Binding studies were carried out running all four cells in series with repetitive cycles of 100-300 µl gRNA injection at 5-10 µl/min (association of varying concentrations of gRNA), buffer flow (dissociation of gRNA) 5-10 µl/min for 15-60 minutes, and regeneration (50 µl injection of regeneration buffer, two 50 µl injections of running buffer at 50µl/min). These experiments were all run at 27° C. The regeneration buffer for the CYb experiments was 10 mM EDTA or 8 M Urea, the regeneration buffer for the A6 and ND7 experiments was 8 M Urea. The determination of rate constants was performed by fitting theoretical curves to the experimental curves we obtained using BIAevaluation 3.0 software (BIACORE, Uppsala, Sweden). The equation used to calculate the association rate constant was the 1:1 (Langmuir) association formula describing analyte (gRNA) binds to ligand (mRNA):

$$\frac{k_a * Conc * R_{max}}{(k_a * Conc + k_d)} \times \left(1 - e^{\left(-(k_a * Conc + k_d) * (t - t0)\right)}\right) + RI$$, k_a = association rate constant (k_{on}), $Conc$ = molar analyte concentration, RI = bulk refractive index effect (RU), R_{max} = Y_{max} = maximum analyte binding capacity (RU), t = time, $t0$ = time at start, k_d = dissociation rate constant (k_{off}). The equation used to calculate the dissociation rate constants for A6 and ND7 from the Biacore sensograms was the 1:1 (Langmuir) dissociation formula describing analyte (gRNA) dissociates from surface complex (mRNA/gRNA complex): $R0 * e^{\left(-k_d * (t - t0)\right)} + Offset$, $R0$ = Y_{max} = maximum analyte binding capacity (RU), k_d = dissociation rate constant, t = time, $t0$ =

time at start, *Offset* = residual response at infinite time (RU). The equation was slightly altered for the CYb dissociation rate constant: $(R0 - Offset) * e^{(-k_d * (t - t0))} + Offset$. Separate fits for each association and dissociation curve were analyzed globally from each experiment to obtain k_{on} and k_{off}, individually, and the results were averaged. The dissociation equilibrium constant (K_D) was calculated from the averages of the rate constants using the equation: $K_D = \frac{k_d}{k_a}$. The errors reported for the rate constants were based on the variances of all curves obtained (Nordgren et al., 2001).

ACKNOWLEDGEMENTS

This work was supported by National Institutes of Health Grant AI34155 to D.K. We'd like to thank Larissa Reifur, Dr. Ron Patterson, Dr. John Wang, Dr. Charles Hoogstraten, and all other members of the MSU RNA Journal Club for critical reading of the manuscript and helpful discussions. We would like to thank Dr. Joseph Leykam and the members of the Macromolecular Structure Facility in the Biochemistry and Molecular Biology Department for the use the Biacore machine.

Literature Cited

Allen TE, Heidmann S, Reed R, Myler PJ, Goringer HU, Stuart KD. 1998. Association of guide RNA binding protein gBP21 with active RNA editing complexes in Trypanosoma brucei. *Mol Cell Biol 18*:6014-6022.

Bhat GJ, Koslowsky DJ, Feagin JE, Smiley BL, Stuart K. 1990. An extensively edited mitochondrial transcript in kinetoplastids encodes a protein homologous to ATPase subunit 6. *Cell 61*:885-894.

Blom D, Burg J, Breek CK, Speijer D, Muijsers AO, Benne R. 2001. Cloning and characterization of two guide RNA-binding proteins from mitochondria of Crithidia fasciculata: gBP27, a novel protein, and gBP29, the orthologue of Trypanosoma brucei gBP21. *Nucleic Acids Res 29*:2950-2962.

Blum B, Bakalara N, Simpson L. 1990. A model for RNA editing in kinetoplastid mitochondria: "guide" RNA molecules transcribed from maxicircle DNA provide the edited information. *Cell 60*:189-198.

Blum B, Simpson L. 1990. Guide RNAs in kinetoplastid mitochondria have a nonencoded 3' oligo(U) tail involved in recognition of the preedited region. *Cell 62*:391-397.

Chang KY, Tinoco I, Jr. 1997. The structure of an RNA "kissing" hairpin complex of the HIV TAR hairpin loop and its complement. *J Mol Biol 269*:52-66.

Corell RA, Feagin JE, Riley GR, Strickland T, Guderian JA, Myler PJ, Stuart K. 1993. Trypanosoma brucei minicircles encode multiple guide RNAs which can direct editing of extensively overlapping sequences. *Nucleic Acids Res 21*:4313-4320.

Duconge F, Di Primo C, Toulme JJ. 2000. Is a closing "GA pair" a rule for stable loop-loop RNA complexes? *J Biol Chem 275*:21287-21294.

Feagin JE, Jasmer DP, Stuart K. 1985. Apocytochrome b and other mitochondrial DNA sequences are differentially expressed during the life cycle of Trypanosoma brucei. *Nucleic Acids Res 13*:4577-4596.

Feagin JE, Jasmer DP, Stuart K. 1987. Developmentally regulated addition of nucleotides within apocytochrome b transcripts in Trypanosoma brucei. *Cell 49*:337-345.

Feagin JE, Shaw JM, Simpson L, Stuart K. 1988. Creation of AUG initiation codons by addition of uridines within cytochrome b transcripts of kinetoplastids. *Proc Natl Acad Sci U S A 85*:539-543.

Feagin JE, Stuart K. 1988. Developmental aspects of uridine addition within mitochondrial transcripts of Trypanosoma brucei. *Mol Cell Biol 8*:1259-1265.

Franch T, Petersen M, Wagner EG, Jacobsen JP, Gerdes K. 1999. Antisense RNA regulation in prokaryotes: rapid RNA/RNA interaction facilitated by a general U-turn loop structure. *J Mol Biol 294*:1115-1125.

Hayman ML, Miller MM, Chandler DM, Goulah CC, Read LK. 2001. The trypanosome homolog of human p32 interacts with RBP16 and stimulates its gRNA binding activity. *Nucleic Acids Res 29*:5216-5225.

Hayman ML, Read LK. 1999. Trypanosoma brucei RBP16 is a mitochondrial Y-box family protein with guide RNA binding activity. *J Biol Chem 274*:12067-12074.

Katsamba PS, Park S, Laird-Offringa IA. 2002. Kinetic studies of RNA-protein interactions using surface plasmon resonance. *Methods 26*:95-104.

Klostermeier D, Millar DP. 2000. Helical junctions as determinants for RNA folding: origin of tertiary structure stability of the hairpin ribozyme. *Biochemistry 39*:12970-12978.

Koller J, Muller UF, Schmid B, Missel A, Kruft V, Stuart K, Goringer HU. 1997. Trypanosoma brucei gBP21. An arginine-rich mitochondrial protein that binds to guide RNA with high affinity. *J Biol Chem 272*:3749-3757.

Koslowsky DJ, Bhat GJ, Perrollaz AL, Feagin JE, Stuart K. 1990. The MURF3 gene of T. brucei contains multiple domains of extensive editing and is homologous to a subunit of NADH dehydrogenase. *Cell 62*:901-911.

Koslowsky DJ, Reifur L, Yu LE, Chen W. 2004. Evidence for U-Tail Stabilization of gRNA/mRNA Interactions in Kinetoplastid RNA Editing. *RNA Biology 1*:28-34.

Lambert L, Muller UF, Souza AE, Goringer HU. 1999. The involvement of gRNA-binding protein gBP21 in RNA editing-an in vitro and in vivo analysis. *Nucleic Acids Res 27*:1429-1436.

Leung SS, Koslowsky DJ. 1999. Mapping contacts between gRNA and mRNA in trypanosome RNA editing. *Nucleic Acids Res 27*:778-787.

Leung SS, Koslowsky DJ. 2001a. Interactions of mRNAs and gRNAs involved in trypanosome mitochondrial RNA editing: structure probing of an mRNA bound to its cognate gRNA. *RNA 7*:1803-1816.

Leung SS, Koslowsky DJ. 2001b. RNA editing in Trypanosoma brucei: characterization of gRNA U-tail interactions with partially edited mRNA substrates. *Nucleic Acids Res 29*:703-709.

Linnstaedt SD, Kasprzak WK, Shapiro BA, Casey JL. 2006. The role of a metastable RNA secondary structure in hepatitis delta virus genotype III RNA editing. *RNA 12*:1521-1533.

Miller MM, Read LK. 2003. Trypanosoma brucei: functions of RBP16 cold shock and RGG domains in macromolecular interactions. *Exp Parasitol 105*:140-148.

Milligan JF, Groebe DR, Witherell GW, Uhlenbeck OC. 1987. Oligoribonucleotide synthesis using T7 RNA polymerase and synthetic DNA templates. *Nucleic Acids Res 15*:8783-8798.

Mohr S, Stryker JM, Lambowitz AM. 2002. A DEAD-box protein functions as an ATP-dependent RNA chaperone in group I intron splicing. *Cell 109*:769-779.

Moller T, Franch T, Hojrup P, Keene DR, Bachinger HP, Brennan RG, Valentin-Hansen P. 2002. Hfq: a bacterial Sm-like protein that mediates RNA-RNA interaction. *Mol Cell 9*:23-30.

Moore MJ, Sharp PA. 1992. Site-specific modification of pre-mRNA: the 2'-hydroxyl groups at the splice sites. *Science 256*:992-997.

Muller UF, Goringer HU. 2002. Mechanism of the gBP21-mediated RNA/RNA annealing reaction: matchmaking and charge reduction. *Nucleic Acids Res 30*:447-455.

Muller UF, Lambert L, Goringer HU. 2001. Annealing of RNA editing substrates facilitated by guide RNA-binding protein gBP21. *Embo J 20*:1394-1404.

Myszka DG. 1997. Kinetic analysis of macromolecular interactions using surface plasmon resonance biosensors. *Curr Opin Biotechnol 8*:50-57.

Nair TM, Myszka DG, Davis DR. 2000. Surface plasmon resonance kinetic studies of the HIV TAR RNA kissing hairpin complex and its stabilization by 2-thiouridine modification. *Nucleic Acids Res 28*:1935-1940.

Nordgren S, Slagter-Jager JG, Wagner GH. 2001. Real time kinetic studies of the interaction between folded antisense and target RNAs using surface plasmon resonance. *J Mol Biol 310*:1125-1134.

Pelletier M, Miller MM, Read LK. 2000. RNA-binding properties of the mitochondrial Y-box protein RBP16. *Nucleic Acids Res 28*:1266-1275.

Pelletier M, Read LK. 2003. RBP16 is a multifunctional gene regulatory protein involved in editing and stabilization of specific mitochondrial mRNAs in Trypanosoma brucei. *RNA 9*:457-468.

Persson C, Wagner EG, Nordstrom K. 1988. Control of replication of plasmid R1: kinetics of in vitro interaction between the antisense RNA, CopA, and its target, CopT. *Embo J 7*:3279-3288.

Reifur L, Cruz-Reyes J, vanHartesvelt M, Koslowsky DJ. 2006. Anchor binding site accessibility and RNA editing in Trypanosoma brucei. *manuscript in prep.*

Reifur L, Koslowsky DJ. 2006. Secondary structure of the ATPase 6 mRNA/gRNA complex. East Lansing, MI: Personal communication.

Schmid B, Riley GR, Stuart K, Goringer HU. 1995. The secondary structure of guide RNA molecules from Trypanosoma brucei. *Nucleic Acids Res 23*:3093-3102.

Schwille P, Oehlenschlager F, Walter NG. 1996. Quantitative hybridization kinetics of DNA probes to RNA in solution followed by diffusional fluorescence correlation analysis. *Biochemistry 35*:10182-10193.

Simpson L, Aphasizhev R, Gao G, Kang X. 2004. Mitochondrial proteins and complexes in Leishmania and Trypanosoma involved in U-insertion/deletion RNA editing. *RNA 10*:159-170.

Slagter-Jäger JG. 2003. CopA and CopT: The Perfect RNA Couple. *Department of Cell and Molecular Biology*. Uppsala, Sweden: Uppsala University. pp 1-47.

Stuart KD, Schnaufer A, Ernst NL, Panigrahi AK. 2005. Complex management: RNA editing in trypanosomes. *Trends Biochem Sci 30*:97-105.

von der Haar T, McCarthy JE. 2003. Studying the assembly of multicomponent protein and ribonucleoprotein complexes using surface plasmon resonance. *Methods 29*:167-174.

Vondruskova E, van den Burg J, Zikova A, Ernst NL, Stuart K, Benne R, Lukes J. 2005. RNA interference analyses suggest a transcript-specific regulatory role for mitochondrial RNA-binding proteins MRP1 and MRP2 in RNA editing and other RNA processing in Trypanosoma brucei. *J Biol Chem 280*:2429-2438.

Yu LE, Koslowsky DJ. 2006. Interactions of mRNAs and gRNAs involved in trypanosome mitochondrial RNA editing: structure probing of an gRNA bound to its cognate mRNA. *RNA 12*:1050-1060.

CHAPTER 4

INTERACTIONS OF MRNAS AND GRNAS INVOLVED IN TRYPANOSOME MITOCHONDRIAL RNA EDITING: MEASUREMENTS OF RNA BINDING RATES FOR A GRNA BOUND TO ITS MRNA AS EDITING PROGRESSES

INTRODUCTION

In trypanosomes, many of the protein coding regions of mitochondrial transcripts are untranslatable until post-transcriptional editing occurs. This process involves >20 proteins, collectively known as the editosome, precisely inserting and deleting uridylates as directed by a guide RNA (gRNA) template (Blum et al., 1990; Blum & Simpson, 1990; Seiwert & Stuart, 1994; Adler & Hajduk, 1997; Simpson et al., 2004; Stuart et al., 2005). The editing process can extensively alter mRNA transcripts by adding and deleting hundreds of uridylates and may require several gRNAs. Editing creates the proper open reading frame for mitochondrial transcripts including the correct initiation and termination codons. The gRNAs that direct the editing process are short RNA molecules (~50-70 nucleotides) made of three functional elements. At the 5' end of the gRNA is a 5-21 nucleotide region known as the anchor that is complementary to the mRNA just 3' of the editing domain. The second element, known as the guiding region, region is complementary to the mature mRNA (allowing G-U base pairs) and serves as the template for proper editing of the mRNA. The post-transcriptionally added poly-uridylate tail (~15 nts) is the third element (Blum et al., 1990; Blum & Simpson, 1990). It appears to play a versatile role in the editing process.

The gRNA plays key roles in the template directed cleavage, uridylate insertion or deletion and finally religation of the transcript (Simpson et al., 2004; Stuart et al., 2005). Therefore, the ability of the gRNAs to target their cognate substrates efficiently is an important part of the editing process. In previous work, different mRNA/gRNA pairs were used to measure the affinity each initiating gRNA had for its cognate mRNA. One of these substrates was the unedited apocytochrome b (CYb) mRNA with its initiating

gRNA, NgCYb-558 (Koslowsky et al., 2004). Editing of the CYb mRNA is developmentally regulated occurring preferentially in the insect host (procyclic) (Feagin et al., 1985). The interaction between NgCYb-558 and its cognate unedited mRNA is very weak with apparent K_D's in the μM range. Solution structure probing indicates that the CYb mRNA forms a stable stem-loop structure, with the anchor binding site (ABS) sequestered within the double-stranded stem (Leung & Koslowsky, 2001a). We hypothesize that the regulation of the editing of CYb mRNA is thermodynamically controlled by the structure of the mRNA. The initiating gRNA, NgCYb-558, has to invade the mRNA secondary structure to bind to the anchor binding site of the mRNA and almost certainly requires a protein co-factor for efficient interaction. In contrast, for two other gRNAs which show very high affinity for their cognate targets (gA6-14 and gND7-550) no significant secondary structure need be disrupted (Reifur et al., 2006). The structure of the immediate editing domain can profoundly affect the efficiency of the interaction between the mRNA and gRNA. This interaction between the mRNA/gRNA complex leads to editing that results in changes of sequence and structure of the mRNA/gRNA complex.

The structure of the CYb mRNA/gRNA complex has been previously studied. Solution structure probing of the CYb mRNA/gRNA complex reveals a 3 helical junction surrounding the first few editing sites (Fig. 21A) that while modified by editing, can be maintained through the third editing site (Fig. 21B,C) (Yu & Koslowsky, 2006). As editing increases the length of the anchor duplex, the gRNA stem-loop is maintained by alternate base pairs that include the U-tail. This results in a decrease in the number of base-pair interactions between the U-tail and the purine-rich mRNA located upstream of

Figure 21

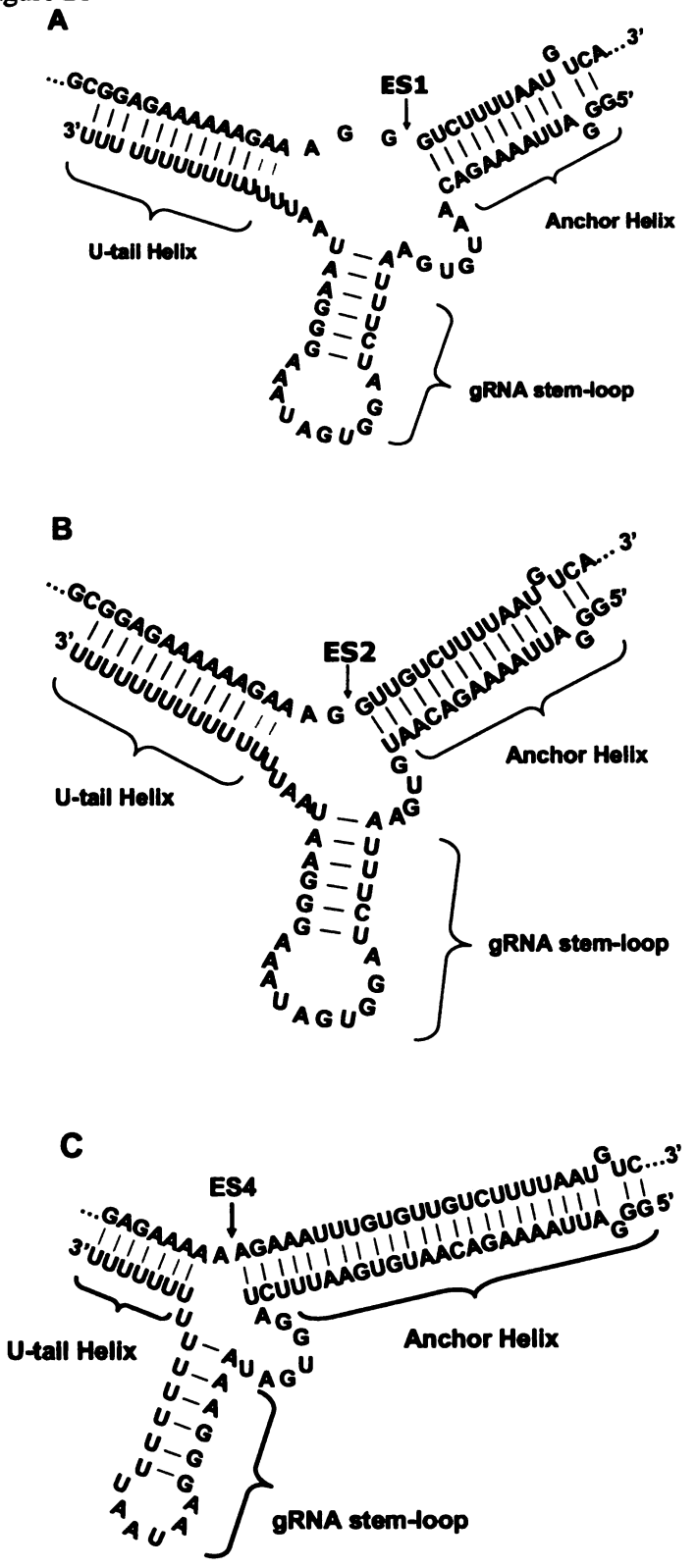
A
ES1
U-tail Helix
Anchor Helix
gRNA stem-loop
B
ES2
U-tail Helix
Anchor Helix
gRNA stem-loop
C
ES4
U-tail Helix
Anchor Helix
gRNA stem-loop

Figure 21. The predicted model for mRNA/gRNA complex secondary structure has three predicted helices: an mRNA/gRNA anchor helix, a gRNA stem-loop of the guiding region, and a U-tail/mRNA duplex. A. 5'CYbUT-NgCYb-558 pair with ES1 showing the first editing site is just 5' (mRNA) of the anchor. B. 5'CYbPES1T-NgCYb-558 pair with ES2 showing the second editing site just 5' (mRNA) of the anchor. C. 5'CYbPES3T-NgCYb-558 pair with ES4 showing the fourth editing site just 5' of the anchor. Notice the anchor has doubled in length.

the editing site. In this study, the kinetic effects of these sequence and structural changes during the initial editing events were investigated. Using both native electrophoretic mobility shift assays (EMSA) and surface plasmon resonance, the ability of NgCYb-558 to pair with the unedited CYb substrate (CYbU) with a substrate edited through site one (ES1, CYbPES1) and a substrate edited through editing site three (ES3, CYbPES3) (Fig. 22) was investigated. Surprisingly, the editing of one site (ES1, the addition of two uridines) decreases the equilibrium dissociation constant (K_D) significantly. Editing through site three (CYbPES3, the addition of 4 uridines and a doubling of the size of the anchor helix) also decreased the dissociation constant. The effects of editing on the stability of the mRNA/gRNA complex were interesting. Analysis of the binding kinetics using the surface plasmon resonance data indicate that stability is controlled by the off-rate (dissociation rate) rather than by the on-rate (association rate). In contrast, data from the EMSA gels indicate that the binding kinetics is controlled both by the on-rate and by the off-rate. Surprisingly, kinetic measurements indicate that the absence of the U-tail results in a two fold slower association rate constant for the gRNA binding the unedited CYb mRNA using both methods. This results in a two fold decrease in the affinity of binding (K_D). In addition, while the U-tail played a significant role in stabilizing the interaction of NgCYb-558 with the unedited substrate, it did not significantly increase the stability of the partially edited substrates. The U-tail was found to interact with the loop and bulge region that surround the anchor binding site. This suggests that the U-tail is helping the CYb gRNA/mRNA complex form by helping disrupt the mRNA stem-loop through binding one side of the helix that hides the anchor binding site.

Figure 22

A

5'CYbUT transcript:

*GGGCGAAUUGGGUACCGUUAAGAAUAAU*GGUUAUAAAUUUUAUAUAAAAGCGGAGAAAAA
AGAAAGGGUCUUUUAAUGUCAGGUUGUUUAUAUAGAAUAUAUGG*auccacuaguucuaga*
gcggcc

5'CYbUT aligned to NgCYb-558:

```
GGUUAUAAAUUUUAUAUAAAAGCGGAGAAAAAAGAAAGGGUCUUUUAAUGUCAGGUUGUUUAUAUAGA..
-----------------------------------------||||||||||#:|
NgCYb558AAUAAGGGAAAUAGUGGAUCUUUAAGUGUAACAGAAAAUUAGGG
```

B

5'CYbPES1T transcript:

GGGCGAAUUGGGUACCGUUAAGAAUAAUGGUUAUAAAUUUUAUAUAAAAGCGGAGAAAAA
AGAAAGGUUGUCUUUUAAUGUCAGGUUGUUUAUAUAGAAUAUAUGG*auccacuaguucua*
gagcggcc

5'CYbPES1T aligned to NgCYb-558:

```
GGUUAUAAAUUUUAUAUAAAAGCGGAGAAAAAAGAAAGGUUGUCUUUUAAUGUCAGGUUGUUUAUAUAG..
--------------------------------------:||||||||||||#:|
NgCYb-558-AAUAAGGGAAAUAGUGGAUCUUUAAGUGUAACAGAAAAUUAGGG
```

C

5'CYbPES3T transcript:

GGGCGAAUUGGGUACCGUUAAGAAUAAUGGUUAUAAAUUUUAUAUAAAAGCGGAGAAAAA
AGAAAuuuGuGuuGUCUUUUAAUGUCAGGUUGUUUAUAUAGAAUAUAUGG*auccacuagu*
ucuagagcggcc

5'CYbPES3T aligned to NgCYb-558:

```
GGUUAUAAAUUUUAUAUAAAAGCGGAGAAAAAAGAAAuuuGuGuuGUCUUUUAAUGUCAGGUUGUUUA..
---------------------------------|||||||::::||||||||||||#:|
NgCYb-558-UUUUAAUAAGGGAAAUAGUGGAUCUUUAAGUGUAACAGAAAAUUAGGG
```

D

NgCYb-558 transcript):

5'GGGAUUAAAAGACAAUGUGAAUUUCUAGGUGAUAAAGGGAAUAAUUAUUUUUUUUUUUUUUU3'

NgCYb-558sU transcript):

5'GGGAUUAAAAGACAAUGUGAAUUUCUAGGUGAUAAAGGGAAUAAUUA3'

gCYb558AnchorComplement:

5'TTGTCTTTTAATCCC3'

gCYb558longAnchorComplement:

5'AGAAATTCACATTGTCTTTTAATCCC 3'

```
                                    gCYb558longAnchorComplement
                                  5'AGAAATTCACATTGTCTTTTAATCCC3'
                                    |||||||||||||||||||||||||
NgCYb-558sU:AAUAAGGGAAAUAGUGGAUCUUUAAGUGUAACAGAAAAUUAGGG5'
                                                 |||||||||||||||
                                               5'TTGTCTTTTAATCCC3'
                                          gCYb558AnchorComplement
```

Figure 22. The sequences of the RNAs used for Chapter 4 experiments. Lowercase, italic letters = vector sequence, # = mismatched sequence, : = GU base-pair, | = complementary sequence, the aligned anchors are bold. A. The 5'CYbUT transcript and 5'CYbUT aligned to NgCYb-558 at the anchors. The CYbU transcript is represented by the underlined portion of 5'CYbUT. B. The 5'CYbPES1T transcript and 5'CYbPES1T aligned to NgCYb-558 at the anchors. The CYbPES1 sequence is represented by the underlined portion of 5'CYbPES1T. C. The 5'CYbPES3T transcript and 5'CYbPES3T aligned to NgCYb-558 at the anchors. The CYbPES3 sequence is represented by the underlined portion of 5'CYbPES3T. Notice that the anchor for 5'CYbUT has 13 base-pairs, the anchor for 5'CYbPES1T has become 16 base-pairs, and the anchor for 5'CYbPES3T has doubled to become 26 base-pairs. D. The NgCYb-558 transcript and the NgCYb-558sU transcript with no U-tail. The gCYb558AnchorComplement sequence is the oligonucleotide added to the CYbU and CYbPES1 dissociation rate constant gels, while the gCYb558longAnchorComplement is the oligonucleotide added to the CYbPES3 dissociation rate constant gels. The oligonucleotides are aligned with the NgCYb-558 sequence.

RESULTS

The binding of the gRNA to mRNA is a fundamental step in RNA editing. From miRNA studies, it is known that a "seed" sequence composed of ~5 nts at the 5' end of the miRNA is responsible for targeting its cognate mRNA for destruction or repression (Lewis et al., 2005). Similarly, substrate recognition between the gRNA and mRNA is mediated by base pairing interactions between the 5' anchor sequence (~5-21 nts) of the gRNA and its mRNA (Blum et al., 1990). Understanding the elements that confer both affinity and specificity on this interaction is critical to understanding the editing process.

In this study, electrophoretic mobility shift assays (EMSA), or gel shift assays, were used to find the equilibrium dissociation constant (K_D) for the binding interaction of the gRNA with the mRNA during editing. Additionally, EMSA and surface plasmon resonance were used to discover how the dissociation rate constants (k_{off}) as well as the association rate constants (k_{on}) change as editing proceeds. Taking a direct measurement of association and dissociation rates allowed for a more accurate assessment of the kinetics of binding (Young & Wagner, 1991).

RNA substrates

Three progressively edited CYb partial mRNAs composed of the first 88 nts from the CYb 5' end were used (Fig. 22). The 5'CYbUT sequence is an unedited substrate and has been previously described. The 5'CYbPES1T and 5'CYbPES3T substrates were edited through the first editing site (2 uridylate residues inserted) and the first three editing sites (a total of 6 uridylates inserted), respectively, and have also been previously described. The CYbU, CYbPES1, and CYbPES3 substrates were identical to the "T" substrates except the tag vector sequence had been removed (Fig. 22) (Leung & Koslowsky, 2001a).

In previous work, the structure of the unedited CYb mRNA alone was found to be a strongly base paired stem-loop with the first three editing sites contained in a terminal 5 nt loop (Fig. 23A) (Leung & Koslowsky, 2001a). Editing of the first site was predicted to add 2 uridylates to the terminal loop (Fig. 23B). Editing of the first three sites appeared to add an additional 6 uridines to the terminal loop, but otherwise did not significantly change the structure found within the stem region (Fig. 23C) (Yu & Koslowsky, 2006). Editing changed the structure of the mRNA. The anchor binding site (ABS) of the unedited CYb mRNA was composed of 13 base pairs. With the first editing event, 2 uridines were inserted at the 5' end of the ABS and were predicted to extend it 3 bps (15 bps total) exposing the three residues in a terminal loop of 9 bps (Fig. 23B). After the third editing event, the mRNA (5'CYbPES3T) structure changed again and now had 4 additional uridylates inserted into two more editing sites. The ABS was composed of 26 bps (doubled in length) and the loop region of 13 bps was single stranded and available to bind the CYb gRNA (Fig. 23C).

The gRNA construct, NgCYb-558, is 59 nucleotides long including a 15 nt. uridylate tail (U-tail) and has been described previously (Fig. 22) (Leung & Koslowsky, 2001b). NgCYb-558 is almost identical to wildtype and directs 21 uridylate insertions at the first 7 editing sites. The effects caused by the absence of the U-tail during the binding interaction was also investigated using a 44 nt. NgCYb-558sU (no U-tail) gRNA (Leung & Koslowsky, 2001b).

Equilibrium binding studies

The CYb mRNA and gRNA substrates for the EMSA (electrophoretic mobility shift assays) experiments were transcribed *in vitro*. The gRNAs were 5' end labeled by

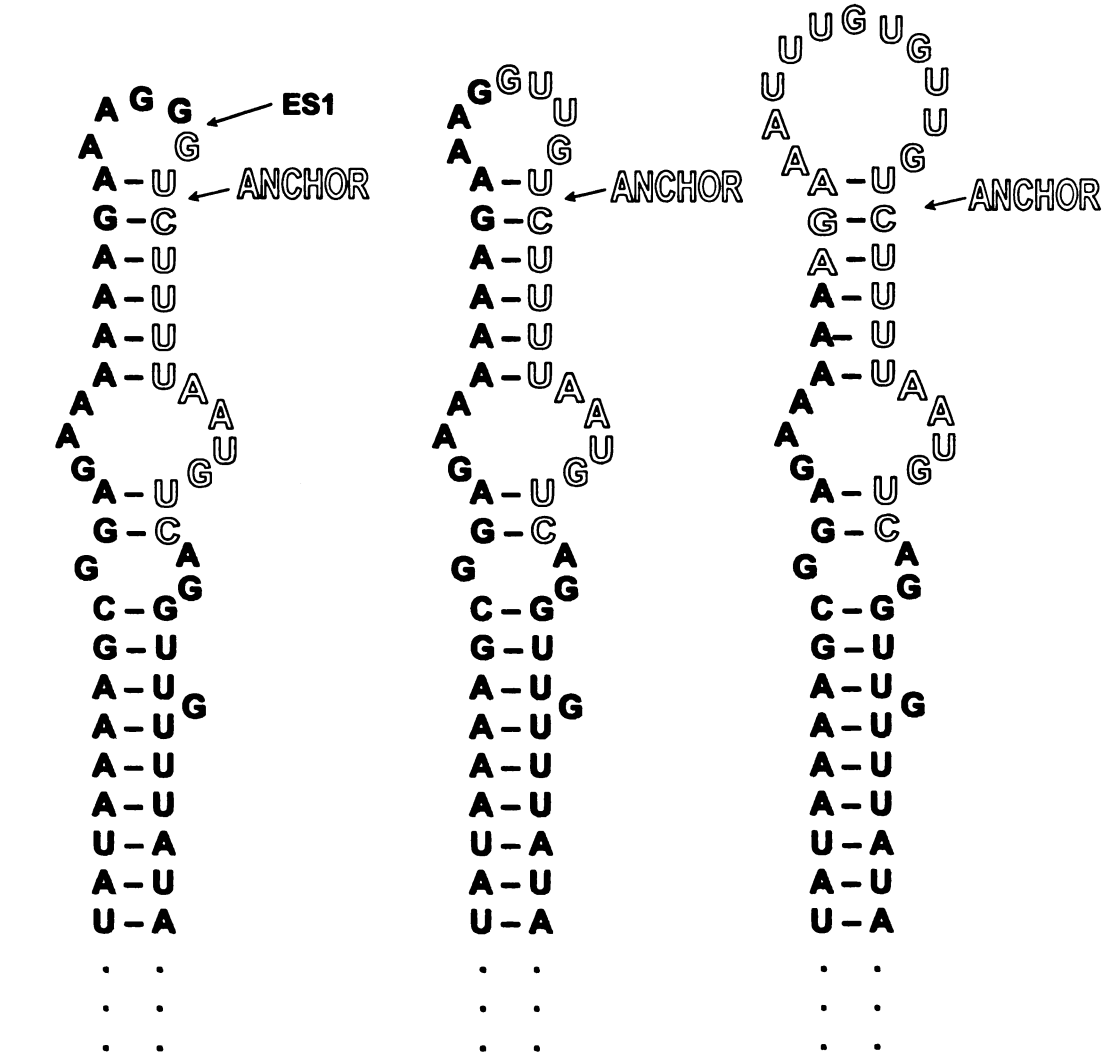

Figure 23. Predicted secondary structures of the CYb mRNAs. A. 5'CYbUT, the unedited mRNA, forms a stable stem-loop with the first few editing sites positioned within the terminal loop of 5 base pairs. B. 5'CYbPES1T, a partially edited mRNA, also forms a stem-loop with the two uridines added at the first editing site enlarging the terminal loop by three bases. C. 5'CYbPES3T, another partially edited mRNA, forms a stem-loop with a large 11 base terminal loop that includes the six uridines inserted into the first three editing sites. The hollow nucleotides represent the anchor binding site (ABS) where the gRNA anchor binds to form the mRNA/gRNA complex.

treatment with calf intestinal phosphatase (Invitrogen) using T4 kinase and [γ ^{32}P] rATP, combined in the indicated concentrations of magnesium (0 mM, 1 mM, 2 mM, and 10 mM Mg^{2+}). To determine equilibrium dissociation constants (K_D), the gRNAs were combined with increasing concentrations of unlabeled mRNA substrate (Table 8), denatured at 70° C for two minutes and slowly cooled to room temperature. The mRNA/gRNA pairs were allowed to anneal for 3 hours to make sure the mRNA/gRNA complex formation reached equilibrium. Samples were loaded under current onto 6% polyacrylamide native gels with magnesium concentrations of the gel and running buffer matching that of the annealing buffer. The apparent equilibrium dissociation constants were derived by quantifying the fmols/µl mRNA/gRNA complex formation for a range of mRNA concentrations from 4 gels. There was a large amount of diffuse signal between the band shifts of the complex and the free gRNA indicating that a lot of dissociation was occurring during electrophoresis.

The EMSA experiments for the apparent dissociation rate constants were similar to the experiments above except that one concentration of mRNA (two times the apparent K_D) and gRNA were incubated for 20 hours at 27° C. Then an oligonucleotide, complementary to the gRNA anchor, was added and time points were taken at the indicated times and snap-frozen on dry ice. Each sample was individually thawed and run as above. The EMSA gels for the apparent observed rate constants also used one concentration of mRNA and gRNA and were incubated at 27° C for the indicated times, snap-frozen, and run as above. The apparent observed rate constant for CYbU was calculated using a single exponential fit based on the reaction mechanism

$mRNA + gRNA \underset{k_{off}}{\overset{k_{on}}{\leftrightarrow}} {}^{gRNA}/_{mRNA}$ where the mRNA and gRNA bind to form the

Lanes	mRNA	Concentration
1, 2	5'CYbUT	0 nM
3, 4	5'CYbUT	75 nM
5, 6	5'CYbUT	125 nM
7, 8	5'CYbUT	250 nM
9, 10	5'CYbUT	500 nM
11, 12	5'CYbUT	750 nM
13, 14	5'CYbUT	1000 nM
15, 16	5'CYbUT	1500 nM
17, 18	5'CYbUT	2000 nM
19, 20	5'CYbUT	3000 nM
1, 2	5'CYbPES1T	0 nM
3, 4	5'CYbPES1T	15.125 nM
5, 6	5'CYbPES1T	31.25 nM
7, 8	5'CYbPES1T	62.5 nM
9, 10	5'CYbPES1T	125 nM
11, 12	5'CYbPES1T	250 nM
13, 14	5'CYbPES1T	500 nM
15, 16	5'CYbPES1T	750 nM
17, 18	5'CYbPES1T	1000 nM
19, 20	5'CYbPES1T	2000 nM
1, 2	5'CYbPES3T	0 nM
3, 4	5'CYbPES3T	7.563 nM
5, 6	5'CYbPES3T	15.125 nM
7, 8	5'CYbPES3T	31.25 nM
9, 10	5'CYbPES3T	62.5 nM
11, 12	5'CYbPES3T	125 nM
13, 14	5'CYbPES3T	250 nM
15, 16	5'CYbPES3T	500 nM
17, 18	5'CYbPES3T	750 nM
19, 20	5'CYbPES3T	1000 nM

Table 8. Concentrations of 5'CYbUT, 5'CYbPES1T, and 5'CYbPES3T mRNAs used in the gel shifts to determine the dissociation constant (K_D).

mRNA/gRNA complex. For the partially edited mRNAs, CYbPES1 and CYbPES3, the best line fit for the data points was a double exponential fit using the reaction mechanism:

$mRNA^{*}+gRNA \xrightarrow{k_{on1}} gRNA/_{mRNA} \underset{k_{off}}{\overset{k_{on2}}{\leftrightarrow}} mRNA+gRNA$ where the mRNA* represents an alternate conformation of the mRNA that allowed a significantly faster association rate with no noticeable dissociation along with a slower mechanism of binding similar to the unedited CYb reaction. The first observed rate constant for CYbPES1 and CYbPES3 could only be measured by the first data point at one minute, and therefore the first observed rate constant could not be reliably measured using EMSA. Since the first binding event was too rapid, only the second, slower observed rate constant was reported and used to calculate the apparent association rate constant (k_{on}). This first binding event may have been a helix nucleation event or initial interaction that is not stable enough to measure using EMSA. The on-rates calculated from the apparent observed rate constant and apparent dissociation rate constant ($k_{off\,app}$) were larger than those calculated from the $K_{D\,app}$ and $k_{off\,app}$. However, the apparent observed rate constant gel band shift assays visually demonstrated the thermodynamic trends of association for the CYb mRNA/gRNA complex during editing.

Surface Plasmon Resonance Studies

The association and dissociation rate constants were then measured using surface plasmon resonance (SPR). This real time kinetic technique also allowed measurements of the binding rate of the mRNA/gRNA complex at different stages of the editing process. The hybridization kinetic rate constants generated from the Biacore experiments had much less variation than the EMSA experiments and were probably more accurate. (The SPR experiments were described more in depth in chapter 3.)

In these experiments, a deoxyoligonucleotide tag with a 3' biotin label was ligated onto the 3' ends of the target mRNAs using T4 DNA ligase (Moore & Sharp, 1992). The biotin labeled mRNA was then immobilized to the streptavidin covered surface of the SA chip (Biacore, Uppsala, Sweden) in two of the four channels of a BIACORE 2000 (Biacore, Uppsala, Sweden). In order to see reliable gRNA binding to the mRNA, 100 to 600 resonance units of mRNA was attached to the chip surface. One channel remained empty and was used as a reference surface and one contained the biotinylated tag as a control for background binding. A continuous flow of gRNA solution at various concentrations (50 to 7400 nM) was injected over the immobilized mRNAs to monitor the gRNA association with its target mRNA. The dissociation phase was monitored by chasing the gRNAs with buffer alone.

The analysis method of the CYbU interactions with NgCYb-558 was described in chapter 3. The CYbU and CYbPES1 dissociation rate constant equation was slightly altered (see materials and methods) to create a better line fit for the data. The CYbPES3 dissociation rate constant data had a better line fit using the 1:1 (Langmuir) dissociation formula (see Materials and Methods). In addition, the experiments done without the U-tail had very high background and should probably be repeated using another method that can detect slower association rates. The individual rate constants were averaged and the equilibrium dissociation constant was calculated from the rate constants. The errors reported were based on the variances of all curves obtained (Nordgren et al., 2001).

The NgCYb-558/5'CYbUT Interaction

Previous experiments involving the unedited CYb mRNA/gRNA complex suggest that the mRNA structure hinders the mRNA/gRNA interaction (Fig. 23A) (Leung &

Koslowsky, 2001a; Koslowsky et al., 2004). Using EMSA experiments, the binding kinetics of the unedited CYb mRNA/gRNA interaction was studied at different concentrations of magnesium. No mRNA/gRNA interaction was detected when no magnesium was added. At 1 mM magnesium, the unedited mRNA/gRNA interaction did not come to equilibrium and had a K_D = 0.8 μM with the U-tail. The K_D of the interaction could not be calculated in the absence of the U-tail at 1 mM magnesium. Using higher concentrations of magnesium, the dissociation constant for the unedited CYb mRNA/gRNA interaction was ~0.5 μM when the U-tail was present and ~0.9 μM when the U-tail is absent. The presence of the U-tail greatly increased the binding affinity of the unedited CYb mRNA/gRNA interaction (Koslowsky et al., 2004). These previous experiments had an incubation time of 45 minutes; however, only the EMSA experiments using the higher concentrations of magnesium were able to come to equilibrium. In an effort to understand this reaction at physiological magnesium levels, these experiments were repeated and allowed to incubate for three hours. When the unedited mRNA/gRNA complex was allowed to incubate for three hours, there was a slight amount of complex formation at 0 mM magnesium not observed using shorter incubation times (Fig. 24A); however, a believable dissociation constant could not be calculated. The unedited CYb mRNA/gRNA interactions were able to come to equilibrium with three hours incubation time at 1 mM magnesium and the dissociation constants were similar to the rates calculated previously for the 2 mM magnesium interactions (Figs. 24A, 25A). At 10 mM magnesium, the dissociation constants appeared to be slightly reduced with the longer incubation time (Figs. 24A, 25A).

Figure 24

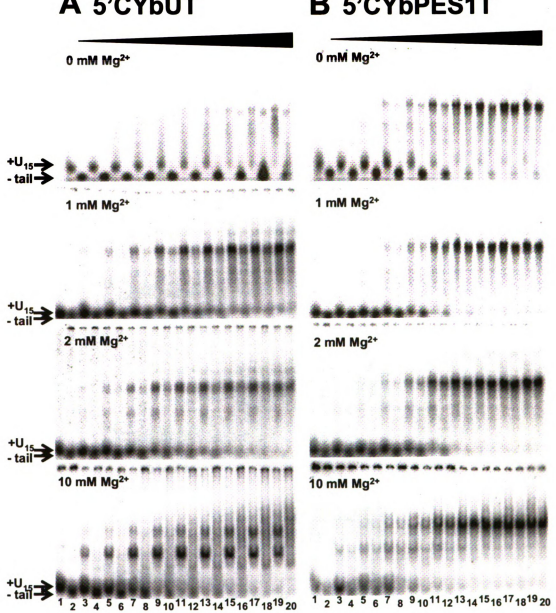
A 5'CYbUT
B 5'CYbPES1T
0 mM Mg2+
1 mM Mg2+
2 mM Mg2+
10 mM Mg2+
+U15
- tail
1 2 3 4 5 6 7 8 9 10 11 12 13 14 15 16 17 18 19 20

Figure 24 continued

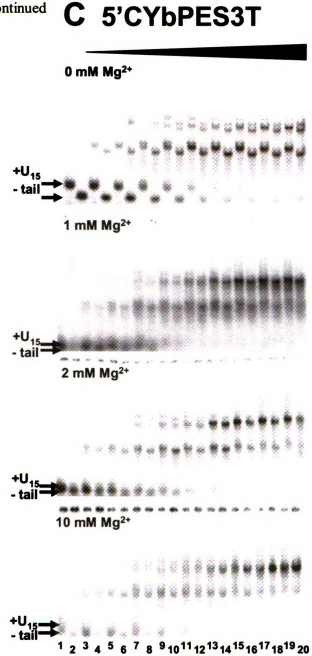

Figure 24. Gel band shift assay looking at the CYb gRNA binding increasing concentrations of the cognate CYb mRNAs. Representative autoradiographs of 6% polyacrylamide native gels are shown with the concentration of magnesium indicated in the top left-hand corner of each gel. The odd number lanes have 5' end labeled NgCYb-558 with a U-tail (+U-tail), while even numbers have 5' end labeled NgCYb-558 without a U-tail (-tail). The positions of the free gRNAs are indicated with bold arrows. A. 5'CYbUT + NgCYb-558, B. 5'CYbPES1T + NgCYb-558, and C. 5CYbPES3T +NgCYb-558.

Figure 25

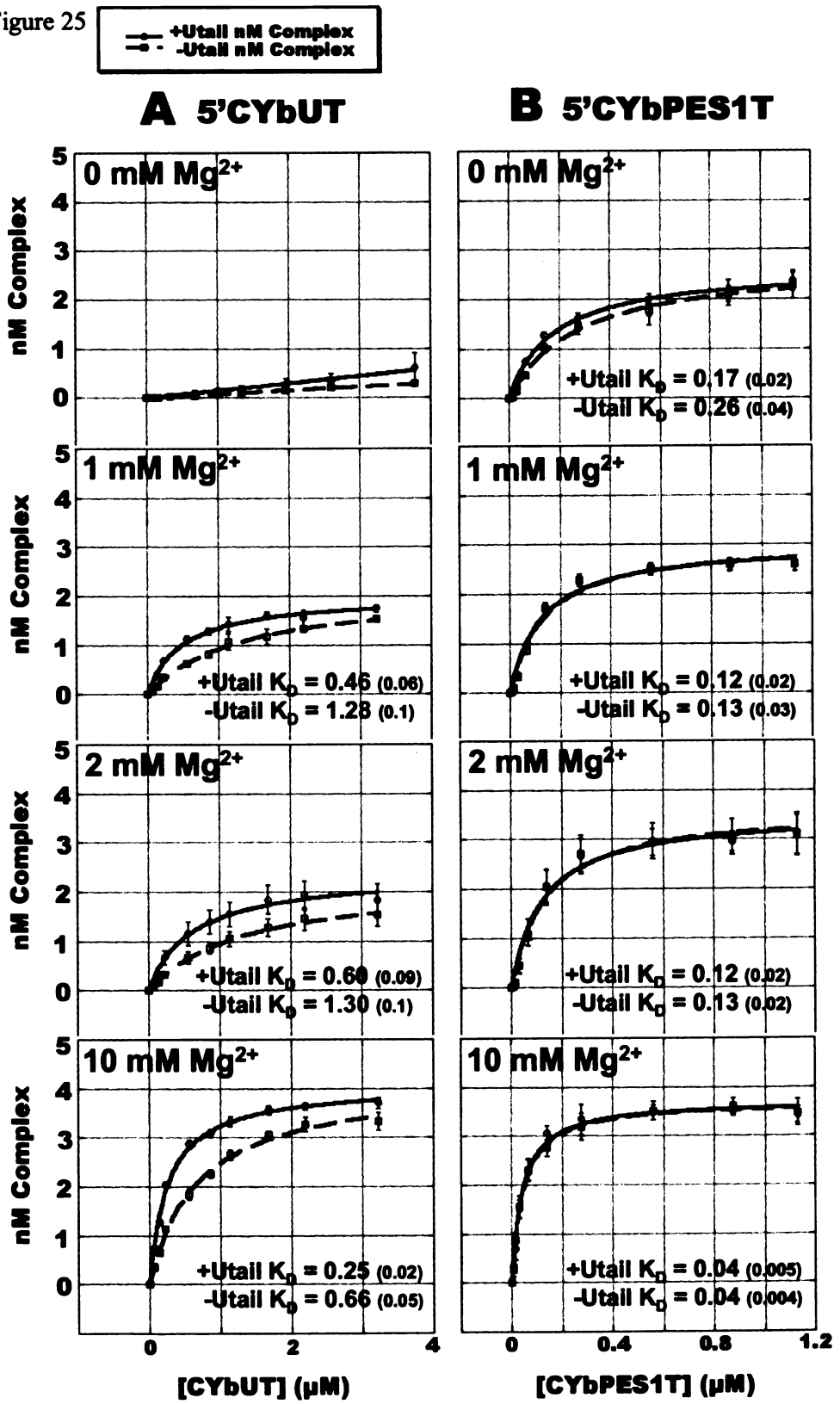
+Utail nM Complex
-Utail nM Complex
A 5'CYbUT
B 5'CYbPES1T
0 mM Mg2+
1 mM Mg2+
2 mM Mg2+
10 mM Mg2+
nM Complex
+Utail KD = 0.17 (0.02)
-Utail KD = 0.26 (0.04)
+Utail KD = 0.46 (0.06)
-Utail KD = 1.28 (0.1)
+Utail KD = 0.12 (0.02)
-Utail KD = 0.13 (0.03)
+Utail KD = 0.60 (0.09)
-Utail KD = 1.30 (0.1)
+Utail KD = 0.12 (0.02)
-Utail KD = 0.13 (0.02)
+Utail KD = 0.25 (0.02)
-Utail KD = 0.66 (0.05)
+Utail KD = 0.04 (0.005)
-Utail KD = 0.04 (0.004)
0
1
2
3
4
5
0
2
4
0
0.4
0.8
1.2
[CYbUT] (μM)
[CYbPES1T] (μM)

Figure 25 continued

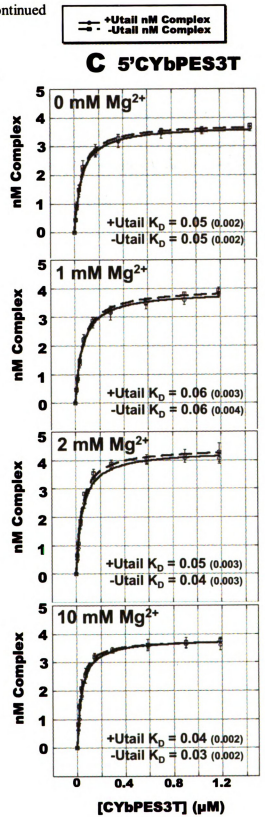

Figure 25. Graphs showing the analysis of CYb gRNA/mRNA complexes at various magnesium concentrations. The x axis represents the concentration of mRNA used in pmols/μl (μM), while the y axis represents the amount of mRNA/gRNA complex formation in fmols/μl (nM). The solid line indicates complexes containing NgCYb-558 (with U-tail); the dashed line indicates complexes containing NgCYb-558sU (no U-tail). The error bars indicate the standard deviation in complex formation observed between gels. The dissociation constants (μM) are written below the curves with the calculated error shown in parentheses A. 5'CYbUT (unedited mRNA) binding NgCYb-558. B. 5'CYbPES1T (partially edited mRNA, first editing site contains 2 uridines) binding NgCYb-558. C. 5'CYbPES3T (partially edited mRNA, first three editing sites contain 6 uridines) binding NgCYb-558.

Calculated dissociation constants were consistent in general with previous experiments and data (Koslowsky et al., 2004).

Gel shifts were also used to look at the apparent dissociation rate constant ($k_{off\ app}$) and the apparent observed rate constant ($k_{obs\ app}$) for CYbU (Fig. 26A,D and 27A,D, Table 9); the apparent observed rate constant and the apparent dissociation rate constant were used to calculate the apparent association rate constant ($k_{on\ app}$) (Table 9). These dissociation gels had 1500 nM CYbU binding to 1 nM gRNA at 27°C for 20 hours at 1 mM magnesium, then an oligonucleotide, complementary to the short gRNA anchor, was added at ten times the concentration of the mRNA. Time points were taken and run on a native gel. The complex dissociation happened quickly with almost all complexes dissociated by five hours. There was one main band of complex formation, and dissociation occurred faster in the absence of the U-tail (Fig. 26D). The apparent dissociation rate constant for CYbU at 1 mM magnesium was ~1 x 10^{-4} s^{-1} (Table 9) both with and without the U-tail. Native gels were also used to find the observed rate constant, so that an association constant could be calculated. Each sample had 1500 nM CYbU and 1 nM gRNA incubated at 27°C at the time points indicated. A single exponential equation was used to calculate the CYbU observed rate constant. The complex associated slowly, and the absence of the U-tail resulted in an even slower association rate. In addition, the bands of complex formation were very blurry indicating dissociation was occurring rapidly during electrophoresis. The apparent association rate constant at 1 mM magnesium was 59 $M^{-1}s^{-1}$ with the U-tail and 38 $M^{-1}s^{-1}$ without the U-tail (Table 9). The U-tail increased the association rate two fold as observed in the plus

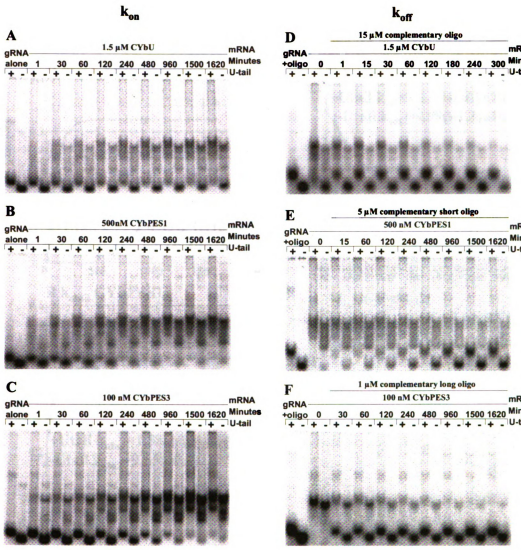

Figure 26. Electrophoretic mobility shift assay looking at the binding of the CYb gRNA to one concentration of the cognate CYb mRNA at 1 mM magnesium in order to determine the association rate constants and the dissociation rate constants for the unedited and partially edited mRNAs. Representative autoradiographs of 8% polyacrylamide native gels. A. Association rate constant gel for CYbU+NgCYb-558. B. Association rate constant gel for CYbPES1+NgCYb-558. C. Association rate constant gel for CYbPES3+NgCYb-558. D. Dissociation rate constant gel for CYbU+NgCYb-558. E. Dissociation rate constant gel for CYbPES1+NgCYb-558. F. Dissociation rate constant gel for CYbPES3+NgCYb-558.

Figure 27

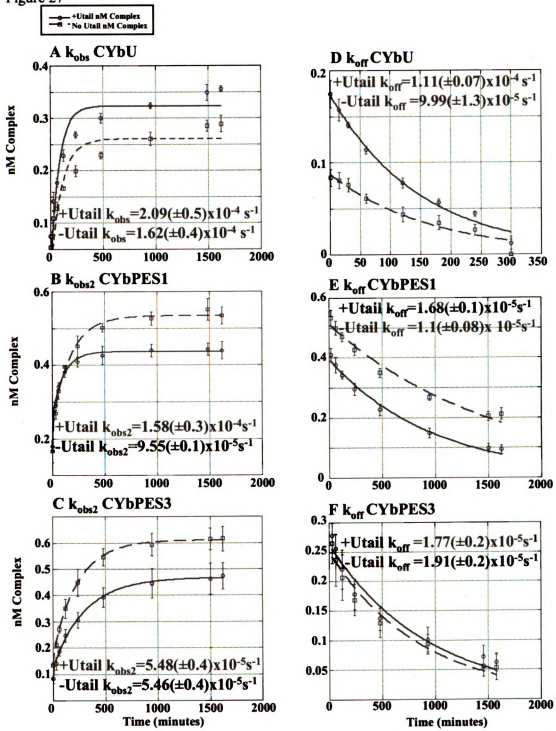
+Utail nM Complex
-No Utail nM Complex
A k_{obs} CYbU
nM Complex
+Utail k_{obs}=2.09(±0.5)x10^{-4} s^{-1}
-Utail k_{obs}=1.62(±0.4)x10^{-4} s^{-1}
B k_{obs2} CYbPES1
nM Complex
+Utail k_{obs2}=1.58(±0.3)x10^{-4}s^{-1}
-Utail k_{obs2}=9.55(±0.1)x10^{-5}s^{-1}
C k_{obs2} CYbPES3
nM Complex
+Utail k_{obs2}=5.48(±0.4)x10^{-5}s^{-1}
-Utail k_{obs2}=5.46(±0.4)x10^{-5}s^{-1}
Time (minutes)
D k_{off} CYbU
+Utail k_{off}=1.11(±0.07)x10^{-4} s^{-1}
-Utail k_{off} =9.99(±1.3)x10^{-5} s^{-1}
E k_{off} CYbPES1
+Utail k_{off}=1.68(±0.1)x10^{-5}s^{-1}
-Utail k_{off} =1.1(±0.08)x 10^{-5}s^{-1}
F k_{off} CYbPES3
+Utail k_{off} =1.77(±0.2)x10^{-5}s^{-1}
-Utail k_{off} =1.91(±0.2)x10^{-5}s^{-1}
Time (minutes)

Figure 27. Graphs showing the observed rate constant and the dissociation rate constant analyses of CYb gRNA/mRNA complexes at 1 mM magnesium. These rate constants can then be used to calculate the association rate constant. The x-axis represents time in minutes, while the y-axis represents the amount of mRNA/gRNA complex formation in fmols/µl (nM). The solid line indicates the curve for the complexes containing NgCYb-558, while the dashed line indicates the complexes containing NgCYb-558sU (no U-tail). The error bars indicate the standard deviation in complex formation observed between gels with the calculated error in apparent dissociation rate constants shown in parentheses. A. CYbU (unedited mRNA) binding NgCYb-558. B. CYbPES1 (partially edited mRNA, first editing site contains two uridines) binding NgCYb-558. C. CYbPES3 (partially edited mRNA, first three editing sites contain six uridines) binding NgCYb-558. Notice that the CYbU anchor contains 13 bps, the CYbPES1 anchor contains 16 bps, and the CYbPES3 anchor has doubled in length to 26 bps.

mRNA	gRNA	$K_{D\ app}$ (M)	$k_{obs\ app}$ (sec^{-1})	$k_{on\ app}$ ($M^{-1}s^{-1}$)	$k_{off\ app}$(s^{-1})
5'CYbUT	NgCYb-558	$4.6(\pm0.6)x10^{-7}$	$2.09(\pm0.5)x10^{-4}$	59.1	$1.11(\pm0.07)x10^{-4}$
	NgCYb-558sU	$1.3(\pm0.1)x10^{-6}$	$1.62(\pm0.4)x10^{-4}$	37.5	$9.99(\pm1.3)x10^{-5}$
5'CYbPES1T	NgCYb-558	$1.2(\pm0.2)x10^{-7}$	$1.58(\pm0.3)x10^{-4}$	$2.47x10^{+2}$	$1.68(\pm0.1)x10^{-5}$
	NgCYb-558sU	$1.3(\pm0.3)x10^{-7}$	$9.55(\pm0.1)x10^{-5}$	$1.49x10^{+2}$	$1.05(\pm0.08)x10^{-5}$
5'CYbPES3T	NgCYb-558	$6.0(\pm0.3)x10^{-8}$	$5.48(\pm0.4)x10^{-5}$	$4.15x10^{+2}$	$1.77(\pm0.2)x10^{-5}$
	NgCYb-558sU	$6.0(\pm0.4)x10^{-8}$	$5.46(\pm0.4)x10^{-5}$	$5.68x10^{+2}$	$1.91(\pm0.2)x10^{-5}$

Table 9. Table of rate constants and dissociation constants calculated from gel band shift data. Column 1: mRNA, Column 2: gRNA, Column 3: apparent dissociation equilibrium constants, Column 4: apparent observed rate constants, Column 5: apparent association rate constants, and Column 6: apparent dissociation rate constants from gels run at 1 mM magnesium.

U-tail lanes of the association gel shifts that formed more complex than the minus U-tail lanes (Fig. 26A).

This trend of binding was confirmed by using real time kinetics to find the dissociation rate constant (k_{off}), the association rate constant (k_{on}), and then calculating the dissociation equilibrium constant (K_D) at 2 mM magnesium. Using surface plasmon resonance (SPR), for CYbU+NgCYb-558 (Table 10) a dissociation equilibrium constant (K_D) of 4.7 μM (4.7×10^{-6} M) and 26 μM (2.6×10^{-5} M) without the U-tail (Fig. 28A, Table 11) were observed. The same trend was observed in the gel shifts where the presence of the U-tail resulted in a higher affinity of binding between the CYb mRNA and gRNA. These numbers were calculated from separate line fits of the association and dissociation curves from the Biacore sensograms (Fig. 28A). The association rate constant (k_{on}) for CYbU+NgCYb-558 is 570 $M^{-1}s^{-1}$ (5.7×10^2 $M^{-1}s^{-1}$) and this is two fold faster than without the U-tail with 240 $M^{-1}s^{-1}$ (2.4×10^2 $M^{-1}s^{-1}$). The dissociation rate constant (k_{off}) for CYbU is 2.7×10^{-3} s^{-1} with and 6.1×10^{-3} s^{-1} without the U-tail. The U-tail has been predicted to slow dissociation; interestingly, for the CYb substrate it increased NgCYb-558 association with CYbU.

The NgCYb-558/5'CYbPES1T Interaction

Surprisingly, with the addition of two uridylates from the first editing event (a three bp increase in the size of the anchor duplex), there was a large increase in mRNA/gRNA complex stability at all concentrations of magnesium (Fig. 24B). Similar to the unedited transcript, the 5'CYbPES1T/NgCYb-558 interaction resulted in the formation of one

main complex at all magnesium concentrations (Fig. 24B). The major complex formed was similar in mobility to that formed by the 5'CYbUT, unedited substrate.

RNA	Analyte or Ligand	Sequence	No. of nts.
CYbU+BigSK	Ligand	5'GGUUAUAAAUUUUAUAUAAAAGCGG AGAAAAAAGAAAGGGUCUUUUAAUGUC AGGUUGUUUAUAUAGAAUAUAUGGAUC atatggaagtaattagaagga-biotin3'	100
CYbU+Biatag1	Ligand	5'GGUUAUAAAUUUUAUAUAAAAGCGGA GAAAAAAGAAAGGGUCUUUUAAUGUCAG GUUGUUUAUAUAGAAUAUAUGGAUCcacua guucuagagcggcc-biotin3'	98
CYbPES1+ CYbBia	Ligand	5'GGUUAUAAAUUUUAUAUAAAAGCGGAG AAAAAAGAAAGGUUGUCUUUUAAUGUCAG GUUGUUUAUAUAGaatttataaccggg+biotin3'	83
CYbPES3+ CYbBia	Ligand	5'GGUUAUAAAUUUUAUAUAAAAGCGGAG AAAAAAGAAAUUUGUGUUGUCUUUUAAU GUCAGGUUGUUUAUAUAGaatttataaccggg+biotin3'	87
NgCYb-558	Analyte	5'GGGAUUAAAAGACAAUGUGAAUUUCUA GGUGAUAAAGGGAAUAAUUUUUUUUUUU UUUU3'	59
NgCYb-558sU	Analyte	5'GGGAUUAAAAGACAAUGUGAAUUUCUA GGUGAUAAAGGGAAUAA3'	44

Table 10. List of all Biacore substrates used. The biotinylated DNA tags were ligated on using DNA bridges listed in Table 8 and are indicated by lowercase letters. Column 1: RNA name. Column 2: Ligands were biotinylated and attached to streptavidin coated SA chips (Biacore, Uppsala, Sweden) and Analytes were injected in running buffer and flowed across the surface of the chip to bind the Ligand. Column 3: Sequence of the Biacore substrates. Column 4: number of nucleotides.

Figure 28

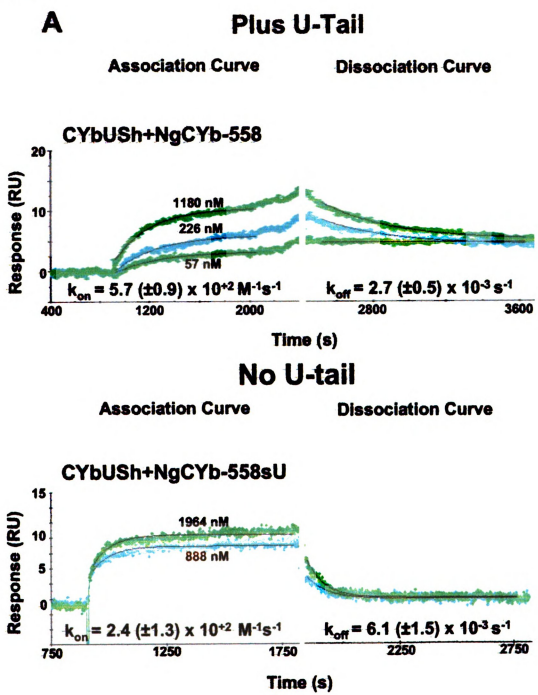
A
Plus U-Tail
Association Curve
Dissociation Curve
CYbUSh+NgCYb-558
Response (RU)
20
10
0
1180 nM
226 nM
57 nM
k_{on} = 5.7 (±0.9) x 10^{+2} $M^{-1}s^{-1}$
k_{off} = 2.7 (±0.5) x 10^{-3} s^{-1}
400
1200
2000
2800
3600
Time (s)
No U-tail
Association Curve
Dissociation Curve
CYbUSh+NgCYb-558sU
Response (RU)
15
10
5
0
1964 nM
888 nM
k_{on} = 2.4 (±1.3) x 10^{+2} $M^{-1}s^{-1}$
k_{off} = 6.1 (±1.5) x 10^{-3} s^{-1}
750
1250
1750
2250
2750
Time (s)

Figure 28 continued

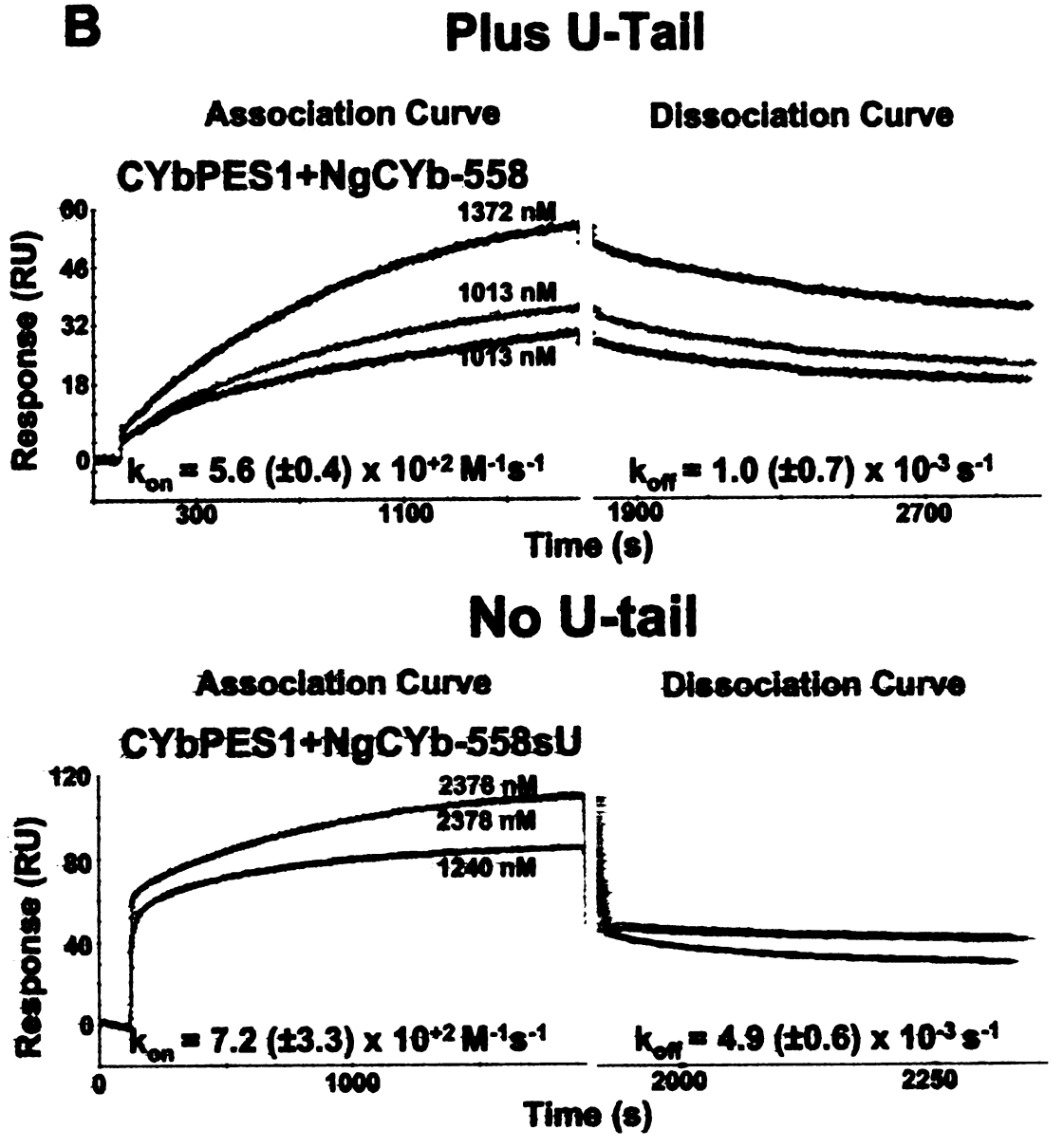

Figure 28 continued

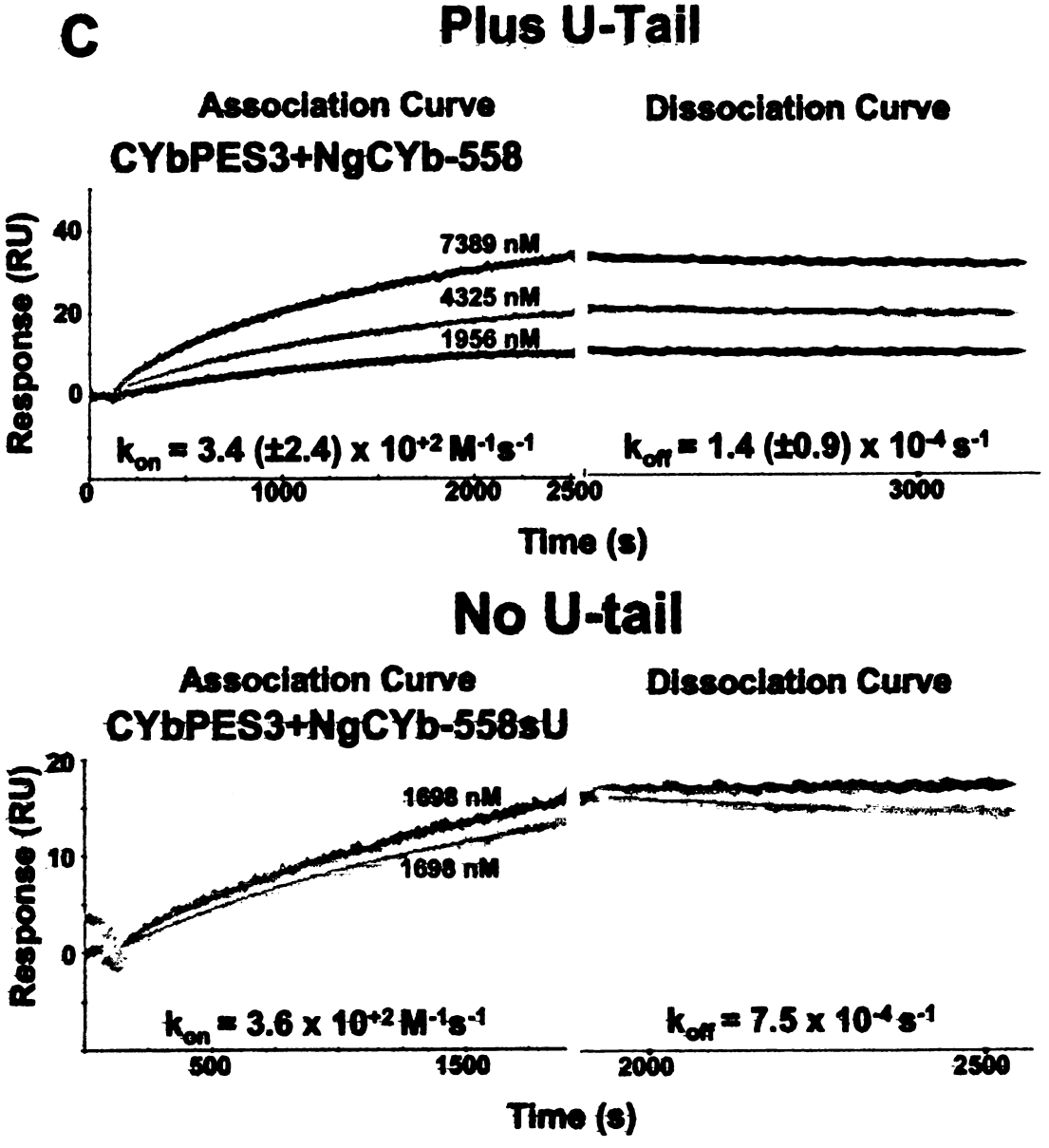

Figure 28. Separate association and dissociation line fits of the CYb Biacore sensograms. Each sensogram represents injections of gRNA over a channel with attached mRNA. The concentration of gRNA is indicated on each graph above each line. A. Sensogram of CYbU + NgCYb-558 and CYbU + NgCYb-558sU (no U-tail) with first the association line fit and then the dissociation line fit. B. Sensogram of CYbPES1 + NgCYb-558 and CYbPES1 + NgCYb-558sU (no U-tail) with first the association line fit and then the dissociation line fit. C. Sensogram of CYbPES3 + NgCYb-558 and CYbPES3 + NgCYb-558sU (no U-tail) with first the association line fit and then the dissociation line fit. Each association rate constant (k_{on}) and dissociation rate constant (k_{off}) is listed with the error in parentheses. RU = resonance units and s = seconds. The CYbPES1+NgCYb-558sU and CYbPES3+NgCYb-558sU experiments need to be repeated to verify these results.

mRNA	gRNA	K_D (M)	k_{on} ($M^{-1}s^{-1}$)	k_{off} (s^{-1})
CYbU	NgCYb-558	4.7×10^{-6}	$5.7 (\pm 0.9) \times 10^{+2}$	$2.7 (\pm 0.5) \times 10^{-3}$
	NgCYb-558sU	2.6×10^{-5}	$2.4 (\pm 1.3) \times 10^{+2}$	$6.1 (\pm 1.5) \times 10^{-3}$
CYbPES1	NgCYb-558	1.8×10^{-6}	$5.6 (\pm 0.4) \times 10^{+2}$	$1.0 (\pm 0.7) \times 10^{-3}$
	NgCYb-558sU	6.9×10^{-7}	$7.2 (\pm 3.3) \times 10^{+2}$	$4.9 (\pm 0.6) \times 10^{-3}$
CYbPES3	NgCYb-558	4.0×10^{-7}	$3.4 (\pm 2.4) \times 10^{+2}$	$1.4 (\pm 0.9) \times 10^{-4}$
	NgCYb-558sU	2.1×10^{-7}	$3.6 \times 10^{+2}$	7.5×10^{-5}

Table 11. Table of rate constants and dissociation constants calculated from CYb Biacore data. Column 1: mRNA, Column 2: gRNA, Column 3: dissociation equilibrium constants, Column 4: association rate constants, and Column 5: dissociation rate constants from surface plasmon resonance experiments run at 2 mM magnesium. Only one experiment was used for the CYbPES3+NgCYb-558sU experiment, so no error is reported and the experiment should be repeated to verify this result.

However, in contrast to the 5'CYbUT substrate, increasing the magnesium levels to 10 mM, did not cause a significant change in the appearance or mobility of the main complex (Fig. 24A, B). At 10 mM magnesium, a second distinct complex of faster mobility was observed at low mRNA concentrations (Fig. 24B, lanes 3-11). In addition, with increasing concentrations of magnesium, there was increased complex formation and lowering of the apparent affinity constant. In the absence of magnesium, the presence of the U-tail significantly decreased the apparent affinity constant (+U-tail $K_{D\ app}$ = 0.17 μM (1.7 x 10^{-7} M), -U-tail $K_{D\ app}$ = 0.26 μM (2.6 x 10^{-7} M)) (Fig. 25B). Surprisingly however, at 1 mM and 2 mM magnesium, there was no statistically significant effect of the U-tail on complex formation. The apparent affinity constants ($K_{D\ app}$) for 1 mM and 2 mM magnesium were 0.12 μM (1.2 x 10^{-7} M) (Fig. 25B). The $K_{D\ app}$ further decreased another two fold to 0.04 μM (4 x 10^{-8} M) (Fig. 25B) with 10 mM magnesium.

Gel shifts were also used to look at the apparent dissociation rate constant ($k_{off\ app}$) and the apparent observed rate constant ($k_{obs\ app}$) for CYbPES1 (Fig. 26B, E and 27B, E, Table 9); the apparent observed rate constant and the apparent dissociation rate constant were used to calculate the apparent association rate constant ($k_{on\ app}$) (Table 9) at 1 mM magnesium. These dissociation gels had 500 nM CYbPES1 binding to 1 nM gRNA at 27°C for 20 hours at 1 mM magnesium. An oligonucleotide complementary to the short gRNA anchor was then added at ten times the concentration of the mRNA. Time points were taken and run on a native gel. The CYbPES1 mRNA/gRNA complex dissociated more slowly than CYbU requiring 27 hours before most of the complex dissociated. There were multiple bands of complex formation with a minor, weaker band that

migrated very slowly and only in the presence of the U-tail. In addition, there appeared to be equal amounts of dissociation plus and minus the U-tail (Fig. 26E). The apparent dissociation rate constant for CYbPES1 was 1.7×10^{-5} s^{-1} and without the U-tail it was 1.1×10^{-5} s^{-1} (Table 9). The dissociation rate was 10 fold slower than CYbU. Native gels were also used to find the observed rate constant, and the association rate constant was calculated. Each sample had 500 nM CYbPES1 and 1 nM gRNA incubated at 27°C at the time points indicated. A double exponential equation was used to extract the CYbPES1 observed rate constant. The CYbPES1 mRNA/gRNA complex also associated slowly, but had clearer bands of complex formation indicating less dissociation was occurring during electrophoresis. Multiple conformations were forming (~3), but they were difficult to differentiate. In addition, there was a small fraction of complex formation that occurred by one minute that appeared to occur with a faster association rate that represented the first rate constant that was too fast to measure (Fig. 26C). The apparent association rate constant at 1 mM magnesium was 250 $M^{-1}s^{-1}$ with the U-tail and 150 $M^{-1}s^{-1}$ without the U-tail (Table 9). The association rate was slightly faster in the presence of the U-tail. Also, the CYbPES1 association rate was four fold faster than CYbU.

At 2 mM magnesium, this trend of binding was confirmed using SPR (Fig. 28B, Table 11. The dissociation rate constant (k_{off}) with the U-tail was 1.0×10^{-3} s^{-1} and 4.9×10^{-3} s^{-1} without the U-tail (Fig. 27B, Table 11). The association rate constant (k_{on}) was 560 $M^{-1}s^{-1}$ (5.6×10^{2} $M^{-1}s^{-1}$) with the U-tail and 720 $M^{-1}s^{-1}$ (7.2×10^{2} $M^{-1}s^{-1}$) without the U-tail (Table 11). There did not appear to be a statistically significant difference in the association or dissociation rate between plus or minus the U-tail for CYbPES1 at 2 mM

magnesium. For CYbPES1+NgCYb-558 (Table 10), the dissociation equilibrium constant (K_D) was calculated using the association and dissociation rate constants, and the K_D is 1.8 μM (1.8×10^{-6} M) with and 6.9 μM (6.9×10^{-6} M) without the U-tail (Table 11). The Biacore rate constants showed the same trend as the EMSA derived rate constants, and the differences between plus and minus the U-tail were not statistically significant (Table 11). In addition, the CYbPES1-gCYb-558 complex had a three fold higher affinity of binding than CYbU that was the result of a two fold decrease in the dissociation rate.

It was evident that the first editing event decreased the affinity constant for the CYb mRNA/gRNA binding, and this may be because the terminal loop now included part of the ABS and appeared to greatly increase the efficiency of binding. Also, it appeared that at 2 mM magnesium the three additional base pairs in the anchor helix decreased the dissociation rate and thereby increased the efficiency of anchor target binding.

The NgCYb-558/5'CYbPES3T Interaction

Additional editing adds four more uridylates into the next two editing sites and effectively doubled the anchor binding site. EMSA analyses indicated that these sequence changes resulted in a further two fold decrease in the apparent affinity constant to ~ 0.05 μM (5×10^{-8} M) (Fig. 25C). With the doubling of the anchor duplex (26 bps), stable complexes were observed even in the absence of magnesium and no U-tail contribution to complex formation was observed. In contrast to 5'CYbUT and 5'CYbPES1T, the addition of magnesium did not significantly increase the apparent affinity constant between the mRNA and gRNA. In addition, the 5'CYbPES3T substrate formed multiple complexes of different mobilities at all four magnesium levels tested.

There were two slower complexes and a faster complex in all gels; however, in the absence of magnesium, the higher mobility complex appeared to predominate.

EMSA experiments were also used to find the apparent dissociation rate constant (k_{off}) and the apparent observed rate constant (k_{obs}) for CYbPES3 (Fig. 26C, F and 27C, F, Table 9); the apparent observed rate constant and the apparent dissociation rate constant were used to calculate the apparent association rate constant (k_{on}) (Table 9) at 1 mM magnesium. These dissociation rate gels had 100 nM CYbPES3 binding to 1 nM gRNA at 27°C for 20 hours at 1 mM magnesium, then an oligonucleotide, complementary to the long gRNA anchor, was added at ten times the concentration of the mRNA. Time points were taken and run on a native gel. The dissociation of the CYbPES3 mRNA/gRNA complex happened very slowly with one main band of complex formation. The CYbPES3 dissociation rate required a much smaller concentration of mRNA and 27 hours of dissociation time. There was also a minor weaker band observed in the presence of the U-tail whose migration was much slower (Fig. 26F). CYbPES3+NgCYb-558 had an apparent dissociation rate constant (k_{off}) of ~1.8×10^{-5} s^{-1} with and without the U-tail. This was similar to the CYbPES1 dissociation rate constant and was ~10 fold slower than CYbU. Native gels were also used to find the observed rate constant, so that an association constant could be calculated. Each sample had 100 nM CYbPES3 and 1 nM gRNA incubated at 27°C at the time points indicated. A double exponential equation was used to calculate the CYbPES3 observed rate constant. The CYbPES3 mRNA/gRNA complex association occurred slowly; however, a small fraction associated by one minute with a faster association that represented the first rate constant that was too fast to measure. The bands of complex formation were much more distinct and there was much

less blurriness indicating even less dissociation was occurring. There were three main bands of complex formation (Fig. 26C). The apparent association rate constant (k_{on}) was ~500 $M^{-1}s^{-1}$ (5.0×10^2 $M^{-1}s^{-1}$) with and without the U-tail. This was two fold faster than the CYbPES1 association rate constant and ~10 fold faster than CYbU (Table 9).

This trend of binding was confirmed using SPR. The dissociation rate constant (k_{off}) is 1.4×10^{-4} s^{-1} with and 7.5×10^{-5} s^{-1} without the U-tail (Fig. 28C, Table 11). This was a nineteen fold slower dissociation rate than CYbU and seven fold slower than CYbPES1. The association rate constant (k_{on}) was 340 $M^{-1}s^{-1}$ (3.4×10^2 $M^{-1}s^{-1}$) with and 360 $M^{-1}s^{-1}$ (3.6×10^2 $M^{-1}s^{-1}$) without the U-tail (Fig 28C, Table 11). There did not appear to be a statistically significant difference in the association rate between CYbU, CYbPES1 and CYbPES3 according to the SPR data at 2 mM magnesium. The equilibrium dissociation constant (K_D) was 0.4 μM (4.0×10^{-7} M) with and 0.2 μM (2.1×10^{-7} M) without the U-tail (Table 11). There was a four fold decrease of K_D, resulting from 3 more uridylates added to the next editing site, when comparing 5'CYbPES1T to 5'CYbPES3T binding to NgCYb-558.

Photoaffinity crosslinking and mapping of U5 and U10 of the CYb U-tail

Whereas it has been shown that the mRNA structure influences gRNA target binding, it was unclear where the U-tail was binding during editing. The EMSA and SPR studies indicated that the presence of the U-tail resulted in an increased association rate for the CYbU/NgCYb-558 complex.

Photoaffinity crosslinking was one way to observe direct interactions between molecules such as the editing complex, and incorporation of the crosslinking agents did not change the nucleotide characteristics enough to interrupt most structures. In an

effort to discover where the U-tail was interacting in the CYb mRNA/gRNA complex, a 4-thio-uridine (4sU) was placed at the fifth (U5) or tenth (U10) position in a U-tail (Table 12) (Dharmacon, Boulder, CO). The 4-thio uridine moiety is a zero-distance crosslinking agent. The U-tails were 5' end labeled and ligated to NgCYb-558sU (no U-tail) using an oligonucleotide bridge (gCYb558(sU) bridge, Table 13) to join the two halves (Leung & Koslowsky, 2001b). P-azido-phenacyl bromide (APA) was added to half of the sample to increase the reach of the crosslink upon irradiation by converting the azido group into a nitrene that crosslinks to nearby residues (has a reach of up to 9 Å away). The gRNAs were annealed to either 5'CYbUT or 5'CYbPES3T and then the mRNA/gRNA complex was UV crosslinked. The crosslinks were isolated on a 6% polyacrylamide gel (Fig. 29). Positions of the crosslinks were then mapped by using primer extension analysis with reverse transcriptase (RT) and RNase H analysis (Fig. 30,31).

There were two crosslinked bands with different migration patterns in the gel for all four pairs of gRNA/mRNA complex and with either U-tail that were labeled band 1 and 2 (Fig. 29). The reactions without APA had a lower percentage of crosslinking. With APA, there was a much higher percentage for the slowest crosslink band, which was labeled band 1 (B1), than for the faster band 2 (B2). The control lanes consisted of a no UV control and a no mRNA control. The only crosslinks of interest were mRNA/gRNA interactions.

For primer extension analysis (Fig 30A), a 5' end labeled primer (BigSK, Table 13) was annealed to 2-5ng of crosslink. AMV reverse transcriptase (RT) (Seikugaku) was used to extend the primer along the mRNA (Leung & Koslowsky, 1999). When the RT

Name	Sequence	Length(nts.)
U15-thioU5	5'-UUUUUUUUU-4sU-UUUUU	15
U15-thioU10	5'-UUUU-4sU-UUUUUUUUUU	15

Table 12. Oligoribonucleotides ordered from Dharmacon. 4sU = 4-thio-uridine.

Name	Sequence	Length(nts.)
T7 22mer	5'-AATTTAATACGACTCACTATAG-3'	22
NgCYb-558(sU)	5'-TTATTCCCTTTATCACCTAGAAAT TCACATTGTCTTTTAATCCCTATAGT GAGTCGTATTAAATT-3'	65
NgCYb-558	5'-AAAAAAAAAAAAAAAATTATTCCCTT TATCACCTAGAAATTCACATTGTCTTTT AATCCCTATAGTGAGTCGTATTAAATT-3'	80
T7CYbShort	5'-AATTTAATACGACTCACTATAGGGT TATAAAT-3'	32
CYb(-BigSK)	5'-GATCCATATATTCTATATAAACAA CCTGACATT-3'	33
CYbU(-)	5'-CTATATAAACAACCTGACATTAAAAG ACCC-3'	30
3'BigSK-biotin	5'-CACTAGTTCTAGAGCGGCC-biotin-3'	19
CYbbigskBIAbridge	5'-GCTCTAGAACTAGTGGATCCATATAT TCTA-3'	30
Biatag1	5'-ATATGAGTAGGTAATTAGTA-biotin-3'	20
Biatag1CYbbridge	5'-ATTACCTACTCATATGATCCATAT ATTCTA-3'	30
BigSK	5'-GGCCGCTCTAGAACTAGTGG-3'	20
gCYb558(sU) bridge	5'-AAAAAAAAAAAAAAATTATTCCC TTTATCACC-3'	32
CYb-1	5'-ATTTATAACC-3'	10
New CYbH-2	5'-ACCATTATTCT-3'	11
5'CYbH-1	5'-CAACCTGACATT-3'	12

Table 13. List of oligodeoxyribonucleotides ordered from Integrated DNA Technologies.

Figure 29

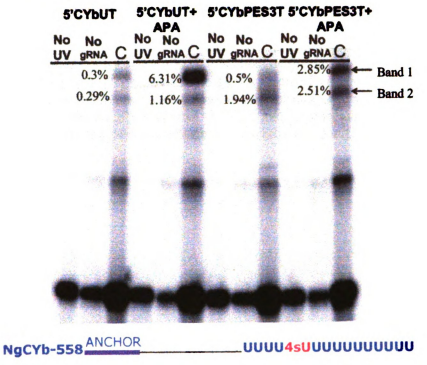
A
CYb mRNAs xlinked to NgCYb-558U5
5'CYbUT
5'CYbUT+ APA
5'CYbPES3T
5'CYbPES3T+ APA
No UV
No gRNA
C
0.3%
0.29%
6.31%
1.16%
0.5%
1.94%
2.85%
2.51%
Band 1
Band 2
NgCYb-558 ANCHOR
UUUU4sUUUUUUUUUU
B
CYb mRNAS xlinked to NgCYb-558U10
5'CYbUT
5'CYbUT+ APA
5'CYbPES3T
5'CYbPES3T+ APA
0.37%
0.69%
4.6%
1.6%
0.66%
1.27%
4.63%
1.78%
Band 1
Band 2
NgCYb-558 ANCHOR
UUUUUUUUU4sUUUUUU

Figure 29. The crosslinks of 5'CYbUT+NgCYb-558 and 5'CYbPES3T+NgCYb-558 run out on gels. A. 5'CYbUT+NgCYb-558 and 5'CYbPES3T+NgCYb-558 crosslinks with the 4-thio U in the fifth position. A diagram of the gRNA is below the gel. B. 5'CYbUT+NgCYb-558 and 5'CYbPES3T+NgCYb-558 crosslinks with the 4-thio U in the tenth position. A diagram of the gRNA is below the gel. Notice that each set of crosslinks has a No UV control and a no gRNA control for each crosslinking reaction. C = crosslink lane. There is a middle crosslink that appears to be mRNA specific that is faintly visible in the no gRNA control. Bands 1 and 2 are indicated with arrows. The percentage of crosslink is indicated next to each crosslink band.

Figure 30

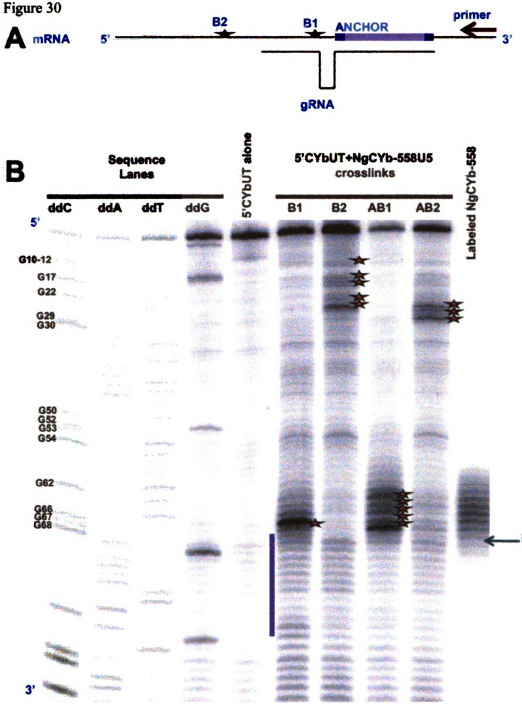
A
mRNA
5'
B2
B1
ANCHOR
primer
3'
gRNA
B
Sequence Lanes
ddC
ddA
ddT
ddG
5'CYbUT alone
5'CYbUT+NgCYb-558U5 crosslinks
B1
B2
AB1
AB2
Labeled NgCYb-558
5'
G10-12
G17
G22
G29
G30
G50
G52
G53
G54
G62
G66
G67
G68
3'
ES1

Figure 30 continued

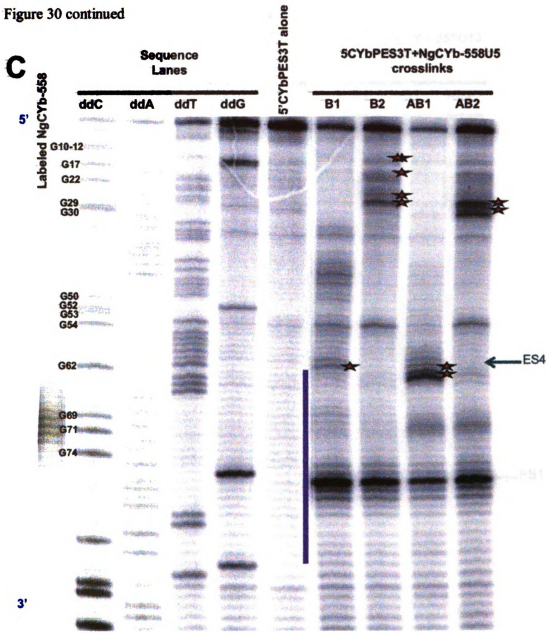

Figure 30 continued

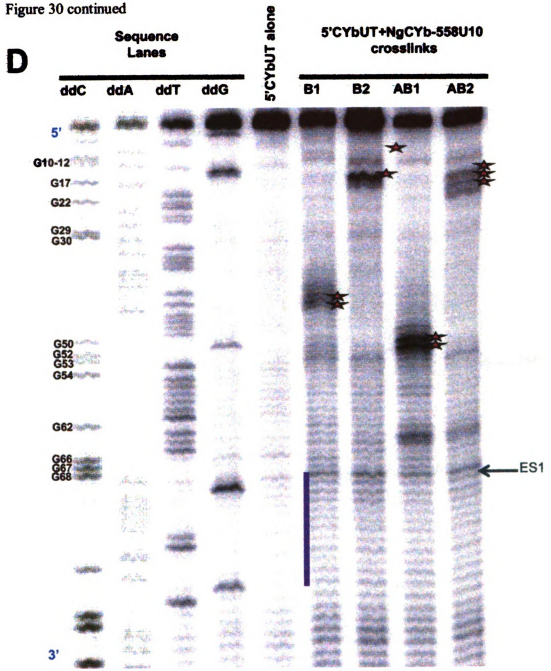

Figure 30 continued

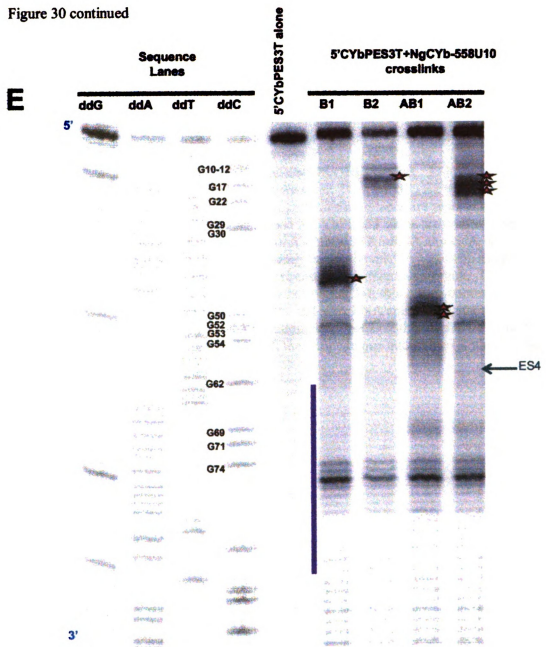

Figure 30. Primer extension analysis of the crosslink bands. A. Diagram of the primer extension analysis. The primer represents the BigSK primer extended by reverse transcriptase. The stars represent covalent crosslinks between the U-tail of the gRNA and the mRNA where the reverse transcriptase will fall off and leave a hard stop on the primer extension gel. B. Primer extension analysis of 5'CYbUT+NgCYb-558 U5 crosslink. C. Primer extension analysis of 5'CYbPES3T+NgCYb-558 U5 crosslink. D. Primer extension analysis of 5'CYbUT+NgCYb-558 U10 crosslink. E. Primer extension analysis of 5'CYbPES3T+NgCYb-558 U10 crosslink B1 = band 1, B2 = B2, AB1 = APA+band1, AB2 = APA+band2. The dideoxy sequencing lanes are represented by ddC, ddA, ddT, and ddG. 5'CYbUT alone and 5'CYbPES3T alone are control lanes showing primer extension of the 5'CYbUT or 5'CYbPES3T mRNA alone. A bar is placed vertically to represent the anchor binding site on the mRNA. Stars on the gels represent hard stops where the reverse transcriptase encountered a crosslink. The 5'CYbPES3T gels have a hard stop in the anchor region, but this stop is believed to be caused by secondary structural elements of the mRNA/gRNA anchor sequence interaction. This strong binding causes the strong stop, because this stop is the same for the U5 and U10 crosslinks. The RT falls off the template one nucleotide (3') before the crosslink.

Figure 31

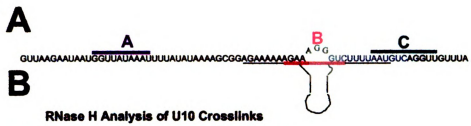
A
B
C
GUUAAGAAUAAUGGUUAUAAAUUUUAUAUAAAAGCGGAGAAAAAAGAA
A U G
GUCUUUUAAUGUCAGGUUGUUUA

B

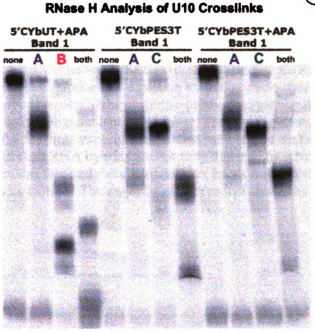
RNase H Analysis of U10 Crosslinks
5'CYbUT+APA
Band 1
none A B both
5'CYbPES3T
Band 1
none A C both
5'CYbPES3T+APA
Band 1
none A C both

C

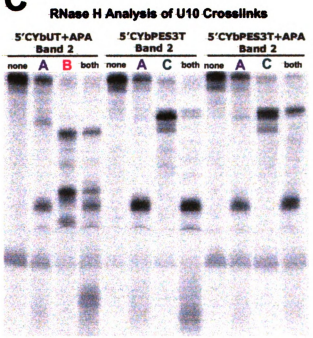
RNase H Analysis of U10 Crosslinks
5'CYbUT+APA
Band 2
none A B both
5'CYbPES3T
Band 2
none A C both
5'CYbPES3T+APA
Band 2
none A C both

Figure 31. RNase H analysis of the U10 crosslinks. A. Diagram of the oligonucleotides used to check the position of the crosslink. The oligonucleotide binds the crosslinked molecules and RNase H digests the DNA/RNA hybrid. The position of the crosslink can be placed based on the digestion pattern of two oligonucleotides separately and together. Oligonucleotide A = New CYbH-2, Oligonucleotide B = CYb-1, and Oligonucleotide C = 5'CYbH-1. B. RNase H analysis of the U10 band 1 crosslinks. Notice that digestion with both oligonucleotides results in the smallest product suggesting that the crosslink position of band 1 is between the two oligonucleotides. C. RNase H analysis of the U10 band 2 crosslinks. Notice that digestion with oligonucleotide A and with both oligonucleotides results in the same size product suggesting the position of the band 2 product is before oligonucleotide A. Note: There was not enough of 5'CYbUT band 1 without APA for these experiments, so that sample was excluded. Also, sometimes the oligonucleotide/mRNA hybrids are not fully digested by RNase H, so when both oligonucleotides are used there may be extra bands from partial digestion from one or the other oligonucleotide. The majority of the product should be a double digestion.

hit the crosslink, it fell off the template. This created a strong stop one nucleotide (3') before the crosslink that was observed when the primer extension analysis was run on a denaturing polyacrylamide gel beside a sequencing reaction of the mRNA.

The main crosslinks for 5'CYbUT/NgCYb-558U5 B1 included A60-G66 (Fig. 30B, 32B); this was also true for 5'CYbPES3T/NgCYb-558U5 B1 (now A60-G69) (Fig. 30C, 32E). The APA group seemed to increase the spread of crosslinks by one or two nucleotides for B1 U5 substrates, but there were still crosslinks near the first few editing sites. 5'CYbUT/NgCYb-558U5 for B2 had a crosslink spread mainly of A20-U25 (+APA=G22-U25, -APA=A20-A23) (Fig. 29B, 32B); the same was true for 5'CYbPES3T/NgCYb-558U5 the crosslinks included A20-A35 (Fig. 30C, 32E). APA again increased the spread of the crosslinks.

The crosslinks from 5'CYbUT/NgCYb-558U10 for B1 without APA included A42-A44, with APA C51-A54 (Fig. 30D, 32C) were observed. 5'CYbPES3T/NgCYb-558U10 B1 crosslinks were one to two nucleotides upstream of 5'CYbUT/NgCYb-558U10 B1 crosslinks (-APA U43-U45) (+APA G50-G53) (Fig. 30E,32F). Crosslinks for 5'CYbUT/NgCYb-558U10 B2 included G17-U18 without APA and G17-A20 with APA (Fig. 30D,32C); 5'CYbPES3T/NgCYb-558U10 B2 appeared to once again have the same spread but a few nucleotides upstream (-APA C16-G17) (+APA C15-U19) (Fig. 30E,32F).

When there was more than one stop, there may have been multiple crosslinks indicating secondary and tertiary interactions. There could have been multiple interactions caused by structural breathing. It appeared that the U-tail was binding and

Figure 32

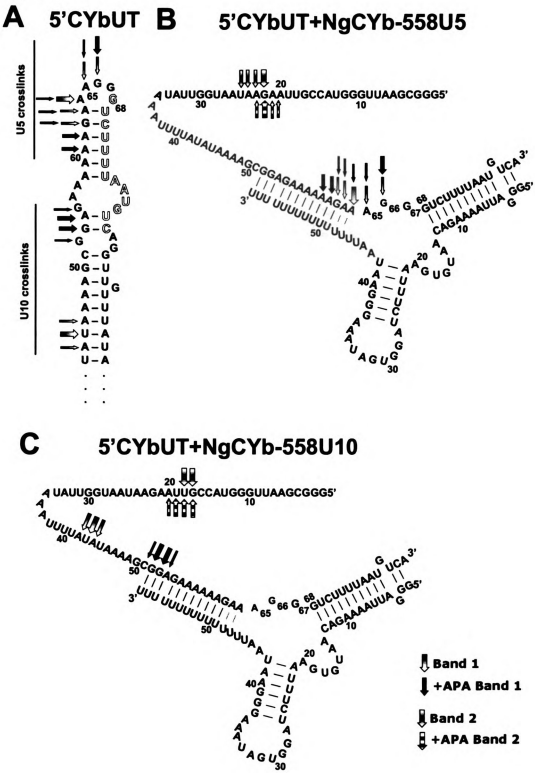
A
5'CYbUT
U5 crosslinks
U10 crosslinks
B
5'CYbUT+NgCYb-558U5
UAUUGGUAAUAAGAAUUGCCAUGGGUUAAGCGGG5'
3'
C
5'CYbUT+NgCYb-558U10
Band 1
+APA Band 1
Band 2
+APA Band 2

Figure 32 continued

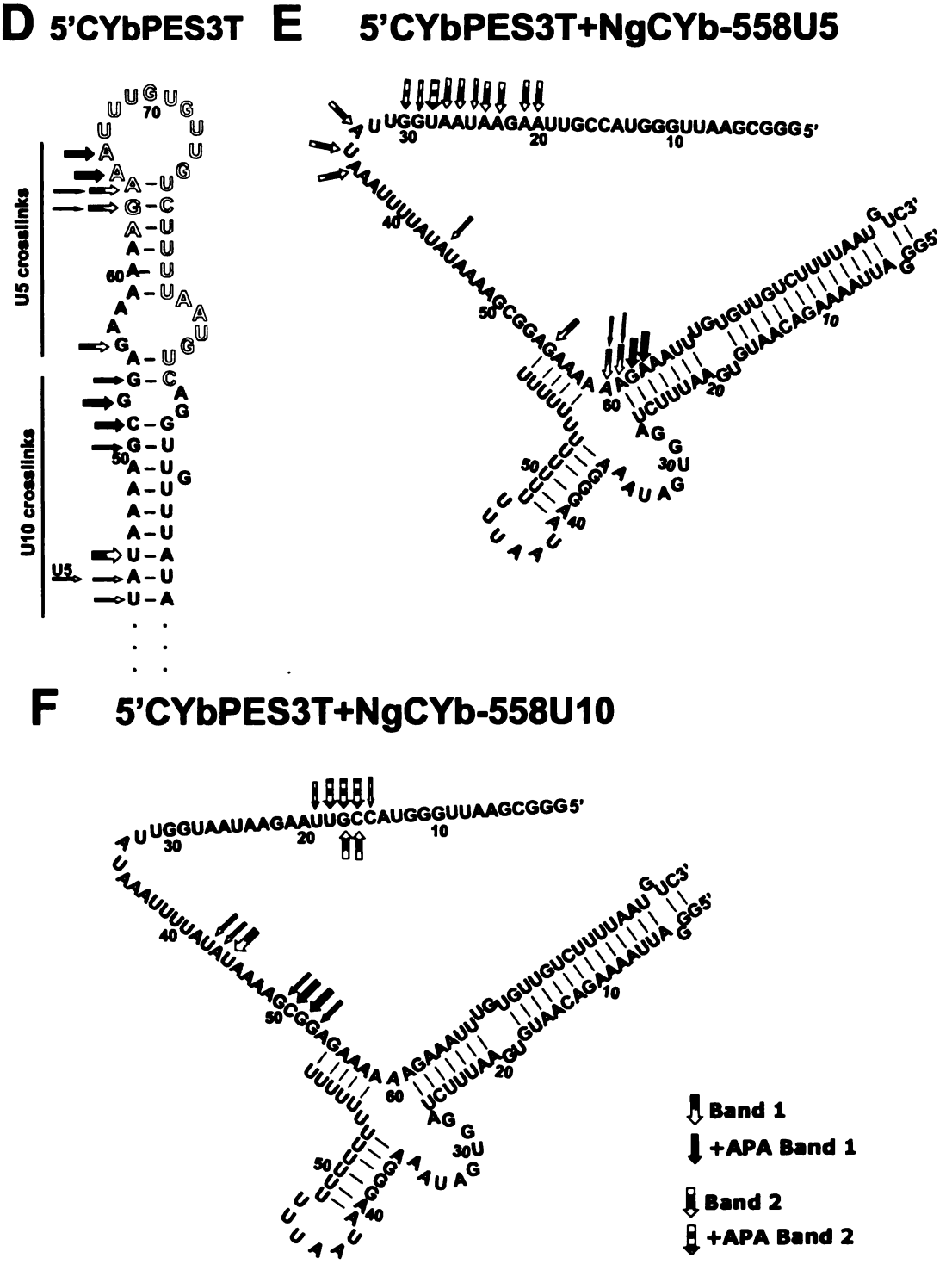

Figure 32. Diagram of the U5 and U10 crosslinks on the mRNA alone and the mRNA/gRNA complex. A. 5'CYbUT alone with the band 1 U5 and U10 crosslink positions indicated by vertical bars. Notice that the U-tail appears to bind the loop and bulge regions. B. 5'CYbUT+NgCYb-558 U5 crosslinks. C. 5'CYbUT+NgCYb-558 U10 crosslinks. D. 5'CYbPES3T alone with the band 1 U5 and U10 crosslink positions indicated by vertical bars. E. 5'CYbPES3T+NgCYb-558 U5 crosslinks. F. 5'CYbPES3T+NgCYb-558 U10 crosslinks. Arrows indicate the bases where covalent crosslinks are detected. The thickness of the arrow indicates intensity of the RT band.

dissociating from the purine rich upstream area of the mRNA that base pairs with the anchor binding site.

RNase H analysis was used to verify the primer extension results and showed that stops were caused by crosslinks and not structural obstacles or other artifacts. Twenty pmols of DNA oligonucleotides (Table 13) were used to surround the crosslinks that were observed on the RT analyses (Fig. 31). RNase H (Takara) was used to digest these areas of RNA duplexed to DNA. DNA oligonucleotides were selected to bracket a crosslink band, and when the digest was run on a gel, a migration pattern was observed that ran faster when the oligos bind closer to the crosslink. If multiple digested bands were observed, there was more than one crosslink. The RNaseH results verified the mRNA/gRNA crosslinks (example shown in Fig. 31).

In comparing crosslinks using 5'CYbUT, the unedited transcript, and 5'CYbPES3T, the partially edited transcript, the same U-tail interactions were found even as editing progressed supporting the previous work done with a 3' terminal crosslinker (Leung & Koslowsky, 1999). The B1 crosslinks were very interesting. The fifth residue of the U-tail was binding the loop of the stem-loop that was on one side of the anchor binding site (G34-G38) (Fig. 32A, D). The tenth U residue was binding the bulge region on the other side of the anchor binding site (C23-A26) (Fig. 32A, D). The U5 crosslinks appeared to be 5-10 nucleotides downstream of the U10 crosslinks; this made sense as the crosslinking agent was moved downstream too. The U5 crosslinks appeared to have a wider spread of crosslinks than the U10 tail; this correlated well with the secondary structure predictions as the U5 crosslinking agent was much closer to the sites for editing and this area was expected to be more dynamic or have more activity and

movement. Kinetic binding studies showed that the U-tail was helping the gRNA to bind the unedited CYb mRNA. These B1 crosslinking positions indicated that the U-tail was binding the bulge regions surrounding the anchor binding site of the unedited mRNA. The U-tail appeared to be helping disrupt the stem-loop of the CYb mRNA by base pairing with the complement to the ABS. This U-tail action may be critical for CYb editing as down regulation of the protein that adds U-tails to the gRNAs resulted in ablation of CYb editing (Nebohacova et al., 2004). However, the presence of mitochondrial proteins such as a helicase or annealing factor may alter this U-tail activity.

The B2 crosslinks were less easy to understand and these crosslinks may represent tertiary interactions with down stream mRNA that occurred after the mRNA/gRNA anchor helix is fully base-paired. However, these crosslinks were interacting with vector sequence on the mRNA, and these crosslinks could also be experimental artifacts. These mRNA/gRNA crosslinks appeared to have a more compact structure as the B2 crosslinks were the faster crosslink band in the gel (Fig. 29).

DISCUSSION

One of the interesting results of these experiments is that the U-tail appears to increase the association rate of the gRNA with the unedited CYb mRNA two fold in the absence of protein co-factors. This trend is observed both in the EMSA gels and in the Biacore data. The crosslinking data shows that the U-tail is binding and releasing the nts of the bulge region and loop region surrounding the anchor binding site. The U-tail may be acting as an evolutionary molecular tool that assists in opening mRNA stem-loops to allow anchor helices to form. The CYb anchor binding site sequence is U/C rich, so the

U-tail will not bind the anchor binding site. The sequence base paired to the anchor binding site is A/G rich, so the U-tail can bind this sequence easily. This makes the U-tail the perfect tool to help the gRNA invade the stem-loop to bind the ABS. Also, the A-U and G-U base pairs are weaker interactions with only 2 hydrogen bonds holding the base pairing interaction together; perhaps this makes the U-tail more flexible as it can make and then break these interactions as needed to maintain structures during editing such as the gRNA stem-loop. However, the U-tail may behave differently in the presence of proteins such as helicases or annealing factors that affect mRNA/gRNA binding.

The effects of editing on the stability of the mRNA/gRNA complex are interesting. The introduction of two uridylates into the first editing site causes a significant decrease in the affinity constant ($K_{D\,app}$) (Fig. 25B) of the 5'CYbPES1T/NgCYb-558 complex. When binding a single stranded region versus loop regions, the efficiency of the interaction depends on RNA structure and accessibility to the target sequence (Lima et al., 1992). The ABS helix must be disrupted in order for gRNA binding to occur (Franch et al., 1999) so that editing can begin. In the unedited mRNA, disruption of the ABS helix region is unfavorable as only four of the twelve nts on the ABS are accessible for anchor target binding, but this increases to seven accessible nts after one editing event. The next two editing events add four additional uridylates to the terminal loop (Fig. 23C) and again lower the affinity constant (Fig. 25C). However, the gRNA forms a stable stem-loop structure that is composed of a section of this CYbPES3 anchor. In fact, some of the newly single stranded anchor complement in the gRNA is part of the gRNA stem-loop and is unavailable to bind the newly single stranded ABS. The 5'CYbPES3T/NgCYb-558 complex has the lowest dissociation constant, and this may be

because the ABS target site is the most accessible with the least disruption of the target structure necessary for binding (Lima et al., 1992). However, the secondary structure of the gRNA may compete with the CYbPES3 anchor target binding resulting in no increase of association rate or possibly a cancellation of the effect of an increased ABS size. However, once the gRNA binds the interaction is more stable, because the anchor helix length has doubled. This effect is shown in the slower dissociation rate for the CYbPES3-gCYb-558 complex. Additionally, there are differences at 1 mM magnesium versus 2 mM magnesium. The increased magnesium may increase the stability of the mRNA and gRNA stem-loops resulting in a smaller association rate of the mRNA binding the gRNA despite the longer ABS. This sequestering of the gRNA long anchor (complement to partially edited ABS) may be an evolutionary gRNA strategy that keeps free gRNAs from competing with the gRNAs bound to the mRNAs once editing has begun.

The unedited CYb mRNA/gRNA interaction appears to be regulated kinetically and requires a chaperone or RNA annealing factor for gRNA target binding. However, such a protein does not co-purify with the main editing complex responsible for RNA editing (Simpson et al., 2004; Stuart et al., 2005). This implies that once editing has begun, this CYb initiating co-factor may be released from the complex. The fact that the very first editing event improves the binding interaction of the CYb mRNA/gRNA complex may be important for developmental regulation. With editing of the first site, the barrier to begin editing is greatly reduced. Once editing begins with the help of the cofactor, the mRNA/gRNA pair may need to be able to proceed through the editing process in the

absence of a co-factor. The kinetics of the interaction improve with each editing event; this may be an important part of editing progression.

An interesting result of the gel shift assays are the multiple bands of different mobility. In the presence of magnesium there appear to be alternate conformations of the mRNA/gRNA complex that are kinetically trapped into stable intermediates. While complexes of more than one mRNA/gRNA cannot be ruled out, it is unlikely as there is no sequence complementarity in the rest of the molecules. It is more likely that different band shift mobilities represent differing amounts of base pair formation along with target structure disruption (Lima et al., 1992). Increasing the magnesium concentration may stabilize multiple folding intermediates of the mRNA/gRNA complex, and these alternate structures of the complex would travel through the gel with different mobilities.

One puzzling aspect of these experiments is that the SPR obtained rate constants show slightly different results than the gel shift obtained rate constants (Table 14). The SPR rate constants show less variation as editing increases versus the gel shift data. The presence of the U-tail increases the association rate of the unedited CYb complex by two fold using both methods. Also, the rate constants from the gel shift data show a faster association rate as editing progresses along with a ten fold decrease in dissociation only after the first editing event. However, the SPR data shows a progressive decrease in dissociation rate with each editing event with no significant increase of association rate observed with increased editing (Table 14). The dissociation constants (K_D) for the gel shift data show the same trend as the Biacore data; however, the gel shift K_D's range from 10^{-6} to 10^{-8}, while the Biacore K_D's range from 10^{-5} to 10^{-7} (Table 14). While the trends of binding are the same, the numbers are not. Another difference is that only a slower

Table 14. Comparison between gel shift data and SPR data. Column 1: mRNA, Column 2: gRNA, Column 3: dissociation equilibrium constants, Column 4: association rate constants, Column 5: dissociation rate constants.

mRNA	gRNA	$K_{D\ app}$ (M)	$k_{on\ app}$ ($M^{-1}s^{-1}$)	$k_{off\ app}$(s^{-1})
5'CYbUT	NgCYb-558	$4.6(\pm0.6)x10^{-7}$	59.1	$1.11(\pm0.07)x10^{-4}$
	NgCYb-558sU	$1.3(\pm0.1)x10^{-6}$	37.5	$9.99(\pm1.3)x10^{-5}$
5'CYbPES1T	NgCYb-558	$1.2(\pm0.2)x10^{-7}$	$2.47 \times 10^{+2}$	$1.68(\pm0.1)x10^{-5}$
	NgCYb-558sU	$1.3(\pm0.3)x10^{-7}$	$1.49 \times 10^{+2}$	$1.05(\pm0.08)x10^{-5}$
5'CYbPES3T	NgCYb-558	$6.0(\pm0.3)x10^{-8}$	$4.15 \times 10^{+2}$	$1.77(\pm0.2)x10^{-5}$
	NgCYb-558sU	$6.0(\pm0.4)x10^{-8}$	$5.68 \times 10^{+2}$	$1.91(\pm0.2)x10^{-5}$

Table of rate constants and dissociation constants calculated from gel band shift data. from gels run at 1 mM magnesium.

mRNA	gRNA	K_D (M)	k_{on} ($M^{-1}s^{-1}$)	k_{off}(s^{-1})
CYbU	NgCYb-558	4.7×10^{-6}	$5.7\ (\pm0.9) \times 10^{+2}$	$2.7\ (\pm0.5) \times 10^{-3}$
	NgCYb-558sU	2.6×10^{-5}	$2.4\ (\pm1.3) \times 10^{+2}$	$6.1\ (\pm1.5) \times 10^{-3}$
CYbPES1	NgCYb-558	1.8×10^{-6}	$5.6\ (\pm0.4) \times 10^{+2}$	$1.0\ (\pm0.7) \times 10^{-3}$
	NgCYb-558sU	6.9×10^{-7}	$7.2\ (\pm3.3) \times 10^{+2}$	$4.9\ (\pm0.6) \times 10^{-3}$
CYbPES3	NgCYb-558	4.0×10^{-7}	$3.4\ (\pm2.4) \times 10^{+2}$	$1.4\ (\pm0.9) \times 10^{-4}$
	NgCYb-558sU	2.1×10^{-7}	$3.6 \times 10^{+2}$	7.5×10^{-5}

Table of rate constants and dissociation constants calculated from CYb Biacore data run at 2 mM magnesium. Only one experiment was used for the CYbPES3+NgCYb-558sU experiment, so no error is reported and the experiment should be repeated to verify this result.

observed rate constant was detectable using the gel shifts, while the Biacore experiments did not detect or separate two rate constants. However, there is also evidence that hybridization kinetics using techniques such as SPR where one molecule is bound can result in altered hybridization kinetics when compared to experiments done in solution (Sekar et al., 2005). In addition, immobilization of the mRNA may alter the thermodynamics of mRNA/gRNA complex formation by constraining the molecule's rotational and diffusional freedom (Nair et al., 2000). Also, when comparing different RNA-RNA interactions, some interactions measured using SPR have lower association rate constants when compared to other methods measuring the same interaction (Slagter-Jäger, 2003). The CYb association rate constant is at the detection limit of the Biacore machine; however, this range may be extended under favorable conditions (Myszka, 1997). This made these experiments difficult requiring very high concentrations of gRNA in order to observe binding causing possible mass transport problems. However, the variation between experiments using SPR was much lower than with the gel shift method indicating that the surface plasmon resonance method is more accurate and precise than the gel shift method. The gel shift method is a powerful tool to observe binding interactions, but the variation between experiments is relatively high. In addition, in order for the gel shifts to come to equilibrium in a reasonable amount of time, the mRNA and gRNA had to be heated and cooled slowly together. This method of annealing probably acts as a chaperone protein such as a helicase that would allow the gRNA to bind the mRNA much easier when the ABS mRNA stem-loop is melted or disrupted. This method appears to result in a higher affinity of binding as observed by

the variation in our dissociation constants between the gel shifts and the SPR experiments. The Biacore data reveals a similar trend, but provide more reliable kinetic data showing how the CYb mRNA/gRNA complex comes together in the absence of any chaperones or annealing factors, while the gel shift data show how this interaction may change in the presence of accessory factors. Although, there are differences, similar trends of binding are confirmed using both techniques.

Each editing event appears to increase the affinity of the mRNA for the gRNA. This indicates that once editing begins, even if a required protein co-factor is released or is displaced by the editosome, the CYb mRNA/gRNA complex will continue in the editing process, and with each editing event, the mRNA becomes more likely to finish editing. Progressivity may be an important part of the editing process, and the increased affinity of the RNA-RNA interaction added with each editing event could be important for editing continuity. In addition, the secondary structure of the gRNA (gRNA stem-loop) may keep free gRNAs from competing with gRNAs already bound in mRNA/gRNA partially edited complexes.

MATERIALS AND METHODS

Oligodeoxyribonucleotides

All oligodeoxyribonucleotides (Table 13) were ordered from Integrated DNA Technologies, Inc. (Coralville, IA).

RNA Synthesis and Labeling

The templates and sequences for 5'CYbUT, 5'CYbPES1T, and 5'CYbPES3T (Fig. 22) have been previously described (Koslowsky et al., 1992; Koslowsky et al., 1996). The templates and sequences for CYbU, CYbPES1, and CYbPES3 (Fig. 22) were similar

to the above sequences but had the vector sequence removed. NgCYb-558 and NgCYb-558sU (no U-tail) (Leung & Koslowsky, 1999, 2001a, b) (Fig. 22) were synthesized using the Uhlenbeck single-stranded T7 transcription method (Milligan et al., 1987) with the oligonucleotides described in Table 13. All RNAs were synthesized by T7 RNA polymerase using a Ribomax Large Scale RNA production kit (Promega) according to the manufacturer's directions. RNAs were gel purified as described previously (Koslowsky et al., 2004). The gRNAs used for the gel shifts were 5' end labeled by treating with calf intestinal phosphatase (Invitrogen) followed by T4 kinase (Invitrogen) with [γ^{32}P] rATP as described previously (Koslowsky et al., 2004).

Serial Dilutions of mRNA

All mRNA concentrations (Table 8) were measured using an ND-1000 spectrophotometer (NanoDrop Technologies, Wilmington, DE).

Gel Band-shift Analysis

The apparent equilibrium constants of the gRNA binding to the mRNA were found using a direct band-shift electrophoresis assay (Koslowsky et al., 2004). The mRNAs were serially diluted (Table 8). The serial diluted concentrations of mRNA were mixed with 50 fmols of 5'end-labeled gRNA (50 mM Tris pH 7.5, 0.1 mM EDTA, 100 mM KCl, 3% glycerol, 0.05% xylene cyanol, and MgOAc as indicated) in 10 µl (Koslowsky et al., 2004). Each sample was heated to 70°C for 2 minutes and allowed to cool to room temperature for 3 hours before being loaded onto a 6% polyacrylamide native gel (50 mM Tris pH 7.5, 50 mM Hepes pH 7.5, 0.1 mM EDTA, indicated concentration of magnesium acetate) under current. The gels were electrophoresed, fixed, and scanned on a phosphorimager (Molecular Dynamics) as described previously (Koslowsky et al.,

2004). The apparent affinity constant of gRNA binding the mRNA was extracted from data-point fitting using Kaleidagraph 3.5 (Synergy Software) with the equation:

$$[Complex] = \frac{\left(\left[gRNA_f\right] * \left[mRNA_f\right]\right)}{\left(\left[gRNA_f\right] + K_D\right)}$$, with $[gRNA_f]$ equal to the concentration of the free gRNA, $[mRNA_f]$ equal to the concentrations of unlabeled free mRNA, $[Complex]$ equal to the concentration of mRNA/gRNA complex, and K_D equal to the dissociation constant. The values reported here represent the average of 4 gels and the error is calculated from the difference in these values.

Dissociation rate gels

The apparent dissociation rate constants of the gRNA binding to the mRNA were found using a direct band-shift electrophoresis assay (Lima et al., 1992). The mRNA was mixed with 10 fmols of 5'end-labeled gRNA (50 mM Tris pH 7.5, 0.1 mM EDTA, 100 mM KCl, 3% glycerol, 0.05% xylene cyanol, and 1 X RNase Secure (Ambion, Austin, TX), and 1 mM magnesium acetate) in 100 µl. Each sample was heated to 60°C for 10 minutes, then held at 27°C for 20 hours before adding an oligonucleotide complementary (Integrated DNA Technologies, Coralville, IA) (Fig. 22) to the gRNA anchor sequence (10X the concentration of the mRNA). A short complementary oligonucleotide was added to the CYbU and CYbPES1 samples, while a long complementary oligonucleotide was added to the CYbPES3 samples (Fig. 22D). This complementary oligonucleotide does not allow the gRNA to rebind the mRNA. Time points were taken at the indicated times and snap frozen on dry ice. The time points were individually thawed and loaded onto an 8% 19:1 polyacrylamide native gel (50 mM Tris pH 7.5, 50 mM Hepes pH 7.5,

0.1 mM EDTA, and 1 mM magnesium acetate) under current. The gels were electrophoresed, fixed, and scanned on a phosphorimager (Molecular Dynamics) as described previously (Koslowsky et al., 2004). The apparent dissociation rate constant of gRNA binding the mRNA was extracted from data-point fitting using Kaleidagraph 3.5 (Synergy Software) with the equation:

$$[Complex_{Total}] = [Complex_{Time1}] * e^{-(k_{off} * Time)}.$$

The $[Complex_{Total}]$ represents total binding of mRNA/gRNA complex formation, $[Complex_{Time1}]$ is the amount of complex formation at the first time point and k_{off} is the apparent dissociation rate constant (Motulsky & Christopoulos, 2003).

Association rate gels

The apparent association rate constants of the gRNA binding to the mRNA were found using a direct band-shift electrophoresis assay (Lima et al., 1992). The mRNA was mixed with 10 fmols of 5'end-labeled gRNA (50 mM Tris pH 7.5, 0.1 mM EDTA, 100 mM KCl, 3% glycerol, 0.05% xylene cyanol, 1 X RNase Secure (Ambion) and 1 mM magnesium acetate) in 100 µl. Each sample was heated to 60°C for 10 minutes, and then held at 27°C. Time points were taken at the indicated times and snap frozen on dry ice. The time points were individually thawed and loaded onto an 8% 19:1 polyacrylamide native gel (50 mM Tris pH 7.5, 50 mM Hepes pH 7.5, 0.1 mM EDTA, 1 mM magnesium acetate) under current. The gels were electrophoresed, fixed, and scanned on a phosphorimager (Molecular Dynamics) as described previously (Koslowsky et al., 2004). The apparent observed rate constant for CYbU was calculated using a single exponential

fit based on the reaction mechanism $mRNA + gRNA \underset{k_{off}}{\overset{k_{on}}{\leftrightarrow}} {}^{gRNA}/_{mRNA}$ where the mRNA and gRNA bind to form the mRNA/gRNA complex. For the partially edited mRNAs, CYbPES1 and CYbPES3, the best line fit for the data points was a double exponential fit using the reaction mechanism:

$mRNA^* + gRNA \xrightarrow{k_{on1}} {}^{gRNA}/_{mRNA} \underset{k_{off}}{\overset{k_{on2}}{\leftrightarrow}} mRNA + gRNA$ where the mRNA* represents an alternate conformation of the mRNA that allows a significantly faster association rate with no noticeable dissociation along with a slower mechanism of binding similar to the unedited CYb reaction. The observed rate constant of gRNA binding the unedited CYb mRNA was extracted from data-point fitting using Kaleidagraph 3.5 (Synergy Software) with the equation:

$[Complex_{SB}] = [Complex_{Total}] * \left(1 - e^{\left(-(k_{obs} * Time)\right)}\right)$ The $[Complex_{SB}]$ represents specific binding of the complex for each time point, $[Complex_{Total}]$ is the amount of specific binding of the complex at equilibrium for a single exponential fit. The observed rate constant of gRNA binding the partially edited CYb mRNAs was extracted from data-point fitting using Kaleidagraph 3.5 (Synergy Software) with the equation:

$[Complex_{SB}] = \left([Complex_1] * \left(1 - e^{\left(-(k_{obs1} * Time)\right)}\right) + \left([Complex_2] * \left(1 - e^{\left(-(k_{obs2} * Time)\right)}\right)\right)\right)$. The $[Complex_{SB}]$ represents specific binding of the complex for each time point, k_{obs} is the observed rate constant, $[Complex_1]$ and $[Complex_2]$ represent two amplitudes of binding for a double exponential fit. The first observed rate constant for CYbPES1 and

CYbPES3 can only be measured by the first data point, and therefore the first observed rate constant cannot be reliably measured using gel shifts. Since the first binding event is so rapid, it cannot be accurately measured using this technique, only the second slower observed rate constant will be reported and used to calculate k_{on}. This first binding event may represent a small fraction of mRNAs that have an open helix due to structural breathing, or it could represent a very unstable helix nucleation event. The limitations of this technique prevent further examination of this phenomenon as it is not stable enough to measure using gel shifts. The apparent association rate constant k_{on} was calculated from the observed rate constant k_{obs} using the equation: $k_{on} = \frac{(k_{obs} - k_{off})}{[mRNA_{Total}]}$ where k_{on} represents the apparent association rate constant, k_{off} is the apparent dissociation rate constant calculated earlier, and the $[mRNA_{Total}]$ is the concentration of mRNA used (Motulsky & Christopoulos, 2003).

Surface Plasmon Resonance Studies

Measurements of the association and dissociation rate constants were performed in a BIACORE 2000 instrument (BIACORE, Uppsala, Sweden). All the solutions used in the binding studies were filtered through a 0.22 μm polyethersulfone membrane (Corning) or a 0.22 μm Millex-GS membrane (Millipore) and degassed. All Biacore mRNA and gRNA substrates are listed in Table 10. The CYbU mRNA was ligated to the BigSK-biotin DNA tag or to Biatag1, a different biotinylated DNA tag. The measurements of CYbU were similar regardless of the DNA tag that was attached. BigSK-biotin or Biatag1 was annealed to the 3' end of CYbU using DNA bridging oligonucleotides (Table 13) as described previously (Yu & Koslowsky, 2006). The bridging

oligonucleotides are listed in Table 13. The CYbU mRNAs were gel extracted without phenol and purified using ultra-free MC membranes (Millipore) and Microcon tubes (YM-50, Millipore) according to the manufacturer's directions. The gRNAs were transcribed as described above and purified using Ultra-free MC and the microcon tubes (YM-10,30) (Millipore) as above. The RNA samples were then diluted in running buffer (20 mM Tris pH 7.5, 0.1 mM EDTA, 2 mM $MgCl_2$, and 100 mM KCl); the CYbU samples were run using 100 mM Tris pH 7.5, while the partially edited substrates, CYbPES1 and CYbPES3, were run in 20 mM Tris pH 7.5. The partially edited CYb mRNAs (CYbPES1 and CYbPES3) were transcribed as described above then ligated to CYbBia, a biotinylated DNA tag, (Table 10) using T4 DNA ligase (Roche). CYbBia is complementary to the CYb mRNAs, and so taking advantage of the stem-loop structure of the CYb mRNA, it was directly annealed to the mRNA and ligated using T4 DNA ligase (Roche). The gRNAs were transcribed as described above. The partially edited CYb mRNAs were gel purified using the Ultra-free MC membranes as above. The partially edited CYb mRNA and gRNA samples were ethanol precipitated and then dialyzed for six hours in running buffer (20 mM Tris pH 7.5, 0.1 mM EDTA, 2 mM $MgCl_2$, and 100 mM KCl) in a Spectra/Por Float-A-Lyzer (5 mM, 300 µl, MWCO 8,000) (Spectrum Laboratories, Inc.) according to the manufacturer's directions. All biotinylated mRNAs were diluted to 10 nM and between 250-600 resonance units (RU) of mRNA was attached at 5 µl/min to a streptavidin coated SA sensor chip (BIACORE, Uppsala, Sweden). Two cells were immobilized with mRNA, one was left unmodified to serve as a reference cell, and one cell was immobilized with the biotinylated DNA tag as a control cell. Binding studies were carried out running all four cells in series with

repetitive cycles of 150-250 µl gRNA injection at 5 µl/min (association of varying concentrations of gRNA, 200-7000 nM), buffer flow (dissociation of gRNA) 5 µl/min for 15-20 minutes, and regeneration (50 µl injection of regeneration buffer, two 50 µl injections of running buffer at 50µl/min). These experiments were all run at 27° C. The regeneration buffer for the partially edited CYb experiments was 1-10 mM EDTA. The regeneration buffer for CYbU experiments was 8 M Urea. The determination of rate constants was performed by fitting theoretical curves to the experimental curves obtained using BIAevaluation 3.0 software (BIACORE, Uppsala, Sweden). The equation used to calculate the dissociation rate constants for CYbPES3 from the Biacore sensograms was the 1:1 (Langmuir) dissociation formula describing analyte (gRNA) dissociates from surface complex (mRNA/gRNA complex): $R0 * e^{(-k_d * (t - t0))} + Offset$, $R0$ = Y_{max} = maximum analyte binding capacity (RU), k_d = dissociation rate constant, t = time, $t0$ = time at start, $Offset$ = residual response at infinite time (RU). The line fit for CYbU and CYbPES1 mRNA/gRNA complexes did not fit the data well, so the equation was slightly altered for the CYbU and CYbPES1 dissociation rate constant: $(R0 - Offset) * e^{(-k_d * (t - t0))} + Offset$. The equation used to calculate the association rate constant was the 1:1 (Langmuir) association formula describing analyte (gRNA) binds to ligand (mRNA):

$\frac{k_a * Conc * R_{max}}{(k_a * Conc + k_d)} \times \left(1 - e^{(-(k_a * Conc + k_d) * (t - t0))}\right) + RI$, k_a = association rate constant (k_{on}), $Conc$ = molar analyte concentration, RI = bulk refractive index effect (RU), R_{max} = Y_{max} = maximum analyte binding capacity (RU), t = time, $t0$ = time at start, k_d = dissociation rate constant (k_{off}). The dissociation rate constant was incorporated into the

association rate constant line fit. Some of the CYbU and CYbPES1 association rate line fits used the dissociation rate constant calculated from the altered dissociation rate equation and some used the dissociation constant calculated from the regular dissociation rate equation. When the line fit the association curve data, the rate constants were similar. The association rate for CYb was actually slower than can be reliably measured by the Biacore 2000 according to machine specifications; however, this range may be extended under favorable conditions (Myszka, 1997). This may account for the differences observed in association rate between the gel shift data and the surface plasmon resonance data. Separate fits for each association and dissociation curve were analyzed globally from each experiment to obtain k_{on} and k_{off}, individually, and the results were averaged. The errors reported for the rate constants were based on the variances of all curves obtained (Nordgren et al., 2001). The dissociation equilibrium constant (K_D) was calculated from the averages of the rate constants using the equation: $K_D = \frac{k_d}{k_a}$.

RNA crosslinking and mapping of crosslinks

A U_{15}-tail containing a 4-thio-uridine (4sU) (Dharmacon, Boulder, CO) either in the fifth or tenth position (Table 12) was 5' trace labeled and ligated to NgCYb-558sU with T4 DNA ligase (Roche) using a DNA bridging oligonucleotide, gCYb558(sU) bridge (IDT, Table 13), as previously described (Leung & Koslowsky, 2001b). Half of the gRNA was treated with p-azidophenacyl bromide (Sigma) as described previously (Leung & Koslowsky, 2001b). The mRNA was then annealed to the gRNA, UV crosslinked, resolved on a 6% acrylamide gel, and recovered as previously described (Leung &

Koslowsky, 2001b). Primer extension analysis was done as previously described (Leung & Koslowsky, 1999) as was the RNase H analysis (Leung & Koslowsky, 2001b).

ACKNOWLEDGEMENTS

This work was supported by National Institutes of Health Grant AI34155 to D.K. We'd like to thank Larissa Reifur, Dr. Ron Patterson, Dr. John Wang, Dr. Charles Hoogstraten, and all other members of the MSU RNA Journal Club for critical reading of the manuscript and helpful discussions. We'd like to thank Dr. Robert Hausinger, Microbiology and Molecular Genetics MSU, and Dr. Zachary Burton, Biochemistry and Molecular Biology MSU, for their help with Kaleidagraph and rate constant equation discussions. We'd like to thank Dr. Hoogstraten for his help with analyzing the Biacore data. Also, we'd like to thank Dr. Karen Friderici and her lab, Microbiology and Molecular Genetics MSU, for the use of their nanodrop spectrophotometer. We would like to thank Dr. Joseph Leykam and the members of the Macromolecular Structure Facility in the Biochemistry and Molecular Biology Department, MSU, for the use the Biacore machine. Many thanks to Remy Brim and Andrea Hingst for many excellent solutions made.

Literature Cited

Adler BK, Hajduk SL. 1997. Guide RNA requirement for editing-site-specific endonucleolytic cleavage of preedited mRNA by mitochondrial ribonucleoprotein particles in Trypanosoma brucei. *Mol Cell Biol 17*:5377-5385.

Blum B, Bakalara N, Simpson L. 1990. A model for RNA editing in kinetoplastid mitochondria: "guide" RNA molecules transcribed from maxicircle DNA provide the edited information. *Cell 60*:189-198.

Blum B, Simpson L. 1990. Guide RNAs in kinetoplastid mitochondria have a nonencoded 3' oligo(U) tail involved in recognition of the preedited region. *Cell 62*:391-397.

Feagin JE, Jasmer DP, Stuart K. 1985. Apocytochrome b and other mitochondrial DNA sequences are differentially expressed during the life cycle of Trypanosoma brucei. *Nucleic Acids Res 13*:4577-4596.

Franch T, Petersen M, Wagner EG, Jacobsen JP, Gerdes K. 1999. Antisense RNA regulation in prokaryotes: rapid RNA/RNA interaction facilitated by a general U-turn loop structure. *J Mol Biol 294*:1115-1125.

Koslowsky DJ, Goringer HU, Morales TH, Stuart K. 1992. In vitro guide RNA/mRNA chimaera formation in Trypanosoma brucei RNA editing. *Nature 356*:807-809.

Koslowsky DJ, Kutas SM, Stuart K. 1996. Distinct differences in the requirements for ribonucleoprotein complex formation on differentially regulated pre-edited mRNAs in Trypanosoma brucei. *Mol Biochem Parasitol 80*:1-14.

Koslowsky DJ, Reifur L, Yu LE, Chen W. 2004. Evidence for U-Tail Stabilization of gRNA/mRNA Interactions in Kinetoplastid RNA Editing. *RNA Biology 1*:28-34.

Leung SS, Koslowsky DJ. 1999. Mapping contacts between gRNA and mRNA in trypanosome RNA editing. *Nucleic Acids Res 27*:778-787.

Leung SS, Koslowsky DJ. 2001a. Interactions of mRNAs and gRNAs involved in trypanosome mitochondrial RNA editing: structure probing of an mRNA bound to its cognate gRNA. *RNA 7*:1803-1816.

Leung SS, Koslowsky DJ. 2001b. RNA editing in Trypanosoma brucei: characterization of gRNA U-tail interactions with partially edited mRNA substrates. *Nucleic Acids Res 29*:703-709.

Lewis BP, Burge CB, Bartel DP. 2005. Conserved seed pairing, often flanked by adenosines, indicates that thousands of human genes are microRNA targets. *Cell 120*:15-20.

Lima WF, Monia BP, Ecker DJ, Freier SM. 1992. Implication of RNA structure on antisense oligonucleotide hybridization kinetics. *Biochemistry 31*:12055-12061.

Milligan JF, Groebe DR, Witherell GW, Uhlenbeck OC. 1987. Oligoribonucleotide synthesis using T7 RNA polymerase and synthetic DNA templates. *Nucleic Acids Res 15*:8783-8798.

Moore MJ, Sharp PA. 1992. Site-specific modification of pre-mRNA: the 2'-hydroxyl groups at the splice sites. *Science 256*:992-997.

Motulsky HJ, Christopoulos A. 2003. Fitting models to biological data using linear and nonlinear regression. *A practical guide to curve fitting*. San Diego: Graphpad Software Inc., www.graphpad.com.

Myszka DG. 1997. Kinetic analysis of macromolecular interactions using surface plasmon resonance biosensors. *Curr Opin Biotechnol 8*:50-57.

Nair TM, Myszka DG, Davis DR. 2000. Surface plasmon resonance kinetic studies of the HIV TAR RNA kissing hairpin complex and its stabilization by 2-thiouridine modification. *Nucleic Acids Res 28*:1935-1940.

Nebohacova M, Maslov DA, Falick AM, Simpson L. 2004. The effect of RNA interference Down-regulation of RNA editing 3'-terminal uridylyl transferase (TUTase) 1 on mitochondrial de novo protein synthesis and stability of respiratory complexes in Trypanosoma brucei. *J Biol Chem 279*:7819-7825.

Nordgren S, Slagter-Jager JG, Wagner GH. 2001. Real time kinetic studies of the interaction between folded antisense and target RNAs using surface plasmon resonance. *J Mol Biol 310*:1125-1134.

Reifur L, Cruz-Reyes J, vanHartesvelt M, Koslowsky DJ. 2006. Anchor binding site accessibility and RNA editing in Trypanosoma brucei. *manuscript in prep.*

Seiwert SD, Stuart K. 1994. RNA editing: transfer of genetic information from gRNA to precursor mRNA in vitro. *Science 266*:114-117.

Sekar MM, Bloch W, St John PM. 2005. Comparative study of sequence-dependent hybridization kinetics in solution and on microspheres. *Nucleic Acids Res 33*:366-375.

Simpson L, Aphasizhev R, Gao G, Kang X. 2004. Mitochondrial proteins and complexes in Leishmania and Trypanosoma involved in U-insertion/deletion RNA editing. *RNA 10*:159-170.

Slagter-Jäger JG. 2003. CopA and CopT: The Perfect RNA Couple. *Department of Cell and Molecular Biology*. Uppsala, Sweden: Uppsala University. pp 1-47.

Stuart KD, Schnaufer A, Ernst NL, Panigrahi AK. 2005. Complex management: RNA editing in trypanosomes. *Trends Biochem Sci 30*:97-105.

Young S, Wagner RW. 1991. Hybridization and dissociation rates of phosphodiester or modified oligodeoxynucleotides with RNA at near-physiological conditions. *Nucleic Acids Res 19*:2463-2470.

Yu LE, Koslowsky DJ. 2006. Interactions of mRNAs and gRNAs involved in trypanosome mitochondrial RNA editing: structure probing of an gRNA bound to its cognate mRNA. *RNA 12*:1050-1060.

CHAPTER 5

CONCLUSIONS AND FUTURE RESEARCH

Summary

The trypanosome is able to effect a rapid change in its development, morphology, and energy metabolism in response to instantaneous differences in temperature (insect 27°C, mammal 37°C), cellular environment, and immune response that is brought on by a change of host (Brown & Neva, 1983). Many of the proteins for energy metabolism that are made in the mitochondria are thought to be developmentally regulated by RNA editing. Developmental regulation of RNA editing may control mitochondrial biogenesis by only allowing production of respiratory proteins during the correct life cycle. However, very little is known concerning how editing is regulated. The gRNA transcripts, the mRNA transcripts, and the editosome protein complexes are always present (Hajduk & Sabatini, 1998). Additionally, very little is known about how the editing complex is assembled onto specific RNAs. There are hundreds of different mRNA/gRNA pairs, but no conserved sequence domains have been found in mRNAs. The only conserved sequence domain shared between the gRNAs is the U-tail. Previous work in this lab suggests that different mRNA/gRNA pairs can form similar structures composed of three helices. Structure recognition may be important for efficient editosome assembly with the mRNA/gRNA pair. Discovering the structure of an mRNA/gRNA pair such as CYb may be the first step in unraveling what RNA structure attracts the editosome, and how the RNA structure changes when in contact with the editosome. This lab is interested in gRNA targeting of the mRNA for binding and how this affects editing efficiency. Specifically, discovering how the mRNA/gRNA complex interaction is occurring and understanding how the anchor sequence, U-tail, and guiding region interact with the mRNA during RNA editing was investigated. The objective of

this study has been to characterize the structure of the CYb gRNA/mRNA complex as well as what role the structure of the CYb mRNA plays in the binding affinity of the gRNA to the mRNA. The effects partial editing of the mRNA have on the gRNA/mRNA complex structure were studied as well as the kinetics of its formation. Additionally, the role the U-tail has in the CYb mRNA/gRNA complex interaction was investigated.

Anchor binding site structure influences editing

Expression of the CYb mRNA is regulated through RNA editing (Feagin et al., 1988) and is needed for mitochondrial respiration in the insect host (Vickerman, 1965). The unedited CYb mRNA forms a stable stem-loop structure, with the anchor binding site (ABS) base paired within the helical stem (Leung & Koslowsky, 2001a). It is clear that the structure of the immediate editing domain on the mRNA can profoundly affect the efficiency of the interaction between the gRNA and the target mRNA (Koslowsky et al., 2004). The unedited CYb mRNA/gRNA binding interaction was compared with two different unedited mRNA/gRNA pairs that have single stranded predicted anchor binding sites (ABS). The ATPase 6 (A6) mRNA/gRNA pair and the NADH dehydrogenase 7 (ND7) mRNA/gRNA pair had a 2000 fold and 8400 fold higher affinity anchor target binding respectively than the CYb mRNA/gRNA pair. The association rate constants and dissociation rate constants show that this is because the A6 pair has a 20 fold faster association rate and a 20 fold slower dissociation rate than the CYb pair. The ND7 results are similar showing that the ND7 mRNA/gRNA pair has a 90 fold faster association rate than the CYbU pair and a similar 20 fold slower dissociation rate comparable to A6. Clearly, the mRNA structure around the immediate editing domain can strongly affect the gRNA anchor target binding and appears to be regulating the CYb

editing kinetically with a slow on-rate and a fast off-rate. The mND7550 substrate and the A6UENDSh substrate are not controlled kinetically as they have a relatively fast on-rate and a very slow off-rate. The mRNA/gRNA complex stability appears to be controlled by the slow off-rate. This slow off-rate may be necessary to allow editing to occur. Both A6 and ND7 mRNAs are predicted to have single stranded anchor binding sites that are easily accessible by the gRNA. However, the ND7 mRNA/gRNA complex is not edited *in vitro* as the constitutively edited A6 pair is, suggesting that an alternative method of editing regulation exists. The editing of the mRNA/gRNA complexes may also be controlled structurally, so that only RNA complexes with the correct tertiary structures are edited. Accessory factors such as chaperones that alter and stabilize structure may be required for editing to occur. Perhaps A6 is the only mRNA/gRNA capable of correct folding in the absence of these factors.

CYb mRNA/gRNA complex structure during editing

In this study, the structure of NgCYb-558 alone and its structure when paired with its cognate unedited mRNA or partially edited mRNA were also investigated. Solution structure probing of the CYb mRNA/gRNA complex reveals a 3 helix structure in the unedited complex that, although modified by editing, is maintained through the third editing site. The changes brought about by partial editing include an anchor duplex doubled in length (Leung & Koslowsky, 2001b; Yu & Koslowsky, 2006). As a consequence of the longer anchor, the stem-loop of the gRNA appears to begin incorporating the U-tail; this results in decreased U-tail interaction with the mRNA (Yu & Koslowsky, 2006). The gRNA stem-loop may be an important structural component of the initial editing complex. Previous work using gel shift analyses indicates that the

U-tail is very important for stabilization of the interaction of some mRNA/gRNA pairs (Koslowsky et al., 2004). RNAi studies have also shown that when the RNA editing terminal uridylyl transferase (RET1), responsible for adding the U-tail to gRNAs is down regulated, there is a decrease in edited mRNAs and inhibited growth of the trypanosome (Aphasizhev et al., 2002) suggesting that the U-tail is necessary for *in vivo* editing (Gott, 2003; Nebohacova et al., 2004). Guide RNAs appear to be able to take advantage of U-tail flexibility through the ability of uridines to base pair with both purine bases. By employing an uridylate tail, the gRNA may increase mRNA/gRNA complex stability, without hampering the U-tail migration needed within the complex during the editing process.

Kinetics of anchor target binding during editing

Using gel band shift assays and surface plasmon resonance, the effects of the changes in structure in the partially edited CYb mRNA/gRNA complex were investigated to discover how the binding interaction changes between the mRNA and gRNA during editing. In this study, the addition of two uridines to the anchor binding site (ABS) of the mRNA decreases the dissociation constant (K_D) significantly. It appears that these three bases increase the size of the terminal loop of the mRNA and make it more accessible. This change in structure leads to an increase in formation of the mRNA/gRNA complex that appears to be caused by a decrease in the dissociation rate. There is an additional decrease in K_D when four more uridylates are added to the next two editing sites. These next two editing events have doubled the size of the mRNA ABS extending through the terminal loop. In addition, the gRNA forms a stable stem-loop structure composed of part of the newly accessible ABS and this section of the gRNA anchor is unavailable for

gRNA binding. This may explain why a large increase of association rate is not observed for this substrate. This may be an evolutionary strategy to keep free gRNAs from disrupting partially edited mRNA/gRNA complexes. This alteration in mRNA structure through editing appears to further increase the stability of the complex by decreasing the dissociation rate. With editing of the first site, the barrier to begin editing is greatly reduced, and the CYb mRNA/gRNA complex becomes more stable with increased editing. The longer anchor helix results in a slower dissociation rate. Once editing begins with the help of cofactors, the mRNA/gRNA pair may need to proceed through the editing process in the absence of a co-factor. The kinetics of the interaction improve with each editing event; this may be an important part of editing progression.

The U-tail has been predicted to slow dissociation; however, one of the interesting results of these experiments is that the U-tail appears to help the gRNA to associate with the unedited CYb mRNA. This trend was observed both in the gel shifts and in the Biacore data. This is the first evidence that shows the U-tail contributes to anchor target binding. However, in the presence of a mitochondrial helicase or an anchor annealing factor this U-tail function may be altered.

Where the U-tail is interacting in the CYb mRNA/gRNA complex was also studied. A 4-thio-uridine (4sU) crosslinking agent was placed in the fifth and then tenth position of the U-tail on NgCYb-558. This gRNA was annealed to either the unedited CYb mRNA or a partially edited substrate and UV crosslinked. These U-tail positions were mapped and the main crosslink band was found to interact with the loop (U5) and bulge region (U10) that surround the anchor binding site. This suggests that the U-tail is helping the CYb gRNA/mRNA complex form. It appears to do this through disruption of

the mRNA stem-loop, by binding one side of the helix that hides the anchor binding site. The CYb anchor binding site sequence is U/C rich, so the U-tail will not bind the anchor binding site. The sequence base paired to the anchor binding site is A/G rich, so the U-tail can bind this sequence easily. This makes the U-tail the perfect tool to help disrupt the stem-loop. Also, the A-U and G-U base pairs are weaker interactions with only 2 hydrogen bonds holding the base pairing interaction together; perhaps this makes the U-tail more flexible so it is able to continue its migration during editing to become part of the gRNA stem-loop.

The U-tail may not be necessary for the A6 and ND7 mRNA/gRNA interactions, or the U-tail function in these interactions may be different than it is for CYb. Interestingly, the anchor binding site sequence for these mRNAs is U/C rich, so the U-tail will not interfere with anchor helix formation. It will be interesting to see if the anchor binding sites for most mRNA/gRNA pairs have evolved to be U/C rich to avoid U-tail interference.

Much is known about the protein components of the editosome. A growing list of proteins is now known to be necessary for RNA editing. However, while much is known about the proteins, very little is known about how gRNAs target mRNAs for binding and how the editosome proteins target the mRNA/gRNA complexes for editing. There is no sequence homology between the hundreds of different pairs other than the U-tail on the gRNA. This lab is interested in discovering how these protein complexes recognize the mRNA/gRNA complexes, and we hypothesize that the editosome protein complexes recognize elements of structure instead of sequence. This work has made a significant contribution to discovering how the gRNA targets its mRNA and what type of binding

affinity different gRNA/mRNA pairs have. By comparing the double stranded CYb mRNA to other single stranded mRNAs, it was found that the structure of the immediate editing domain is important for gRNA target binding. Also, the editing process appears to improve the mRNA/gRNA interaction, so that mRNA and gRNA pairs that have started editing are more likely to finish with each editing event; this may be important for editing progression. Additionally, the versatility of the U-tail and its role in gRNA binding association along with its role in maintaining important structures such as the gRNA stem-loop provide new insights into its biological function and purpose. This work helps illuminate how RNA hybridization during editing occurs and provides deeper insights into the biological function of this RNA-RNA interaction. This has laid the groundwork for future studies that include mitochondrial proteins to see how the RNA-RNA interactions change in the presence of mitochondrial proteins.

The solution structure probing data show that the structure of the mRNA/gRNA complex appears to form a three way helical junction. RNA helical junctions are versatile structural elements that are able to perform multiple biological functions using differing structural requirements. Some ribozymes containing three way junctions can exist in inactive extended conformations for long periods of time and may require regulatory ligands to form the correct structure (Goldschmidt et al., 2002). The mRNA/gRNA complexes may require multiple chaperones for editing to occur. One example of a functional RNA requiring chaperones is the group I self-splicing intron. For group I introns, CYT-18 appears to stabilize group I intron structures, while CYT-19, an ATP dependent nucleic acid helix-destabilizer, uses ATP hydrolysis to unfold kinetically trapped intermediates to allow correct folding. Both proteins appear to be

necessary for self-splicing of this group I intron (Lorsch, 2002; Mohr et al., 2002). Chaperones similar to these may be required specifically for the CYb mRNA/gRNA complex to destabilize the CYb mRNA stem-loop and stabilize the mRNA/gRNA complex. In addition, other RNA chaperones involved in RNA-RNA matchmaking (Muller et al., 2001) or involved in strand exchange (Arthur et al., 2003) may be necessary to promote faster anchor binding *in vivo* for other mRNA/gRNA pairs. The ND7 and A6 mRNAs are both predicted to have similar secondary structures (three way junctions) and have similar kinetics of binding, but A6 is the only mRNA/gRNA pair capable of *in vitro* editing. Perhaps the ND7 complex forms the incorrect tertiary structure and the editosome can not recognize it, so editing can not occur. This occurs in the hepatitis delta virus where ADAR1, an RNA editing enzyme in humans, only performs adenosine to inosine editing on the RNA genomes with branched structures but not unbranched structures (Linnstaedt et al., 2006). Perhaps editing in trypanosomes is controlled structurally and mRNA/gRNA complexes other than A6 require chaperones to form the correct tertiary structures as well as stabilize this structure in order to be recognized by the editosome.

Editosome recruitment

An objective of this study was to discover the structure and kinetics of the CYb mRNA/gRNA interaction in order to discover how the editosome is recruited to the mRNA/gRNA complex. One possibility for editosome recruitment is that proteins with RNA binding sites are needed to recognize different structural elements of the mRNA/gRNA complex. Solution structure probing of additional mRNA/gRNA pairs may help prove that structure recognition may be how the editosome targets

mRNA/gRNA complexes. One element of structure the editosome may recognize is the mRNA/gRNA anchor helix. The anchor helix is the first element of structure formed during editing, and the gRNA anchor binding the mRNA ABS is thought to be the first step in editing. The endonucleases of the editosome have double-stranded RNA binding domains that may target the anchor helix for binding to cleave the mRNA strand (Panigrahi et al., 2006). This anchor binding step needs to be extremely accurate in order to eliminate incorrect editing that could result in a non-functional protein.

The anchor helix may not be the only element of RNA structure necessary for editing. The local structure at the editing site may determine which protein editing complex is recruited. Different editosome complexes (U-deletion or U-insertion) must bind during editing, so there must be additional structural elements necessary for the correct complex to be recruited. One of the editosome proteins that binds RNA, KREPA4, appears to bind gRNA U-tails or U-rich sequence with a putative S1 motif similar to a cold shock domain (Salavati et al., 2006). Proteins that prefer U-rich sequence could function as sensors to detect U's needing deletion. Perhaps the key factor in deciding which editing complex is recruited is an mRNA bulge detector. The editosome may recognize the 3-helix mRNA/gRNA structure and bind. If the single stranded bulge is U-rich next to the anchor helix, a U-deletion complex is recruited. If the single stranded bulge next to the anchor helix is not U-rich, a U-insertion complex is recruited. In addition, there may be proteins of the editosome that bind various elements of RNA structure such as the gRNA stem-loop in order to correctly position the editosome on the complex.

One method of characterizing mRNA/gRNA structure and protein positioning would be using crosslinking agents in various positions in the gRNA and mRNA, annealing the

two RNA molecules, and adding editosome complexes. Once this has been done, the RNA/protein complexes would be UV crosslinked and resolved on SDS page gels. Antibodies against the various proteins could be used to identify which proteins are binding in which positions. Additionally, changing the sequence of the mRNA and gRNA from U-insertion to U-deletion and vice versa would allow differentiation of different proteins involved as bulge sensors for U-insertion and U-deletion. If a specific protein always binds the same element of structure such as the gRNA stem-loop, anchor helix, editing bulge, or U-tail, these elements of structure could serve as points of orientation that each protein binds to correctly position the editosome for editing. Removal of these elements of structure could disrupt editing.

In addition to crosslinking studies, monitoring conformational changes in the mRNA/gRNA secondary and tertiary structure through time resolved fluorescence resonance energy transfer (FRET) would give detailed information about secondary and tertiary structure changes of the mRNAs and gRNAs separately and together. FRET describes experiments where donor and acceptor dyes are attached to two sites on the molecule to measure the distance between two regions of a molecule. The donor fluorophore donates its energy to the acceptor fluorophore in a distance dependent manner, so that the change in fluorescence between two dyes indicates a change in conformation. Using FRET would enable study of single-molecule conformation changes, conformation changes caused by protein binding, and thermodynamics of protein binding (Ha et al., 1999). In addition, FRET measurements would be able to detect faster association events that SPR and gel shifts cannot detect. Investigating how

each new accessory factor affects the mRNA/gRNA complex conformation would provide much new information.

Editing Accessory Factors

Although a core editosome complex has been identified, this set of proteins is not sufficient to generate editing *in vitro* with any substrate other than the ATPase 6 subunit. Additional accessory factors have been identified that affect editing. Most of these have not been proven to directly affect the editing process. A few of these proteins seem to have direct effects on CYb editing. These proteins include MRP1 and 2 as well as RBP16.

MRP1 and MRP2

The mitochondrial RNA-binding proteins (MRP), MRP1 and MRP2, are accessory factors to the editing process that are arginine rich and bind to gRNAs (Koller et al., 1997; Blom et al., 2001). Both MRP proteins co-purify in a protein complex, and when both proteins are knocked down in RNAi experiments, there are very low amounts of CYb mRNA editing (Vondruskova et al., 2005). MRP1 has an RNA annealing activity (Muller et al., 2001) that is thought to reduce the electrostatic repulsion between the mRNA and gRNA anchor. This is thought to make anchor hybridization favorable. The formation of the anchor helix is thought to release MRP1 from the gRNA, because MRP1 has a low affinity for dsRNA (Muller & Goringer, 2002). The crystal structure of the MRP1/MRP2 complex reveals a heterotetramer with MRP2 binding the gRNA stem-loop and MRP1 holding the anchor sequence in a single stranded conformation. MRP1 presents the anchor sequence with the bases exposed to the solvent ready to bind the pre-mRNA. The beta sheet of the MRP1 protein is electropositive and thought to provide

charge neutralization for the anchor phosphate backbone (Schumacher et al., 2006). The solution structure probing on the CYb gRNA also suggests that the anchor sequence is presented to the mRNA in single-stranded form (Yu & Koslowsky, 2006). It appears that this annealing factor ensures that the anchor is single stranded. The structure data for the gRNA in this complex correlates well with our gRNA alone structure for NgCYb-558 providing evidence that the RNA structures are relevant. In addition, these accessory factors appear to recognize structure not sequence also verifying our hypothesis that the structure and not the sequence of the mRNA/gRNA complex is important for recognition by the editosome proteins as MRP1 and MRP2 are transient members of the editosome complex (Allen et al., 1998). Interestingly, the structure of the gRNA is not altered by the MRP complex (Hermann et al., 1997; Schumacher et al., 2006), and the gRNA guiding region stem-loop is maintained providing additional evidence that the gRNA stem-loop appears to be an important structure for the editing process. The MRP complex only weakly binds the U-tail (Muller et al., 2001; Schumacher et al., 2006) suggesting that while the anchor sequence is bound by MRP1 and the gRNA stem-loop is bound to MRP2 (Schumacher et al., 2006), the U-tail is free to interact with the mRNA. In addition, both previous and present crosslinking studies show that the U-tail interacts with a section of mRNA upstream of the editing sites (Leung & Koslowsky, 1999). One possibility for an U-tail interaction may be formation of Hoogsteen base pairs with the purine rich mRNA sequence upstream of the first editing site forming a pyrimidine/purine/pyrimidine triplex that destabilizes the ABS helix and allows the gRNA anchor to bind the ABS (Rajagopal & Feigon, 1989; Pilch et al., 1990).

MRP1 and 2 may be important co-factors for CYb editing. The CYb gRNA cannot bind the mRNA easily because of the double stranded nature of the anchor binding site (Koslowsky et al., 2004), and it appears that MRP1 and 2 might be involved in the formation of anchor duplexes. The fact that constitutively edited mRNAs such as A6 were unaffected by MRP1 and 2 RNAi knock-down (Vondruskova et al., 2005), shows that these proteins could be specific annealing factors for CYb editing or that A6 editing may only be enhanced with this co-factor. Future experiments with the addition of MRP 1 and 2 could show that these proteins are important chaperone proteins to help the gRNA bind the mRNA. Also, if these proteins were developmentally regulated or involved with proteins that were developmentally regulated, this would allow discovery of how CYb editing is developmentally regulated.

RBP16

Another possible editing accessory factor is, RBP16, a 16 kDa protein that binds U-rich sequences such as the gRNA U-tail. It contains an N-terminal cold shock domain and a C-terminal region rich in arginine and lysine residues (Hayman & Read, 1999). The *in vitro* association between RBP16 and gRNA is increased in the presence of p22, a human p32 homologue (Hayman et al., 2001). RNAi knock-down of RBP16 results in a ~98% reduction in CYb mRNA editing (Pelletier & Read, 2003). Recent studies using enhanced gRNAs show that RBP16 may enhance CYb U-insertion editing (Miller et al., 2006). RBP16 could be important for CYb editing. Additional *in vitro* studies using RBP16 with p22 will need to be done to see if RBP16 can improve the unenhanced CYb gRNA's interaction with the mRNA through structure stabilization or annealing activity.

The studies of these accessory factors are inconclusive. And showing that these accessory factors exist and proving their function *in vivo* is very difficult. In addition, studying these mRNA/gRNA pairs in the presence of these mitochondrial proteins will show if the mRNA/gRNA complex structure changes in the presence of protein. Adding the editosome complexes to the mRNA/gRNA complexes after exposure to these accessory factors could result in more *in vitro* editing for other mRNAs besides A6.

One of the objectives of these studies was to discover the function of the U-tail. The U-tail appears to have multiple functions during editing in the CYb mRNA/gRNA complex. It appears to improve association between the gRNA and the mRNA by binding the complementary strand to the ABS to help disrupt the helix. Additional mRNAs both with single stranded and double stranded anchor binding sites could be investigated to see if they have similar kinetics of anchor target binding as well as association and dissociation rates. The U-tail also maintains the gRNA stem-loop by feeding into the gRNA stem-loop as the anchor helix grows during editing. It will be interesting to see if other mRNA/gRNA pairs employ the U-tail for this function.

Literature Cited

Allen TE, Heidmann S, Reed R, Myler PJ, Goringer HU, Stuart KD. 1998. Association of guide RNA binding protein gBP21 with active RNA editing complexes in Trypanosoma brucei. *Mol Cell Biol 18*:6014-6022.

Aphasizhev R, Sbicego S, Peris M, Jang SH, Aphasizheva I, Simpson AM, Rivlin A, Simpson L. 2002. Trypanosome mitochondrial 3' terminal uridylyl transferase (TUTase): the key enzyme in U-insertion/deletion RNA editing. *Cell 108*:637-648.

Arthur DC, Ghetu AF, Gubbins MJ, Edwards RA, Frost LS, Glover JN. 2003. FinO is an RNA chaperone that facilitates sense-antisense RNA interactions. *Embo J 22*:6346-6355.

Blom D, Burg J, Breek CK, Speijer D, Muijsers AO, Benne R. 2001. Cloning and characterization of two guide RNA-binding proteins from mitochondria of Crithidia fasciculata: gBP27, a novel protein, and gBP29, the orthologue of Trypanosoma brucei gBP21. *Nucleic Acids Res 29*:2950-2962.

Brown HW, Neva FA. 1983. Ch. 4: Blood and Tissue Protozoa of Man. *Basic Clinical Parasitology*. Norwalk, CT: Appleton Century Croft. pp 45-53.

Feagin JE, Shaw JM, Simpson L, Stuart K. 1988. Creation of AUG initiation codons by addition of uridines within cytochrome b transcripts of kinetoplastids. *Proc Natl Acad Sci U S A 85*:539-543.

Goldschmidt V, Rigourd M, Ehresmann C, Le Grice SF, Ehresmann B, Marquet R. 2002. Direct and indirect contributions of RNA secondary structure elements to the initiation of HIV-1 reverse transcription. *J Biol Chem 277*:43233-43242.

Gott JM. 2003. Two distinct roles for terminal uridylyl transferases in RNA editing. *Proc Natl Acad Sci U S A 100*:10583-10584.

Ha T, Zhuang X, Kim HD, Orr JW, Williamson JR, Chu S. 1999. Ligand-induced conformational changes observed in single RNA molecules. *Proc Natl Acad Sci U S A 96*:9077-9082.

Hajduk SL, Sabatini RS. 1998. Mitochondrial mRNA Editing in Kinetoplastid Protozoa. In: Grosjean H, Benne R, eds. *Modification and Editing of RNA*. Washington, D.C.: ASM Press. pp 377-411.

Hayman ML, Miller MM, Chandler DM, Goulah CC, Read LK. 2001. The trypanosome homolog of human p32 interacts with RBP16 and stimulates its gRNA binding activity. *Nucleic Acids Res 29*:5216-5225.

Hayman ML, Read LK. 1999. Trypanosoma brucei RBP16 is a mitochondrial Y-box family protein with guide RNA binding activity. *J Biol Chem 274*:12067-12074.

Hermann T, Schmid B, Heumann H, Goringer HU. 1997. A three-dimensional working model for a guide RNA from Trypanosoma brucei. *Nucleic Acids Res 25*:2311-2318.

Koller J, Muller UF, Schmid B, Missel A, Kruft V, Stuart K, Goringer HU. 1997. Trypanosoma brucei gBP21. An arginine-rich mitochondrial protein that binds to guide RNA with high affinity. *J Biol Chem 272*:3749-3757.

Koslowsky DJ, Reifur L, Yu LE, Chen W. 2004. Evidence for U-Tail Stabilization of gRNA/mRNA Interactions in Kinetoplastid RNA Editing. *RNA Biology 1*:28-34.

Leung SS, Koslowsky DJ. 1999. Mapping contacts between gRNA and mRNA in trypanosome RNA editing. *Nucleic Acids Res 27*:778-787.

Leung SS, Koslowsky DJ. 2001a. Interactions of mRNAs and gRNAs involved in trypanosome mitochondrial RNA editing: structure probing of an mRNA bound to its cognate gRNA. *RNA 7*:1803-1816.

Leung SS, Koslowsky DJ. 2001b. RNA editing in Trypanosoma brucei: characterization of gRNA U-tail interactions with partially edited mRNA substrates. *Nucleic Acids Res 29*:703-709.

Linnstaedt SD, Kasprzak WK, Shapiro BA, Casey JL. 2006. The role of a metastable RNA secondary structure in hepatitis delta virus genotype III RNA editing. *RNA 12*:1521-1533.

Lorsch JR. 2002. RNA chaperones exist and DEAD box proteins get a life. *Cell 109*:797-800.

Miller MM, Halbig K, Cruz-Reyes J, Read LK. 2006. RBP16 stimulates trypanosome RNA editing in vitro at an early step in the editing reaction. *RNA 12*:1292-1303.

Mohr S, Stryker JM, Lambowitz AM. 2002. A DEAD-box protein functions as an ATP-dependent RNA chaperone in group I intron splicing. *Cell 109*:769-779.

Muller UF, Goringer HU. 2002. Mechanism of the gBP21-mediated RNA/RNA annealing reaction: matchmaking and charge reduction. *Nucleic Acids Res 30*:447-455.

Muller UF, Lambert L, Goringer HU. 2001. Annealing of RNA editing substrates facilitated by guide RNA-binding protein gBP21. *Embo J 20*:1394-1404.

Nebohacova M, Maslov DA, Falick AM, Simpson L. 2004. The effect of RNA interference Down-regulation of RNA editing 3'-terminal uridylyl transferase

(TUTase) 1 on mitochondrial de novo protein synthesis and stability of respiratory complexes in Trypanosoma brucei. *J Biol Chem 279*:7819-7825.

Panigrahi AK, Ernst NL, Domingo GJ, Fleck M, Salavati R, Stuart KD. 2006. Compositionally and functionally distinct editosomes in Trypanosoma brucei. *RNA 12*:1038-1049.

Pelletier M, Read LK. 2003. RBP16 is a multifunctional gene regulatory protein involved in editing and stabilization of specific mitochondrial mRNAs in Trypanosoma brucei. *RNA 9*:457-468.

Pilch DS, Levenson C, Shafer RH. 1990. Structural analysis of the (dA)10.2(dT)10 triple helix. *Proc Natl Acad Sci U S A 87*:1942-1946.

Rajagopal P, Feigon J. 1989. NMR studies of triple-strand formation from the homopurine-homopyrimidine deoxyribonucleotides d(GA)4 and d(TC)4. *Biochemistry 28*:7859-7870.

Salavati R, Ernst NL, O'Rear J, Gilliam T, Tarun S, Jr., Stuart K. 2006. KREPA4, an RNA binding protein essential for editosome integrity and survival of Trypanosoma brucei. *RNA 12*:819-831.

Schumacher MA, Karamooz E, Zikova A, Trantirek L, Lukes J. 2006. Crystal Structures of T. brucei MRP1/MRP2 Guide-RNA Binding Complex Reveal RNA Matchmaking Mechanism. *Cell 126*:701-711.

Vickerman K. 1965. Polymorphism and mitochondrial activity in sleeping sickness trypanosomes. *Nature 208*:762-766.

Vondruskova E, van den Burg J, Zikova A, Ernst NL, Stuart K, Benne R, Lukes J. 2005. RNA interference analyses suggest a transcript-specific regulatory role for mitochondrial RNA-binding proteins MRP1 and MRP2 in RNA editing and other RNA processing in Trypanosoma brucei. *J Biol Chem 280*:2429-2438.

Yu LE, Koslowsky DJ. 2006. Interactions of mRNAs and gRNAs involved in trypanosome mitochondrial RNA editing: Structure probing of a gRNA bound to its cognate mRNA. *RNA 12*:1050-1060.